The Effect of G-Seat Tactile Cueing on Linear Motion Perception

by

Patricia Barrett Schmidt

S.B., Aeronautics and Astronautics

Massachusetts Institute of Technology, 1996

Submitted to the Department of Aeronautics and Astronautics in partial fulfillment of the requirements for the degree of

Master of Science in Aeronautics and Astronautics

at the

MASSACHUSETTS INSTITUTE OF TECHNOLOGY

February, 1998

Author .....
Department of Aeronautics and Astronautics
December 9, 1997

Certified by .....
Laurence R. Young
Apollo Program Professor of Astronautics
Department of Aeronautics and Astronautics
Thesis Supervisor

Accepted by .....
Jaime Peraire
Associate Professor
Department of Aeronautics and Astronautics
Chairman, Department Graduate Committee

The Effect of G-Seat Tactile Cueing on Linear Motion Perception

by

Patricia B. Schmidt

Submitted to the Department of Aeronautics and Astronautics on
January 16, 1998, in partial fulfillment of the requirements for the
degree of Master of Science in Aeronautics and Astronautics

Abstract

Humans obtain information from several sources, including the vestibular system, vision, and tactile and proprioceptive sensation, in order to estimate spatial orientation. A model of this estimation process is particularly useful in flight simulation, where simulator cab motion, visual displays, and other devices are used to create an illusory perception of motion in pilots. Tactile cueing using G-seats has been used in flight simulation for z-axis acceleration and roll and pitch tilt cueing and has been shown to affect pilots' perceived motion. Although models describing the vestibular and visual roles in motion perception have been developed, the tactile contribution to motion perception, while significant, is less well understood. An experiment was conducted using a G-seat to quantify in the frequency domain the contribution of tactile cueing to linear motion perception. Eight blindfolded subjects were presented with uncorrelated sum-of-sines (.06 Hz-.5 Hz) disturbances in horizontal velocity and G-seat pressure and used a hand controller to null the velocity disturbance. Half of the experimental trials used G-seat pressure and sled velocity disturbance, and the other half used only sled velocity disturbance. Transfer functions between sled velocity and control response (vestibular transfer function) and G-seat pressure and control response (tactile transfer function) were computed. Results showed a significant response to G-seat cueing, with a differentiator tactile transfer function. Small but significant increases in vestibular transfer function magnitude were seen when the G-seat was on. Differentiation in the tactile transfer function agrees with previous research on cutaneous tactile receptors and supports the use of the G-seat as an acceleration onset cueing device. The smaller than expected increases in vestibular transfer function magnitude indicate that motion perception is not a simple sum of contributions from linear, time invariant tactile and vestibular estimators. A z-axis acceleration cueing drive algorithm for a pneumatic G-seat and a simulation concept using a pneumatic G-seat and a helmet-mounted display are proposed.

Thesis Supervisor: Laurence Young

Title: Apollo Program Professor of Astronautics

Acknowledgments

I would like to thank Professor Larry Young for giving me the opportunity to work on this project and for providing the guidance that made this thesis possible.

I would also like to thank Dr. Billy Ashworth at NASA Langley Research Center for the loan of the G-seat used in this work.

Many thanks are due to Mike Markmiller, for building the hardware that allowed the G-seat to work on the sled, and most importantly, for trusting a UROP student to do "important" work, and teaching me about everything from soldering to pipe fittings.

I am indebted to Sherry Mowry and Nasos Dousis for their help in experiment development.

Special thanks go to students at the MVL, for making life around here interesting. Thanks to Jen, who knows why the sky is red at sunset but blue at noon, to Keoki for advice and Mardi Gras parties, to Dawn for that awesome banana bread and for putting up with silliness, to Amir for interesting conversation and computer help, and to Prashant for musical entertainment.

Thanks to Marsha Warren, for taking care of all the paperwork and red tape. A big thank you to Dick Perdichizzi and Don Weiner for technical assistance. Special thanks to Subjects A through N for their time and cooperation, which was uncompensated except for one 44 ounce raspberry slurpee.

I owe a huge debt to my parents for making it possible for me to come to MIT, and to Julie and Harry for their support. Thanks to all of my friends from House 4, especially Karen and Rich, my teammates from the sailing team, Hatch and Fran, and the GNC^4 crew, for keeping me sane through five and a half years at MIT.

This work was funded by NASA Grant NAGW-3958.

Table of Contents

List of Figures

List of Tables

Chapter 1

Introduction

1.1 Motivation

The human brain combines information from a number of sources to obtain an estimate of the body's orientation and motion. The two major sources of information are the vestibular system and vision, while additional contributions are made by tactile and proprioceptive sensation. A considerable amount of research has been done to model the relative contributions of visual and vestibular information; however, tactile sensation has recieved relatively little attention in motion estimation modeling efforts. (Borah, Young, and Curry 1978)

Motion sensation through tactile cueing recieved attention beginning in the 1970's as a method of providing additional motion cueing in flight simulation. Flight simulators use a combination of simulator cab motion and visual scene motion to convey to the pilot the motion of the simulated aircraft. (Rolfe and Staples 1986) Tactile stimulation was investigated as a way of providing the sustained linear acceleration cues that simulator cab motion and visual field motion could not reproduce. (Kron 1980)

The device used in flight simulators to produce tactile cues in the simulator is known as a G-seat. A G-seat is a flight simulator seat which has inflatable cushions or hydraulically actuated panels in the seat pan and back. By altering the pressure distribution on the skin of the pilot's back and legs, the G-seat mimics the tactile stimulation produced by contact between the pilot and seat in an accelerating aircraft. Several versions of the G-seat were developed.(Kron 1980) Drive algorithms for G-seats were developed to produce tactile cueing for z-axis acceleration and roll and pitch tilt.(Flach, Riccio, McMillan, Warren 1986, Martin, Osgood, McMillan 1987)

The majority of research on the G-seat has focused on its role in simulation, specifically on the performance of pilots in flight simulators using the G-seat. In order to incorporate tactile sensation into overall models of spatial orientation, a broader understanding of motion sensation through tactile cueing is needed. The objective of this study is to assess the effectiveness of a G-seat at producing illusory linear motion outside of a flight simulation environment and to quantify the contribution of G-seat tactile cueing to linear motion perception.

1.2 Organization

Chapter 1 describes the motivation for this work. Chapter 2 discusses background information about the motion perception process and the G-seat. Chapter 3 describes the equipment used in the experiment and Chapter 4 describes the design and execution of the experiment. Chapter 5 details data analysis, and Chapters 6, 7 and 8 contain the results, discussion, conclusions and recommendations for future work.

Chapter 2

Background

2.1 Vestibular System

The vestibular organs, which are located in the inner ear, are the primary motion sensors in humans. The semicircular canals sense angular velocity, while the otolith organs sense linear acceleration, which may be caused by tilt with respect to gravity, linear motion. or centrifugal acceleration. Fernandez and Goldberg (1976) found that the otolith organs respond to tilt and centrifugal acceleration, by recording from individual otolith neurons.

2.2 Tactile receptors in the skin

The skin contains a variety of specialized receptors which sense touch, heat, cold, and pain. Two types of touch receptors are found in hairy skin: slowly adapting and rapidly adapting receptors.

Slowly adapting receptors sense a sum of velocity and position of skin indentation and stretch. Morphologically and functionally, they fall into two categories. The Type I receptors, or Merkel cells, are found in the epidermis and code a combination of position and velocity of skin indentation. (Burgess and Perl 1973) Linear systems analysis of the response of single Type I receptors shows that the receptors have a fractional integrator transfer function, as a result of their nonlinear dynamics. (Looft and Baltensperger 1990)

Type II receptors, or Ruffini endings, are found in the dermis. Type II receptors are stimulated by lateral stretch of the skin and code a combination of stretch and stretch rate. (Burgess and Perl 1973)

Rapidly adapting mechanoreceptors in the skin, such as the Pacinian corpuscle, sense vibration. The multi-layered corpuscle which surrounds the nerve ending acts as a mechanical high-pass filter, only transmitting velocity and acceleration of skin indenta-

tion.(Loewenstein 1971) Because Pacinian corpuscles respond to skin indentation velocity and acceleration with a high threshold, they are considered to be vibration transducers.(Burgess and Perl 1973)

2.3 Models of spatial orientation

Several models have been developed to describe the motion estimation process in humans. These models primarily deal with motion estimation from visual and vestibular inputs, although one model (Borah, Young, and Curry 1978) includes tactile and proprioceptive inputs.

Zacharias (1977) proposed a linear estimator model and conducted experiments to determine the estimator transfer functions for the visual and vestibular systems in yaw rotation. Subjects in Zacharias's experiment controlled yaw rotation of a flight simulator while viewing a moving visual surround. Zacharias found that the linear estimator model did not fit the experimentally determined transfer functions and proposed a non-linear model, known as the conflict model, in which the visual and vestibular signals are averaged with a weighting that is determined by the amount of conflict between them. For short duration conflict, the weighting is shifted toward the vestibular signal. He used computer simulations of his model to demonstrate that it fit his experimental data.

The Zacharias conflict model was strictly designed to fit experimental data, but a model based on optimal estimation can be derived from first principles, given information about the sensors. Oman (1982) proposed an estimator model which uses a Kalman filter, an estimator which is optimal for a particular set of sensor noise covariances.

Borah, Young, and Curry (1978) simulated a steady-state Kalman filter model, but found that it was necessary to add the conflict nonlinearity of Zacharias's model in order for the results to agree with experimental time response data. The constant-gain Kalman

filter alone did not reproduce the delay in onset of circularvection when a stationary subject is presented with a rotating visual scene, but the combined Kalman filter-conflict model did reproduce the time delay.

Merfeld (1990) conducted an experiment with monkeys on a centrifuge, recording torsional eye movements in response to the changing gravito-inertial vector. He developed a linear model for estimation of the direction of the gravity vector, with estimator gains set to match experimental data. One important difference between Merfeld's model and previous models was that his model used quaternions to represent angles in three-dimensional space. This allowed the model to be give accurate results with large deviations from center.

Pommellet (1990) proposed a time-varying extended Kalman filter estimator model for spatial orientation, using only vestibular inputs. Pommellet's model used quaternions to represent spatial orientation. Since the quaternion representation introduced nonlinearities, Pommellet's estimator applied the Kalman filter equations to a representation of the system dynamics that was linearized about the value of the estimated state at each time step. This type of estimator is known as an extended Kalman filter. Model outputs were found to agree qualitatively with data from Merfeld's experiment in some cases, but in other cases, the model's estimated state converged much more quickly to the true state than Merfeld's experimental results would indicate.

2.4 Previous G-Seat Research

One of the earliest G-seats was built at NASA Langley Research Center and integrated into Langley's Differential Maneuvering Simulator. The Langley G-seat was intended for normal acceleration cueing only. It had eight inflatable bladders, arranged in 2 by 2 arrays on the seat pan and back. The drive algorithm for the Langley G-seat was based on contact

between the pilot's ischial tuberosities and the hard base under the inflatable cushions and required the pilot to be loading the seat pan with his or her weight. For the zero acceleration condition, the cushions were inflated so that the pilot's weight was mostly supported on a cushion of air, with some of the force transmitted through the ischial tuberosities (ITs) to the rigid seat base. In order to simulate headward acceleration, air was let out of the cushions, causing more of the pilot's weight to be supported by the ITs in contact with the hard seat base. To simulate footward acceleration, the cushions were inflated, causing the pilot's weight to be supported by the cushions, rather than contact between the ITs and the seat base. Initial reports by pilots indicated that the tactile cues produced by the G-seat were realistic.(Ashworth 1976) Further testing of the Langley G-seat demonstrated that pilots' performance using the G-seat in fixed-base flight simulation was better than their performance without the G-seat. (Ashworth, McKissick, Parrish 1984)

The next generation of G-seats was the Advanced Low Cost G-Cueing System (ALCOGS), which was developed by the Link Division of Singer Corporation for the Air Force. The ALCOGS G-seat had a seat pan driven in heave, pitch and roll by hydraulic actuators, which was overlaid with pneumatic firmness bladders. The backrest of the seat was hydraulically driven in roll, pitch and heave, while panels located in the lower corners of the backrest were extended and retracted. The ALCOGS design addressed several shortcomings of the pneumatic G-seat. The hydraulic actuators had a higher bandwidth and less time delay than the pneumatic G-seat, and, unlike the Langley G-seat, the height and firmness of the seat pan could be independently controlled. (Krohn and Kleinwaks, 1978)

Extensive research was done to develop roll and pitch drive algorithms for the ALCOGS. Contrary to researchers' expectations, drive laws based on roll velocity and position resulted in better pilot performance than drive laws based on roll acceleration.

(Levison, McMillan, Martin, 1984). Later drive algorithms were developed using psychophysical matching techniques. (Flach, Riccio, McMillan, Warren, 1985) Comparisons between pilot performance using visual cues alone, the ALCOGS alone, and the combination of ALCOGS and visual cues showed that use of the ALCOGS alone resulted in better pilot performance than the use of visual cues alone. (Snell, Flach, McMillan, Warren, 1985)

Research on tactile cueing of motion at MIT has focused on the relative contributions of tactile, vestibular and visual cueing to motion perception, using a Langley G-seat. Markmiller (1996) conducted an experiment in rostro-caudal axis linear motion, analogous to Zacharias's (1977) experiment, using a G-seat and head-mounted display on the MIT sled. Subjects controlled the sled with a hand controller, and their task was to null out a sum-of-sines velocity disturbance, with additional sum-of-sines stimuli presented in the visual field and G-seat. Transfer functions for each of the channels were calculated using a cross-correlation method similar to that proposed by Zacharias (1977).

Chapter 3

Equipment

3.1 G-seat

The G-seat is a flight simulator pilot's seat with inflatable cushions on the seat pan and back. The G-seat used in this experiment, which is shown in Figure 3.1, is a Langley G-seat, as described in Section 2.3, and is pneumatically driven.

Figure 3.1: G-seat

The seat pan, which was the only portion of the G-seat used in this experiment, consists of a 2x2 array of cloth-covered silicone rubber air bladders on a wooden seat base. A pressure transducer is mounted on each air bladder. The dimensions of the seat pan with the G-seat inflated are 14" (35.6 cm) by 16" (40.6 cm) by 6" (15.2 cm). At maximum inflation of the unloaded seat, the cushions are approximately 1.5 " (3.8 cm) in thickness.

One inch diameter steel pipes connect each air bladder to a pipe nipple which extends out the back of the wooden seat base. These pipe nipples are connected by 10 foot (3.05

m) length, 1" (2.54 cm) diameter rubber hose to a valve assembly located under the sled cart. The valve assembly consists of four anti-G-suit valves, actuated by Ling Model 203 shaker motors. The anti-G-suit valves are spool valves which have two positions: open or closed.

Bottled nitrogen was used as the gas supply for the G-seat. Nitrogen was supplied to the G-seat's valve manifold, through a 40 foot (12.2 m) rubber hose at 80 psi (544 kPa), where a regulator on the valve assembly reduced the pressure to 5 psi (34.0 kPa). The long hose was necessary so that the nitrogen cylinder could be secured to the lab wall. The nitrogen at 5psi was then supplied to the four anti-G-suit valves which regulated gas flow into the G-seat cushions.

The G-seat control system is an analog pressure controller, which separately controls pressure in each of the four seat cushions. Seat cushion pressure is measured with a National Instruments Model LX1802GN pressure transducer on each seat cushion. The pressure signal is inverted and low-pass filtered, then summed with the command signal and a user-adjustable bias to form the motor drive signal. The motor drive signal goes to a set of motor amplifiers (Inland Motor EM 1802) which power the motors. A terminal on the G-seat controller chassis allows the low pass filtered pressure signal to be monitored and recorded by a computer.

The control system has several user-adjustable parameters, which are set with potentiometers on the controller boards. They include a pressure signal bias, pressure signal gain, command signal gain, and motor drive signal bias. These gains and biases were set so that the pressure signal is zero when the cushions are not inflated, and the responses of the two front and two back cushions match each other.

The simplicity of the G-seat control system presented two possible problems. The first potential difficulty, which was addressed by Markmiller (1996), was low bandwidth.

Markmiller experimentally determined transfer functions from command to cushion pressure and command to cushion displacement, demonstrating that the G-seat's bandwidth was adequate for a manual control experiment. A bode plot of the G-seat system's response to sinusoidal pressure commands is shown in Figure 3.2

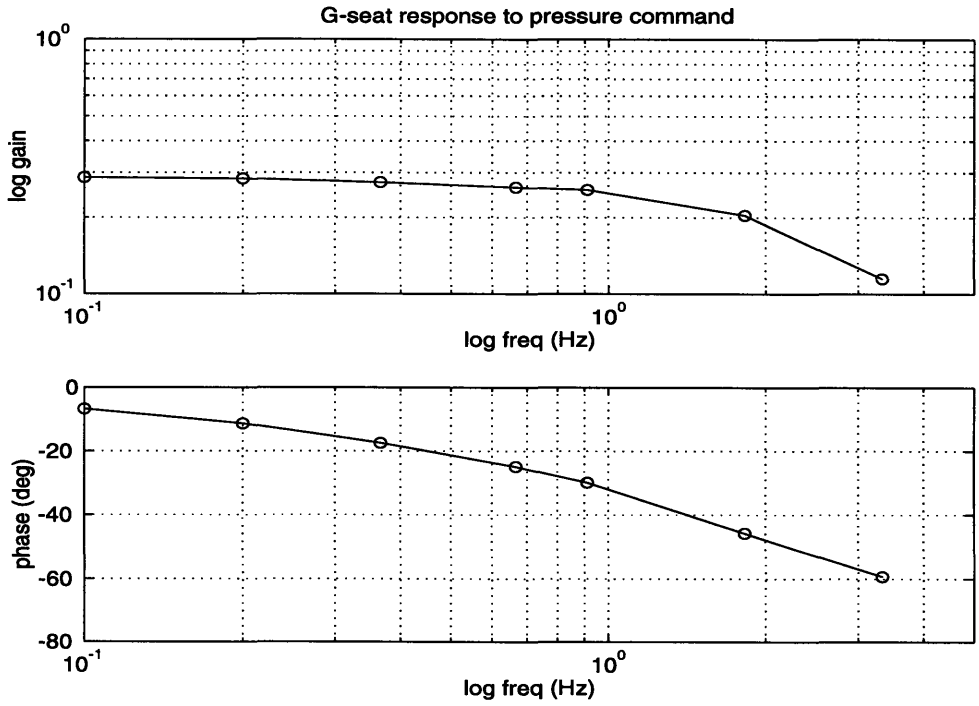

Figure 3.2: G-seat frequency response (Markmiller 1996)

The second potential difficulty was the possibility of a long time delay in the G-seat's response to commands. Markmiller's G-seat transfer functions did not indicate a significant time delay. This was confirmed by testing the response to a step pressure command. Figure 3.3 shows the result of the step response test. Figure 3.3 shows a two-sample delay between pressure command and pressure, which corresponds to a time delay of 20-40 msec.

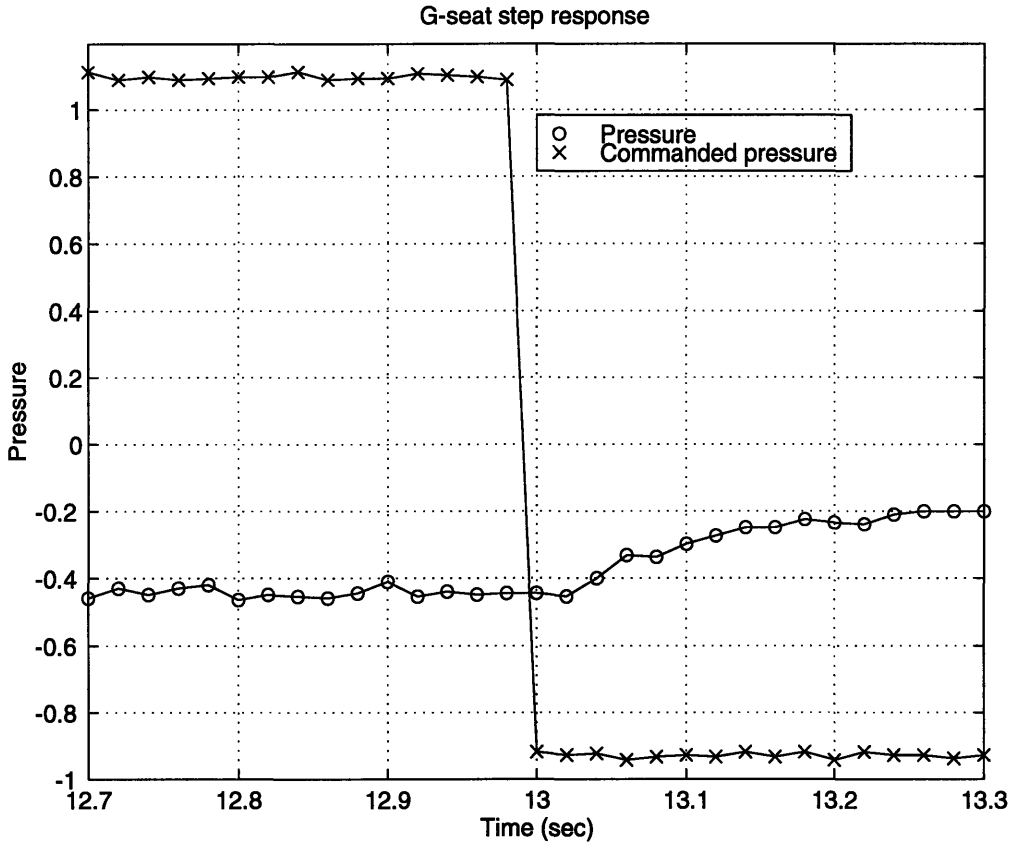

Figure 3.3: G-seat step response

One issue that arose during testing was the need for an acceleration feedforward gain to the G-seat. The G-seat pressure control system obscures the normal tactile cues that a subject receives when the sled is in motion. As the sled accelerates in the headward direction, pressure increases in the G-seat, due to the inertial force of the subject's body on the seat. As a result, the controller lets gas out of the cushions, in order to return the pressure to its commanded value. Footward acceleration of the sled produces the reverse effect, as the seat inflates to maintain a constant pressure. This effect results in the subject sinking into the seat and rising out of it by an abnormally large amount when the sled moves. To counteract this unrealistic effect, sled acceleration was fed forward to the G-seat command signal, in order to raise the commanded pressure when sled acceleration was in the headward direction and lower the commanded pressure when sled acceleration was in the foot-

ward direction. The feedforward gain was selected based on a subjective assessment of the realism of the seat's motion during sled motion.

3.2 Sled

The MIT sled, pictured in Figure 3.4, is a human-rated linear acceleration cart. It has a reorientable subject chair on a cart which moves along two parallel rails. The range of motion of the sled is 4.7 m from one end of the track to the other.

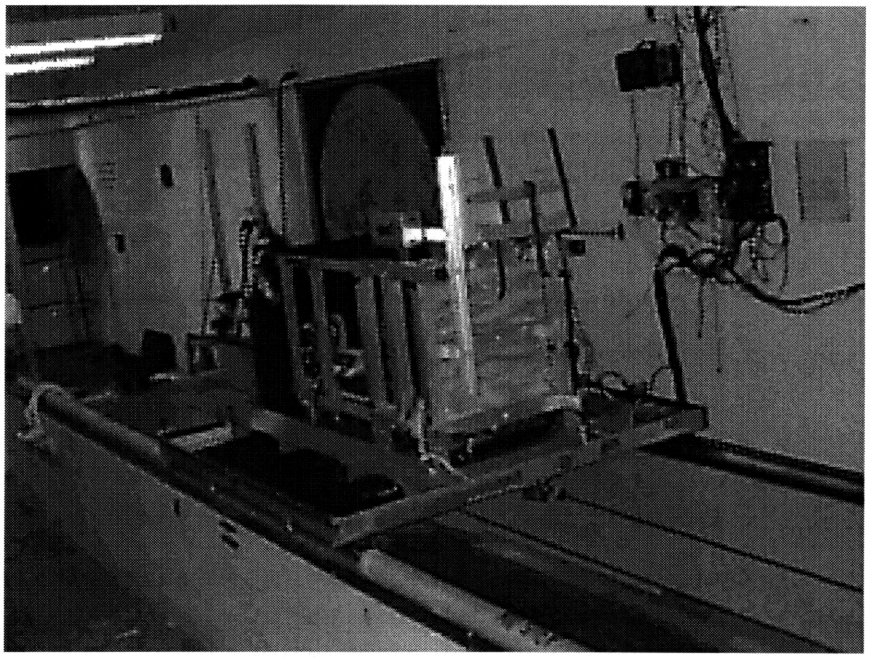

Figure 3.4: MIT sled

The subject seat is enclosed in a fiberglass and aluminum frame. This chair assembly can be oriented for motion in one of three axes: rostro-caudal (z-axis), inter-aural (y-axis), and anterior-posterior (x-axis). Three restraints are provided for subjects: a five-point aircraft harness, an adjustable head restraint made up of padded plexiglass blocks, and nylon straps to restrain the feet on the footrest. Cloth was draped around the outer frame of the seat assembly, in order to prevent subjects from sensing sled velocity through wind cues.

An intercom is provided for two-way voice communication between the subject and the sled operator.

The sled is driven by an Inland Motors permanent magnet servo motor. The motor turns a 1 foot diameter aluminum drum, which drives a steel cable. The cable makes a complete loop between the drum, the sled cart and an idler at the opposite end of the track. The motor is controlled by a GE HiAK pulse width modulation controller.

The sled is commanded by a Northgate 386 PC computer running "sled", a C++ program written specifically for the MIT sled. The computer also outputs an auxiliary command signal, which was used to command the G-seat. The sled software allows the user to set up and execute experiment protocols for both the sled and the auxiliary device.

One issue of concern in this experiment was the likelihood of the sled reaching the end of the track during an experiment run. Several mechanisms exist to prevent injury or damage if the sled hits the end of the track. First, the sled program incorporates a position limiting algorithm which sets the commanded sled velocity to zero if the sum of sled's position and a constant multiplied by velocity exceeds predetermined limits. Second, limit switches are located at either end of the track. The limit switches are triggered when the sled cart comes in contact with them, interrupting a circuit which activates the brake, bringing the sled to a rapid stop. Third, bungee cords and steel bumpers are positioned beyond the limit switches to stop the sled should the limit switches fail. Finally, the operator can either command zero velocity ("Soft Abort") or activate the brake ("Hard Abort") from the operator's console and the subject can activate the brake by pressing the subject's stop button at any time during the run.

In an early experiment run, it was discovered that a failed isolation amplifier in the sled operator's console prevented the sled computer from receiving sled velocity data. Because of the amplifier failure, the sled velocity signal at the computer was a constant -15 volts,

and the velocity input to the position limiting algorithm was a large negative value. As a result, the position limiting algorithm stopped the sled approximately 10cm short of the end of the track on the negative side, and did not stop the sled before it reached the limit switch on the positive side of the track. Because of the other safety mechanisms described above, the lack of a computer-controlled position limit at one end of the track was not considered to be a serious problem.

3.3 Subject's Hand Controller

Subjects controlled sled velocity using a sliding hand controller which was constructed specifically for sled-G-seat experiments by Markmiller (1996). The controller is a rectangular box (10"x5"x3") (25.4 cm x 12.4 cm x 7.62 cm) with a knob on the right side of the box. The knob slides parallel to the axis of motion of the sled. Rubber bands return the knob to the center when it is released. The controller is mounted on the sled chair frame so that the knob is located 22 inches (55.9 cm) above the seat backrest. The controller has a range of motion of 8.5 inches (21.6 cm), and an output range of -15 volts to +15 volts. Headward motion of the controller commands headward motion of the sled.

The controller signal is filtered by an analog filter (Krohn-Hite Model 3340) with a cutoff frequency of 40 Hz. The control signal is then multiplied by a gain and low-pass filtered digitally in the sled program. The control signal gain is set based on the maximum velocity in the sled disturbance profiles, using a method developed by Hiltner (1981). The gain is set so that the velocity commanded by 90% deflection of the subject's controller is equal to the highest disturbance velocity. This algorithm resulted in a control signal gain of .113. The digital low-pass filter has a cutoff frequency of 10 rad/sec.

3.4 Data Acquisition

Data was acquired on a 90 Mhz Pentium PC computer, running Labtech 9.0, using a Keithley Metrabyte DAS-1600 data acquisition board. Four channels of analog signals were recorded: pressure in G-seat cushion #1, sled acceleration, sled velocity, and the subject's command signal. Pressure data came from the pressure output port on the G-seat controller chassis and was low-pass filtered by an analog circuit to attenuate high-frequency noise caused by the G-seat servo amplifiers. Acceleration was measured by a Setra model 110 accelerometer mounted to the sled cart. Velocity was obtained from the tachometer on the sled motor, and the subject's control signal was recorded at the point where it entered the sled operator's console. A schematic of data acquisition and command for the experiment is shown in Figure 3.5.

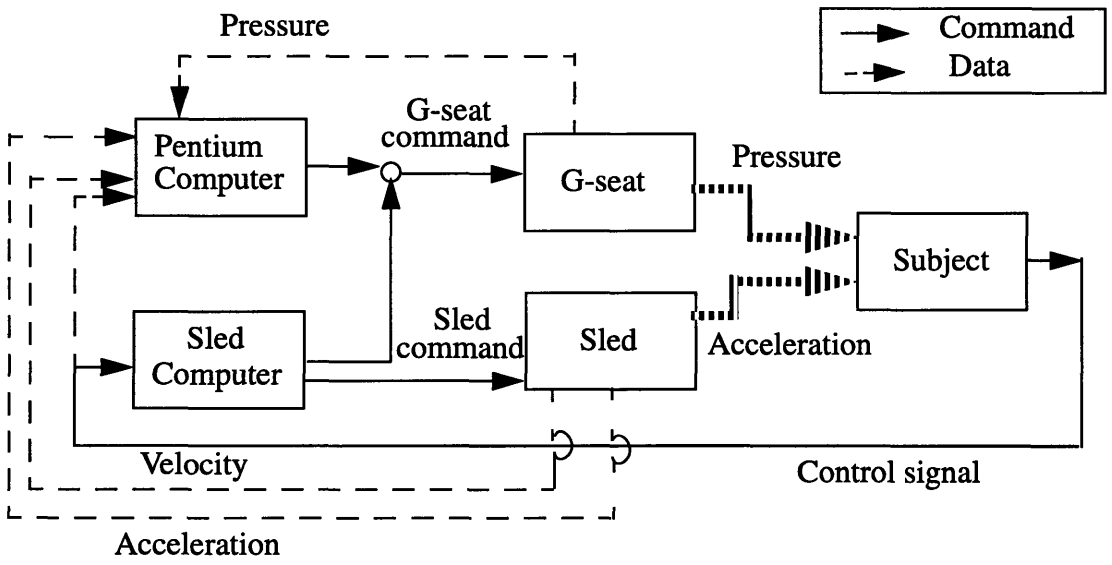

Figure 3.5: Data acquisition and command schematic

Because of the isolation amplifier failure in the operator's console, the velocity signal was not available from the velocity output port on the console. The velocity signal was obtained by tapping into the signal where it entered the console, then buffering it with a unity-gain amplifier and connecting the buffered signal to the computer, thus bypassing

the failed component in the console. The resulting velocity data was more noisy than normal, but the noise was filtered out of the recorded data adequately in Matlab.

The Labtech software acquired data at a 50 Hz sampling rate, displayed, and recorded it. The Labtech data display window is shown in Figure 3.6. Data files were named as follows: <subject><trial number>; for example, e11 is subject E, trial number 11. Subject designators for subjects A, I, and J were aa, ii, and jj, in order to avoid conflicts with variable names. The data files were saved in five-column ascii format, where the columns were time in seconds, pressure, acceleration, velocity, and control signal. Labtech appended an end of file character to the end of each data file, which had to be removed before loading the file in Matlab.

.

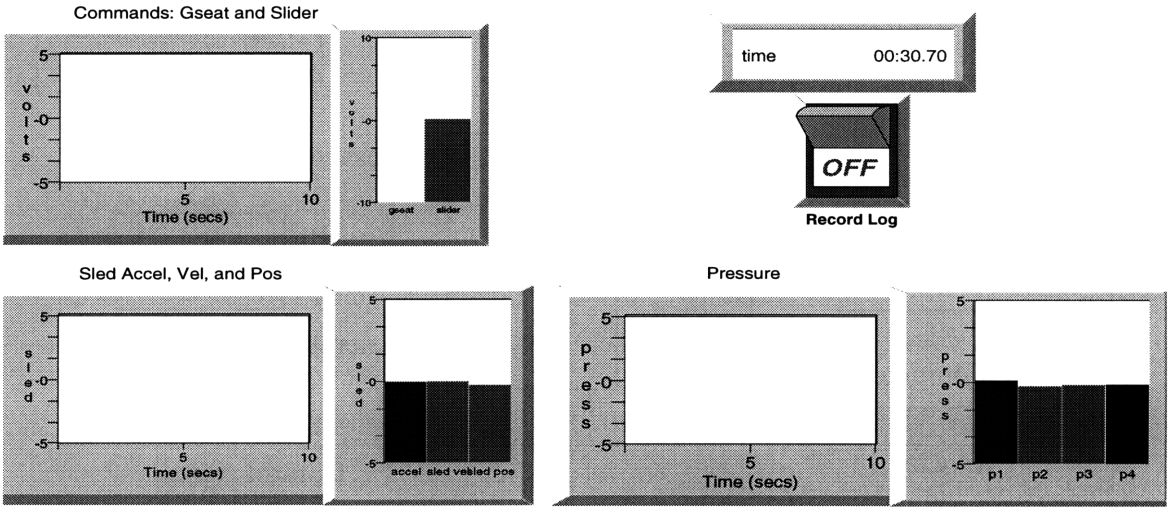

Figure 3.6: Labtech data display window

3.5 Command Generation

Commands to the G-seat originated from both the Pentium and the sled computer. The auxiliary command signal from the sled computer was used to command a sum of sines pressure profile for the G-seat, and the Pentium computer was used to command the accel-

eration feedforward which was described in Section 3.1. The acceleration feedforward command, which was the measured sled acceleration multiplied by a gain, was output using a Keithley Metrabyte DDA-16 analog output board. The two command signals were summed using an analog summer, and the total command signal was connected to the "command in" port on the G-seat controller chassis.

Commands to the sled were generated by the sled computer and originated from two sources: the sum of sines disturbance profiles and the subject's commands. The sled disturbance profiles are discussed in section 4.2. The subject's commands were low-pass filtered and multiplied by a gain, as described in Section 3.2, and summed with the disturbance profiles to result in the total command to the sled.

Chapter 4

Experiment

4.1 Overview

The goal of this experiment is to determine whether tactile cueing using a G-seat affects linear motion perception and to quantify its contribution in the frequency domain. The experiment design is patterned after two experiments with similar goals, done by Zacharias (1977) and Hiltner (1983). Zacharias conducted an experiment in yaw rotation in which subjects viewed a visual display and were instructed to null out a sum-of-sines disturbance in their yaw velocity. The visual display indicated their true angular velocity plus a sum of sines disturbance. Hiltner (1983) developed protocols for a velocity nulling experiment using the MIT sled, and demonstrated that blindfolded subjects could null out a sum of sines linear velocity disturbance on the sled.

The experiment is a closed-loop velocity nulling task. Blindfolded subjects are seated on the sled and given a sum of sines disturbance in sled velocity and G-seat pressure. Their task is to use a hand controller that commands velocity to null out the sled's velocity.

Figure 4.1 is a block diagram representation of the velocity nulling task in the experiment. The shaded portion of the block diagram indicates the estimation and control processes that occur in the human operator, and the unshaded portion indicates the dynamics of the subject's controller, sled and G-seat. The two disturbances given to the subject are d1, the sled velocity disturbance, and d2, the G-seat pressure disturbance.

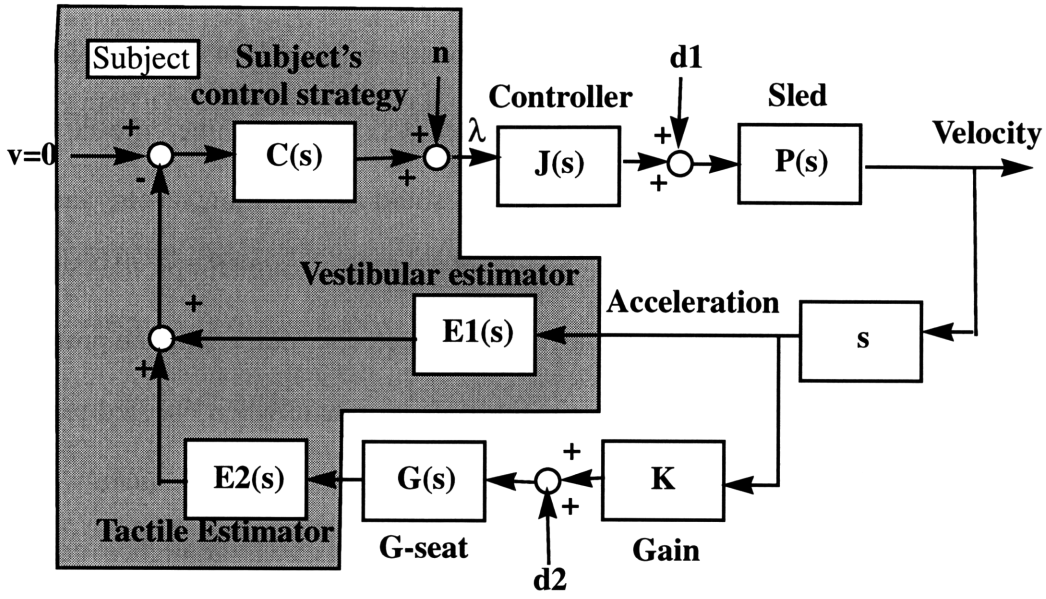

Figure 4.1: Experiment Block Diagram

4.2 Disturbance Profiles

The disturbances provided to the subjects must meet requirements imposed by the human operator, the sled and the G-seat. The disturbance must be unpredictable, in order to evoke realistic disturbance rejection control responses from the subject. Since the human operator's bandwidth is limited, the disturbance must be limited in bandwidth to below approximately .5 Hz. Profiles must also minimize the amount of time spent at sub-threshold accelerations. The disturbance is also subject to limitations on maximum sled position and maximum G-seat pressure.

Hiltner (1983) demonstrated that subjects could perform a velocity-nulling task on the MIT sled. Since the disturbance profiles used in Hiltner's experiment met the necessary conditions, they were adapted for use in this experiment.

Hiltner's disturbance profiles were the sum of sines at 12 different frequencies. The frequencies are prime multiples of a base frequency of .01221 Hz. so that no frequency is

a harmonic of another. The phase difference between sines at successive frequencies is a constant, 253 deg., in order to avoid a large disturbance magnitude at the start of the trial.

Hiltner's sled velocity profiles were determined according to three criteria: sled displacement constraints, minimum time at sub-threshold acceleration levels, and subject performance. Hiltner iterated on relative magnitudes of sines to obtain profiles with minimum time at sub-threshold acceleration levels and selected several candidate protocols for testing with human subjects. Since experiment trials terminate when the sled reaches the end of the track, it is essential to determine that the subjects can adequately null sled velocity for a particular sled disturbance profile. The profiles with the highest completion rates were selected for use in the experiment. (Hiltner 1983)

Since this experiment used two disturbance modalities, sled and G-seat, sines at 6 of the 12 possible frequencies are used for each channel, alternating between sled and G-seat. This results in two disturbance profiles. Profile 1 has sled disturbance at odd-numbered frequencies and G-seat disturbance at even-numbered frequencies. Profile 2 has sled disturbance at even-numbered frequencies and G-seat disturbance at odd-numbered frequencies. The frequencies and magnitudes of the sled and G-seat disturbance profiles are shown in Table 4-1. One of the sled disturbance profiles is shown in Figure 4.2

Data from both profiles is required for computation of vestibular and tactile transfer functions. A group of two trials using Profile 1 and Profile 2 is the smallest unit of data that can be analyzed. This group of trials referred to as a block

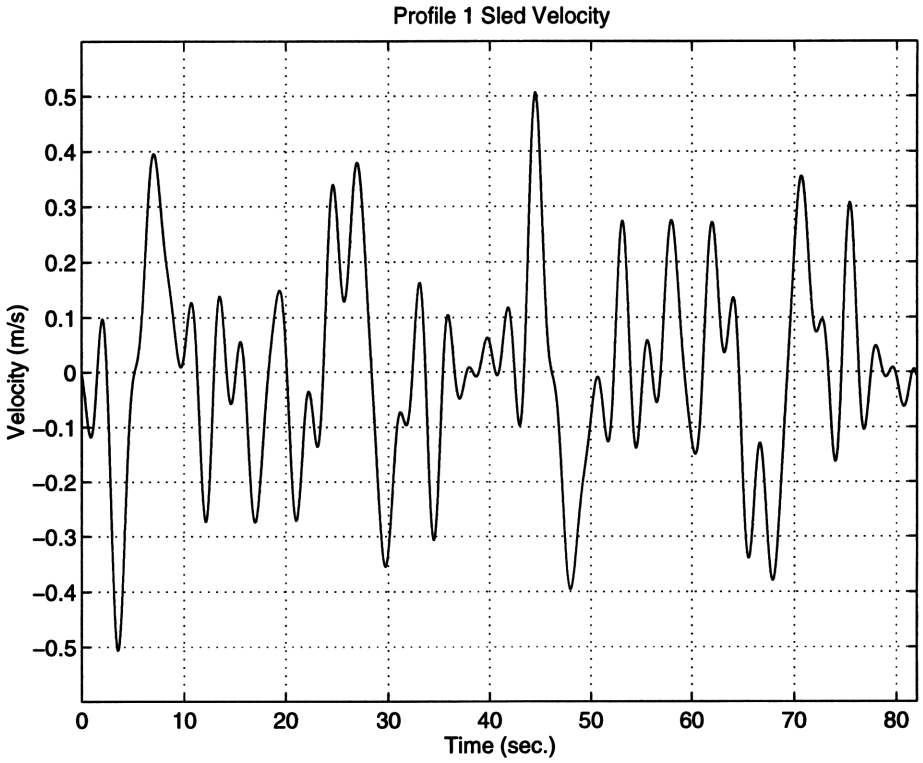

Figure 4.2: Sample sled velocity disturbance profile.

Table 4.1: Disturbance profiles

Frequency (Hz)	**Profile 1** sled velocity (m/s)	G-seat command (volts)	**Profile 2** sled velocity (m/s)	G-seat command (volts)
.0610	.12			2.8
.0854		3.0	.13	
.110	.12			2.8
.134		2.6	.11	
.159	.12			2.8
.208		2.6	.11	
.232	.10			2.3
.281		2.6	.11	

Table 4.1: Disturbance profiles

Frequency (Hz)	**Profile 1** sled velocity (m/s)	G-seat command (volts)	**Profile 2** sled velocity (m/s)	G-seat command (volts)
.354	.09			2.1
.391		1.6	.07	
452	.07			1.6
.500		1.4	.06	

4.3 Experiment Design

The final experiment protocol has three parts: practice trials, blindfolded data trials, and eyes open data trials.

Practice

The practice portion of the experiment was designed to reduce the effect of learning on performance in data trials. The number of practice trials required was determined from the results of a pilot experiment. Three subjects (A, B, and C) completed a pilot protocol which consisted of eight replications of profile 1 and profile 2. (Sled velocity data for subject C was lost due to an instrumentation problem, so no transfer functions were calculated for that subject's data.) Transfer functions were calculated for each set of two trials. Transfer functions for early trials were characterized by a sawtooth pattern, in which magnitudes alternated between high and low. Later trials showed less of a sawtooth pattern. These were attributed to large changes in the subject's performance between successive trials. Based on the qualitative trend in the pilot subjects' transfer functions, it was determined that four practice trials were sufficient.

In the practice protocol used for the first seven subjects, subjects completed four trials with disturbance inputs in both G-seat pressure and sled velocity of the same duration and character of the disturbances used in the data trials. These disturbance profiles were not identical to the disturbance profiles used in the data trials. Practice disturbance profiles can be found in Appendix B. The first trial was conducted without the blindfold, with the room lights on, in order to familiarize the subject with the range of sled motion and the response of the sled to control inputs. The following three trials were conducted with the subject wearing the blindfold. If the sled reached the end of the track during a trial, the run was terminated and repeated. Subjects took an average of 6.4 attempts to complete 4 practice trials.

For the last subject (subject L), the practice protocol was different. This practice protocol took a more incremental approach, with a total of 5 practice trials. In the first trial, the subject "rode" the sled without controlling it, without the blindfold, in a lighted room. The second trial contained no disturbance; the subject was allowed to manipulate the controller and move the sled without wearing the blindfold. The next trial was an eyes-open velocity nulling trial, identical to the other subjects' first practice trials, and the final two trials were identical to the other subjects' last three practice trials. Subject L took 6 attempts to complete the 5 practice trials. The different practice protocol did not result in different performance in the data trials for subject L.

Data Trials

The number and ordering of the data trials was determined by the following requirements: the ability to assess differences between responses when the G-seat is on or off, ability to balance for order effects despite possible inter-subject differences, and the ability to separate the subject's control strategy from the estimator transfer functions. This resulted in an experiment with three conditions, two of which were balanced for order within subjects.

The algorithm used to balance for order effects does not require data from different subjects to be averaged together.(Chapanis 1959) Each block is two trials, one trial with each disturbance profile, and is the smallest amount of data that can be used to compute transfer functions. This design gives four replications of each condition, resulting in 16 blindfolded data trials

In order to separate the subject's control strategy from the velocity estimation process, four additional trials were conducted, without the blindfold. Under these conditions, the subjects could see their surroundings and were able to estimate velocity from visual information. The visual velocity estimation process can be considered very fast compared with the bandwidth of the disturbance profiles; hence the transfer function from sled acceleration to the subject's command output is approximately equal to the transfer function of the subject's control strategy.

For the first 7 subjects, the eyes-open trials were conducted with the room lights on. These subjects had a clear view of the ceiling of the room, which contained several visual features that conveyed very strong position cues. For subject L, the eyes-open trials were conducted with the room lights off. The room was sufficiently lit for the subject to detect visual motion, but dark enough to obscure fine details on the ceiling.

Table 4-2 shows the order of trials in the experiment.

Trial number	G-seat	Vision
Practice 1	On	Yes
Practice 2	On	No
Practice 3	On	No
Practice 4	On	No
1	On	No
2	On	No

Table 4.2: Ordering of trials in experiment profile

Trial number	G-seat	Vision
3	Off	No
4	Off	No
5	Off	No
6	Off	No
7	On	No
8	On	No
9	Off	No
10	Off	No
11	On	No
12	On	No
13	On	No
14	On	No
15	Off	No
16	Off	No
17	Off	Yes
18	Off	Yes
19	Off	Yes
20	Off	Yes

Table 4.2: Ordering of trials in experiment profile

4.4 Subjects

A total of fourteen subjects volunteered for this experiment. Informed consent was obtained from each subject prior to the start of the experiment. The informed consent statement can be found in Appendix A.

Subjects are designated with the letters A-N. Subjects D, E, F, H, I, J, K, and L completed the full experiment protocol. Subjects A, B, and C participated in a pilot experiment described in section 4.3 and did not participate in the full experiment. Subjects G, M, and N did not complete the entire experiment protocol. None of the subjects who participated

in the full experiment had been subjects in a similar experiment, conducted by Markmiller (1996), involving velocity nulling on the sled with the G-seat. The mean age of the subjects who participated in the full experiment is 22 years.

4.5 Experiment Procedure

Prior to the start of the experiment, subjects were read a uniform set of instructions for the experiment (Appendix A), and read and signed the consent form (Appendix A). The G-seat was turned on, and the subject entered the sled. Subjects were strapped in with the five-point aircraft harness and good contact between the subject and the G-seat was verified. Broadband noise from a radio tuned to an AM frequency was played in the subject's headset. Noise volume was set at a level just below that considered by the subject to be uncomfortably loud. The output of the subject's controller was adjusted to zero using a potentiometer at the operator's console. Subjects completed four practice trials and 20 data trials, as described in Section 4.3. A short break was provided between the last trial with the blindfold and the first trial without the blindfold (Trials 16 and 17), in order to allow the subject's eyes to adjust to the light. The entire experiment protocol took approximately 1.5 hours.

Chapter 5

Data Analysis

5.1 Overview

For each experimental trial, G-seat pressure, sled velocity, sled acceleration, and subject's command signal were recorded. Data analysis had three goals:

- Compute transfer functions for the vestibular and tactile feedback paths for each subject in all three experimental conditions.
- Determine whether significant differences exist between the tactile transfer function magnitudes with the G-seat on and with the G-seat off.
- Fit transfer functions to the frequency response data.

5.2 Derivation of transfer functions

Transfer functions for the vestibular and tactile feedback paths were computed from the recorded sled velocity, G-seat pressure, and subject's command signal. The derivation of the estimator transfer functions was adapted from a system identification method proposed by Zacharias (1977). Calculation and plotting of the transfer functions was done in Matlab.

Derivation of transfer function relationships

Given recorded sled velocity, G-seat pressure, subject's command signal, known transfer functions for the sled (P(s)), subject's controller (J(s)) and the G-seat (G(s)) and the known G-seat acceleration feedback gain (K), transfer functions for the tactile and vestibular feedback paths can be calculated for the three experiment conditions. The calculated transfer functions are the product of the estimator transfer function and the subject's control strategy transfer function. A block diagram for the portion of the experiment G-seat on is shown in Figure 5.1.

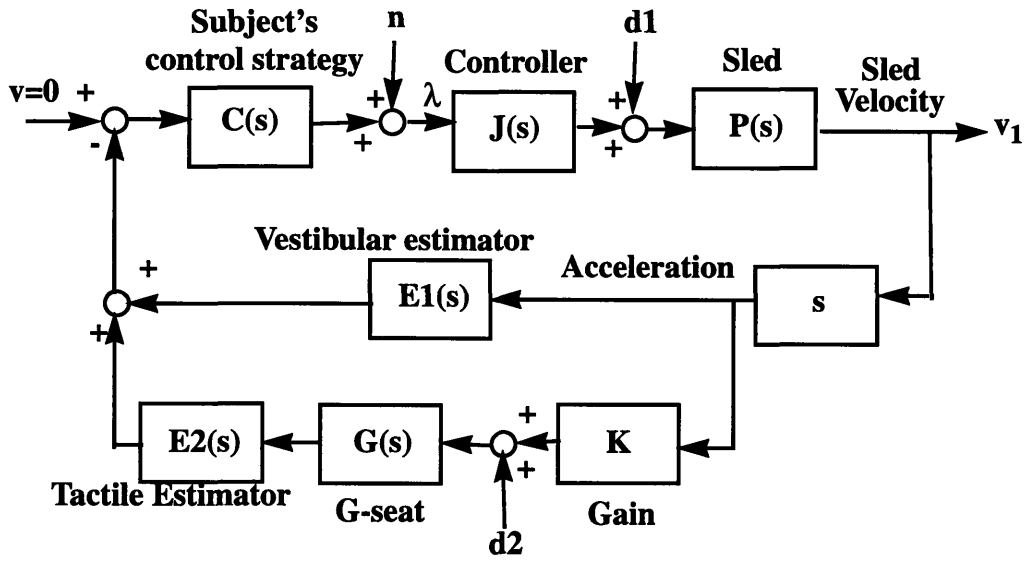

Figure 5.1: G-seat on block diagram

Using the block diagram in Figure 5.1, the sled velocity v_1, the subject's command signal λ, and the G-seat pressure p_g can be written in terms of the inputs: the sled velocity disturbance, d_1, the G-seat pressure disturbance, d_2, and the control remnant, n.

Define the return difference, Δ.

$$\Delta = 1 + JPCs\langle E_1 + KGE_2 \rangle$$

Write v_1, λ, and p_g in terms of the inputs and the return difference.

$$v_1 = \frac{JP}{\Delta}n + \frac{P}{\Delta}d_1 + \frac{GE_2CJP}{\Delta}d_2$$

$$\lambda = \frac{1}{\Delta}n + \frac{Ps(E_1 + KGE_2)C}{\Delta}d_1 + \frac{E_2C}{\Delta}d_2$$

$$p_g = \frac{JPsKG}{\Delta}n + \frac{PsKG}{\Delta}d_1 + \frac{1}{\Delta}d_2$$

The cross spectral densities of outputs v_1, λ, and p_g to inputs d_1 and d_2 can be expressed as functions of the power spectral densities and cross spectral densities of the inputs.

$$\Phi_{v_1 d_1} = \frac{JP}{\Delta}\Phi_{nd_1} + \frac{P}{\Delta}\Phi_{d_1 d_1} + \frac{GE_2CJP}{\Delta}\Phi_{d_2 d_1}$$

$$\Phi_{\lambda d_1} = \frac{1}{\Delta}\Phi_{nd_1} + \frac{Ps(E_1 + KGE_2)C}{\Delta}\Phi_{d_1 d_1} + \frac{E_2C}{\Delta}\Phi_{d_2 d_1}$$

$$\Phi_{pgd_2} = \frac{JPsKG}{\Delta}\Phi_{nd_2} + \frac{PsKG}{\Delta}\Phi_{d_1d_2} + \frac{1}{\Delta}\Phi_{d_2d_2}$$

$$\Phi_{\lambda d_2} = \frac{1}{\Delta}\Phi_{nd_2} + \frac{Ps(E_1 + KGE_2)C}{\Delta}\Phi_{d_1d_2} + \frac{E_2C}{\Delta}\Phi_{d_2d_2}$$

The disturbances d_1, and d_2 are mutually uncorrelated, and the control remnant, n, is, by definition, uncorrelated with the inputs. Therefore,

$$\Phi_{d_1d_2} = \Phi_{nd_1} = \Phi_{nd_2} = 0$$

The cross spectral density relationships thus simplify to

$$\Phi_{v_1d_1} = \frac{P}{\Delta}\Phi_{d_1d_1}$$

$$\Phi_{\lambda d_1} = \frac{Ps(E_1 + KGE_2)C}{\Delta}\Phi_{d_1d_1}$$

$$\Phi_{pgd_2} = \frac{1}{\Delta}\Phi_{d_2d_2}$$

$$\Phi_{\lambda d_2} = \frac{E_2C}{\Delta}\Phi_{d_2d_2}$$

Using these expressions for the cross-spectral densities, the following ratios can be calculated.

$$a_1 = \frac{\Phi_{\lambda d_1}}{\Phi_{v_1d_1}} = s(E_1C + KGE_2C)$$

$$a_2 = \frac{\Phi_{\lambda d_2}}{\Phi_{p_gd_2}} = E_2C$$

The cross-spectral densities, $\Phi_{\lambda d1}$, $\Phi_{\lambda d2}$, Φ_{v1d1}, and $\Phi_{pgd1,}$are computed from the recorded velocity, G-seat pressure, and subject's command signal. Since the ratios a_1 and a_2 are known, the two previous two equations can be solved for E_1c and E_2c, resulting in the following expressions for E_1c and E_2c.

$$E_1C = \frac{1}{s}a_1 - KGa_2$$

$$E_2C = a_2$$

A different set of equations relates the cross-spectral densities and the transfer functions for the experiment trials with the G-seat off. Figure 5.2 shows the block diagram for the G-seat off condition.

In order to assess the magnitude of the subject's computed response at the G-seat disturbance frequencies for G-seat off trials, a transfer function was calculated from nominal G-seat command to subject command input. This transfer function serves only as an indication of manual control remnant, measurement noise and numerical error, and is used as a basis for determining whether the computed tactile transfer function for the G-seat on condition is distinguishable from measurement noise (See Section 5.4). The transfer function was calculated by substituting pre-recorded pressure data for the actual G-seat pressure data and computing power spectral densities and cross-spectral densities using the pre-recorded pressure data.

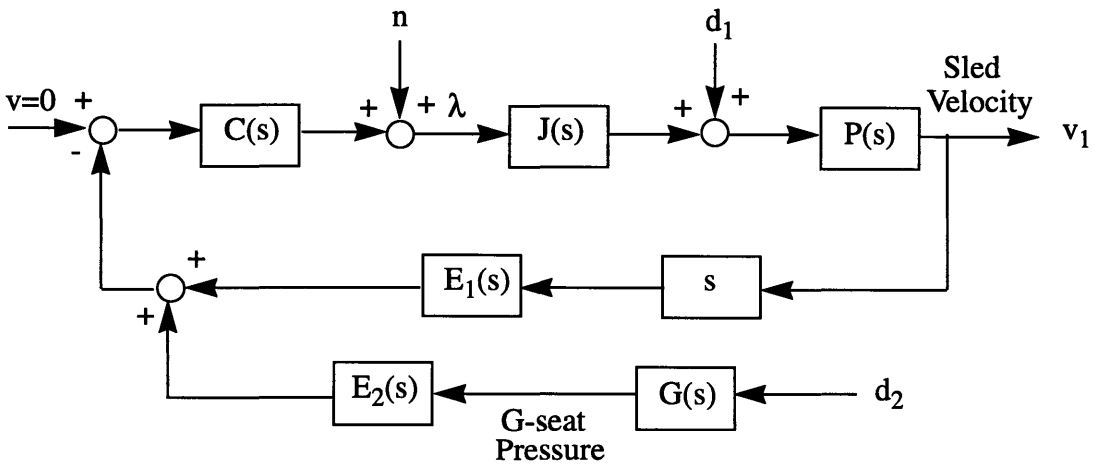

Figure 5.2: G-seat off block diagram

As in the G-seat on case, the relationships between the outputs v_1 and λ and the disturbances d_1 and d_2 can be written based on the block diagram.

$$\Delta = 1 + JPCsE_1$$

$$v_1 = \frac{JP}{\Delta}n + \frac{P}{\Delta}d_1 + \frac{E_2CJP}{\Delta}d_2$$

$$\lambda = \frac{1}{\Delta}n + \frac{PsE_1C}{\Delta}d_1 + \frac{E_2C}{\Delta}d_2$$

The cross spectral densities of outputs to inputs can be written as before, with the cross spectral densities of uncorrelated signals equal to zero.

$$\Phi_{v_1 d_1} = \frac{P}{\Delta}\Phi_{d_1 d_1}$$

$$\Phi_{\lambda d_1} = \frac{PsE_1C}{\Delta}\Phi_{d_1 d_1}$$

$$\Phi_{\lambda d_2} = \frac{E_2C}{\Delta}\Phi_{d_2 d_2}$$

The cross-spectral density ratios a_1 and a_2 are calculated, from the recorded sled velocity, G-seat pressure, and subject's command input.

$$a_1 = \frac{\Phi_{\lambda d_1}}{\Phi_{v_1 d_1}} = sE_1C$$

$$a_2 = \frac{\Phi_{\lambda d_2}}{\Phi_{p_g d_2}} = \frac{E_2C}{\Delta}$$

The vestibular and tactile transfer functions E_1C and E_2C can be calculated in terms of the ratios a_1 and a_2. Since the tactile loop is not closed, the transfer functions are not linear combinations of the cross-spectral density ratios, as they are for the G-seat on condition. The computed tactile transfer function serves only as an indication of control remnant and instrumentation noise.

$$E_1C = \frac{1}{s}a_1$$

$$E_2C = a_2 + a_1 a_2 JP$$

The subject's control strategy transfer function, C, can be computed for trials in which the subject was able to see. Since the visual velocity estimation process is very fast compared to the frequency content of the disturbances, the value of the estimator transfer function approaches unity gain for the frequency range under consideration. Thus, for G-seat off, blindfold off trials:

$$C = \frac{1}{s}a_1$$

5.3 Transfer function calculation

Computation of E_1C, E_2C, and C was done in Matlab, using scripts which can be found in Appendix E. The script cutleadtail.m was first used to remove the portion of the data file recorded before the trial began and after it ended. For trials when the G-seat was off, the script press.m was used to substitute pre-recorded pressure data for the actual pressure data. The script loadsubt.m loaded experiment data files and data files which contained the nominal sled and G-seat commands. It then called the function findtf2.m, which computed the cross-spectral density ratios a_1 and a_2 for each block of two trials. The cross-spectral density ratios were then passed to the function solvefortft.m, which computed the transfer functions E_1C and E_2C from the cross-spectral density ratios for each block of trials with the G-seat on. Another script, nofbktf.m, computed the transfer functions for the blocks with the G-seat on. The transfer functions for each block are then plotted by the script makeplots.m. Loadsubt.m then saves a file containing the cross-spectral density ratios and transfer functions for each subject. Means of transfer functions for all subjects were computed using the scripts grandmean.m for blindfolded trials and eomean.mfor eyes open trials.

Three known transfer functions were used in calculating E_1C and E_2C. J(s) is the transfer function of the subject's controller. The controller dynamics are set in the sled control program and are implemented as a first order digital low-pass filter with a break frequency of 10 rad/sec. P(s) is the sled transfer function. For the frequency range of interest, P(s) is approximately equal to one. G(s), which is the transfer function from G-seat command to G-seat pressure, was found experimentally by Markmiller (1996).

The G-seat acceleration feedforward gain, K, was set as described in Section 3.1. The value of K used in the experiment trials was 15.

5.4 Significance of tactile transfer function magnitudes

At each of the twelve frequencies, the mean transfer function magnitude for the G-seat on condition was compared with the mean magnitude for the G-seat off condition. Satterthwaite's approximation for comparing means of data with different variances was used to assess the significance of the difference between the means. Comparisons were made for each subject and for the mean over all subjects.

The test statistic λ and the approximate number of degrees of freedom were computed as follows. The mean of the base 10 log of magnitudes for G-seat on trials is $\bar{x}$, and s_1 is the standard deviation of the base 10 log of magnitudes for G-seat on trials. The mean of the base 10 log of magnitudes for G-seat off trials is $\bar{y}$, and s_2 is the standard deviaion of the base 10 log of magnitudes for G-seat off trials. The base 10 log of all magnitudes was used in statistical calculations, because the distribution of the log magnitudes was roughly symmetrical about the mean, while the distribution of magnitudes was skewed.

$$\lambda = \frac{\bar{x} - \bar{y}}{\sqrt{\frac{s_1^2}{n_1} - \frac{s_2^2}{n_2}}}$$

$$d' = \frac{\left(\frac{s_1^2}{n_1} + \frac{s_2^2}{n_1}\right)^2}{\frac{\left(\frac{s_1^2}{n_1}\right)^2}{(n_1 - 1)} + \frac{\left(\frac{s_2^2}{n_1}\right)^2}{(n_2 - 1)}}$$

$$d'' = int(d')$$

The null hypothesis (x=y) is rejected if

$$|\lambda| > t_{d'', 95}.$$

where t is obtained from the t distribution table. (Rosner 1990)

These calculations were done in the script tmagstat.m.

5.5 Transfer function fits

The output of the frequency-domain analysis script, loadsubt.m, was the magnitude and phase of the vestibular and tactile transfer functions at the frequencies used in the disturbance profiles. Transfer functions were fitted to this frequency response data.

Examination of the frequency response data showed that the phase data was highly discontinuous, with large positive and negative phase shifts, as discussed in Section 6.1. For this reason, only magnitude data was used in the transfer function fits.

Fitting transfer functions to magnitude data presents several problems which were addressed in the analysis. First, phase data is required to distinguish non-minimum phase zeros from minimum-phase zeros, and stable poles from unstable poles. It can be safely assumed that the tactile and vestibular estimators are stable if the experimental trial was completed. Furthermore, there is no evidence to suggest that the vestibular or tactile feedback paths contain non-minimum phase zeros. Second, pre-existing Matlab functions for computing fitted transfer functions from frequency response data (tfe, invfreqs) have no option to ignore phase data. A script was written to compute fitted transfer functions from magnitude data only.

The transfer function fitting script used an iterative algorithm to find the transfer function of specified order which fits the data best in a least-squares sense. The script fitted a gain and a transfer function containing up to two poles and up to two zeros. A range of allowable stable pole and zero locations and a frequency step were specified; the script found the magnitude response of each transfer function within the range and selected as the best fit the transfer function which had the minimum squared error.

Goodness-of-fit for the transfer functions was assessed using an F-test method for multiple linear regressions. A transfer function was fit to the magnitude data, as described above, and the squared error between the transfer function fit and the data (ResSS) was

computed. The squared difference between the fitted transfer function and the mean magnitude (RegSS) was computed.

The regression mean square and the residual mean square were computed as follows, where k is equal to the number of parameters in the model and n, the number of data points, is equal to 12.

$$RegMS = \frac{ResSS}{k}$$

$$ResMS = \frac{Resss}{(n-k-1)}$$

The test statistic, λ, is the ratio of ResMS to RegMS. The null hypothesis is rejected for $\lambda > F_{k,\, n-k-1,.95}$.

Chapter 6

Results

6.1 Computed transfer functions

Transfer functions were computed for each subject in all trials according to the method described in Section 5.2. Mean transfer functions were computed for each subject for the G-seat on condition, the G-seat off condition and the eyes open condition. The mean of all subjects' transfer functions are shown in Figures 6.1-6.5. Figures 6.1 and 6.2 are the mean vestibular and tactile transfer functions for the G-seat off condition. Figures 6.3 and 6.4 are the mean vestibular and tactile transfer functions for the G-seat on condition. The computed tactile transfer function for the G-seat off condition serves as a measure of noise and manual control remnant, rather than an indication of dynamics in the tactile feedback path. Figure 6.5 is the mean transfer function from sled velocity to subject command for the eyes open condition. Mean transfer functions were computed by separately finding means of magnitudes and phases, rather than by computing the means of the real and imaginary parts of the complex transfer functions. A detailed description of transfer function calculation can be found in Section 5.2.

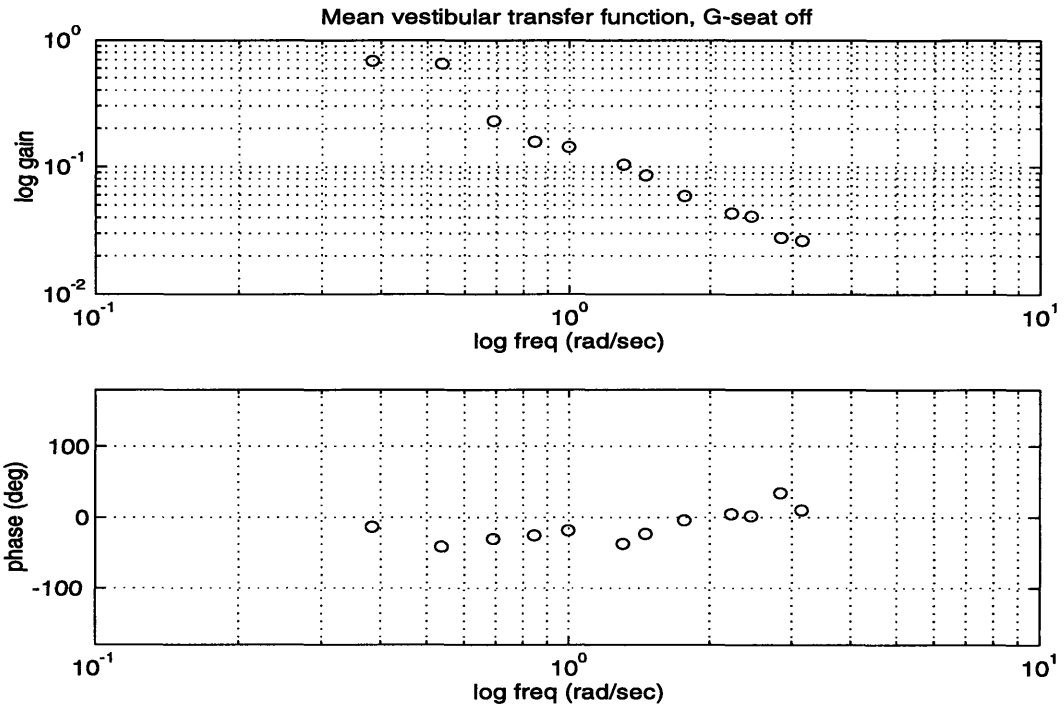

Figure 6.1: Mean vestibular transfer function, G-seat off

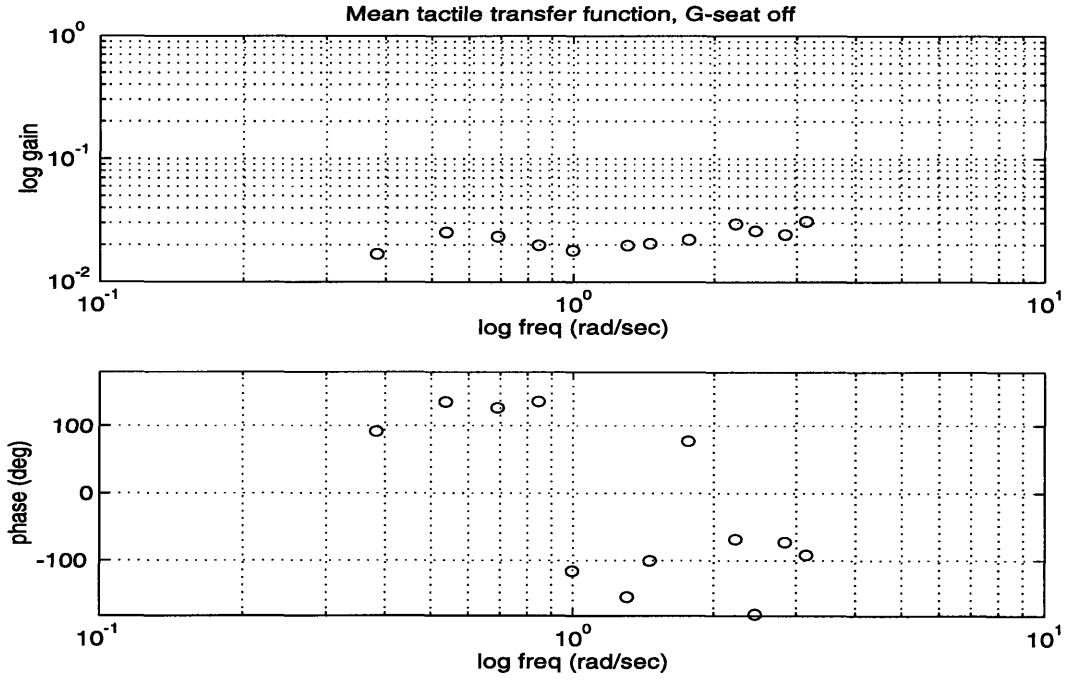

Figure 6.2: Mean tactile transfer function, G-seat off

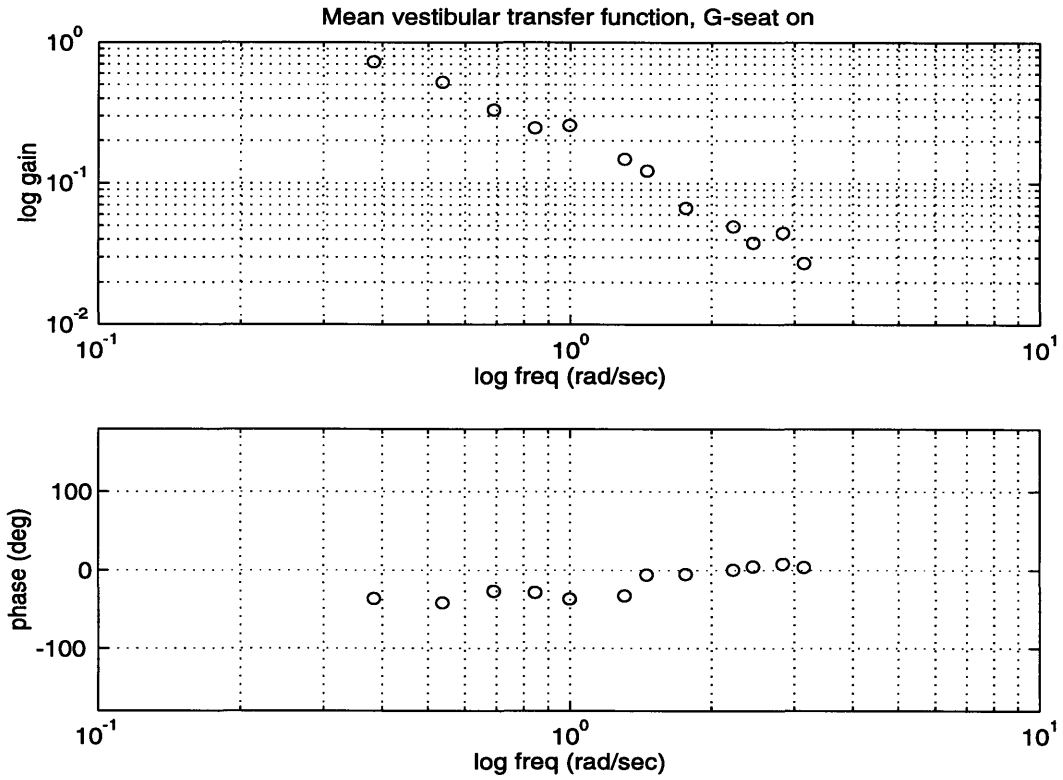

Figure 6.3: Mean vestibular transfer function, G-seat on

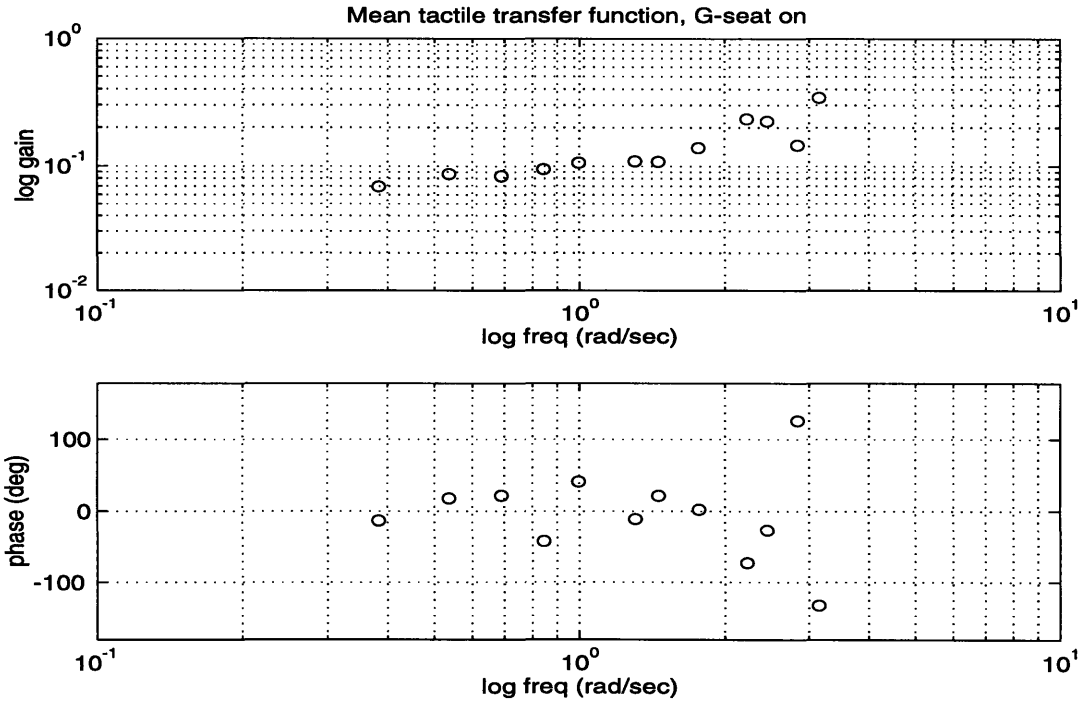

Figure 6.4: Mean tactile transfer function, G-seat on

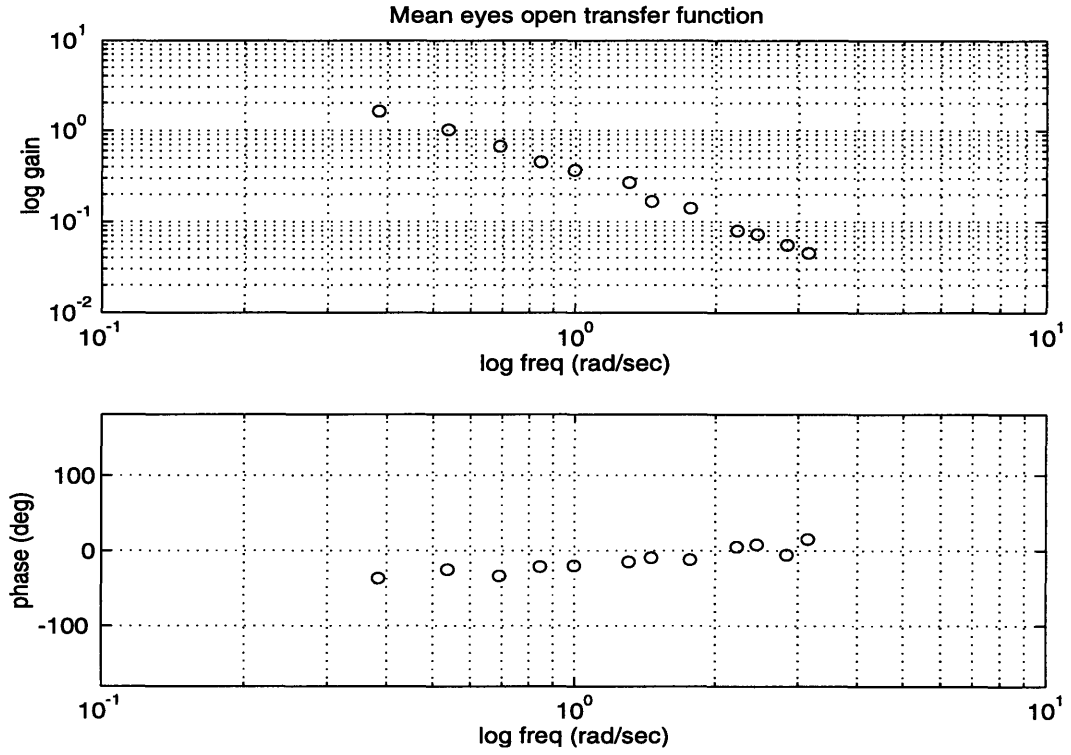

Figure 6.5: Mean transfer function, eyes open

As shown in the Figures above, discontinuities in the phase data for all of the computed transfer functions and the lack of correlation between the magnitude data and the phase data render the computed phases suspect. There are several sources of inaccuracy in the phase data, in both the subject's responses and data analysis. Nonlinearities in subjects' responses, including non-constant time delays and subjects' uncertainty in the direction of estimated velocity, prevent this system identification method from accurately calculating the phase of the subject's transfer function. Numerical artifacts also cannot be ruled out as the source of phase data inaccuracy.

The eyes-open condition was intended to provide a means of estimating the subject's control strategy transfer function. The transfer function from sled velocity to subject command is the product of the velocity estimator transfer function and the control strategy

transfer function. With the subject's eyes open in the light, a visual velocity estimator approaches unity gain, because its dynamics are much faster than the frequency range of interest. As a result, the transfer function from sled velocity to subject command should approach the subject's control strategy transfer function.

The above argument relies on the assumptions that subjects use the same control strategy for both eyes-open and eyes-closed conditions and visually estimate sled velocity in the eyes-open condition. The computed mean eyes-open transfer function in Figure 6.5, however, shows two integrations, indicating that the subjects were estimating position rather than velocity in the eyes-open trials. For this reason, the eyes-open transfer functions were not used to remove the subjects' control strategy from the tactile and vestibular estimators. Tactile and vestibular transfer functions discussed here, therefore, refer to the transfer function of the entire feedback path, including both the estimator and the subject's control strategy.

6.2 Comparison between G-seat on and off conditions

The vestibular and tactile transfer functions under the G-seat on condition were compared to the transfer functions with the G-seat off. Because there was no disturbance at the G-seat frequencies for the G-seat off trials, the G-seat off tactile transfer functions indicate manual control remnant and numerical artifacts in the computed transfer functions, rather than the dynamics of the tactile feedback path. A significantly higher tactile transfer function magnitude for the G-seat on condition than the G-seat off condition indicates that subjects did, in fact, respond to G-seat cues. Tactile transfer function magnitude comparisons were made for each subject at each frequency, as described in Section 5.4. The results of the analysis are given in Table 6.1, where asterisks indicate tactile transfer function magni-

tudes that are significantly higher with the G-seat on.

Table 6.1: Significance of tactile transfer function magnitudes

Freq(Hz)	.061	.085	.110	.134	.159	.208	.232	.281	.354	.391	.452	.500
Subject												
D	*		*	*		*	*	*	*	*	*	*
E	*	*			*	*	*	*			*	*
F	*	*	*	*	*	*	*	*	*	*	*	*
H	*	*			*		*	*	*	*		*
I	*	*	*	*	*	*	*	*	*	*	*	*
J	*			*	*	*	*	*	*	*	*	*
K						*				*		*
L	*	*	*	*	*	*	*	*	*	*	*	*

Tactile transfer function magnitudes were significantly higher with the G-seat on for 9 of the 12 frequencies in 7 of 8 subjects. The larger number of non-significant tactile transfer function magnitudes for subject K can be accounted for by the loss of data files for one block of trials. Eight of the tactile transfer function magnitudes for subject K were, however, significant at the .10 level. In no case was the G-seat off tactile transfer function magnitude significantly higher than the G-seat on tactile transfer function magnitude.

Figure 6.6 shows the mean of all subjects plus and minus one standard deviation for the tactile transfer functions under the G-seat on and off conditions. The differences in the magnitudes were significant at all frequencies.

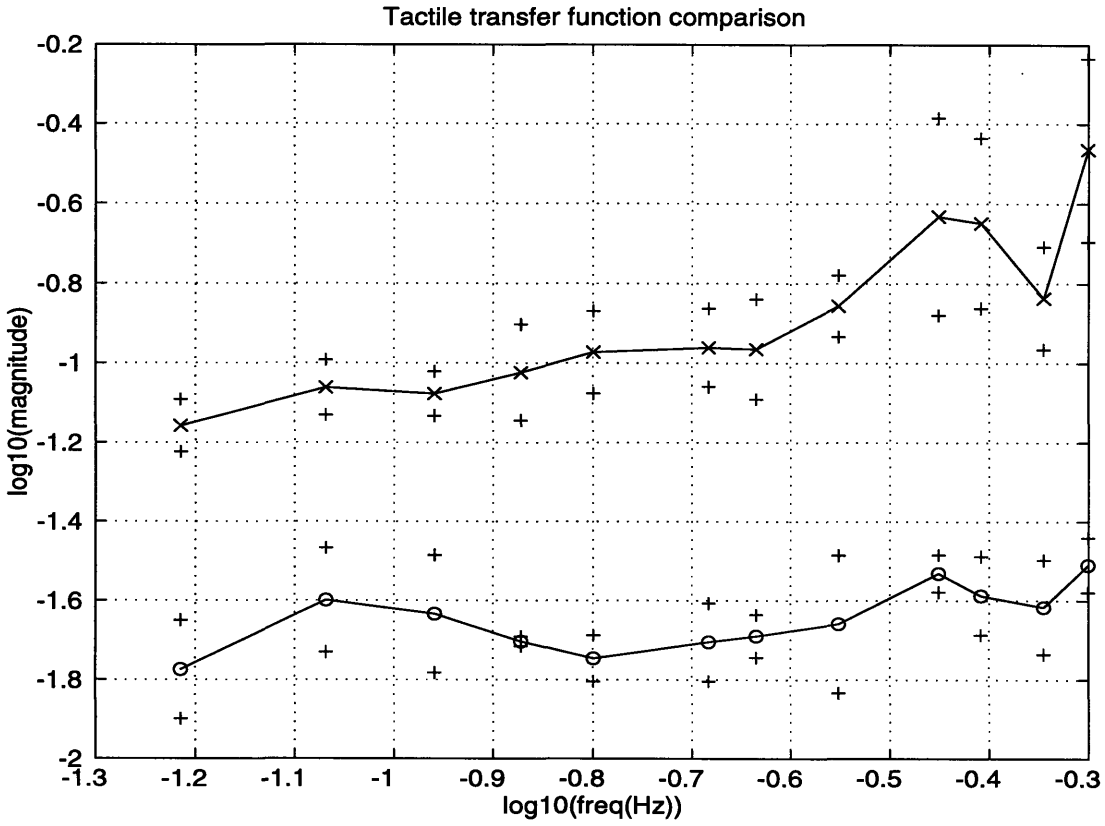

Figure 6.6: Mean over all subjects, tactile transfer function comparison. x indicates G-seat on, o indicates G-seat off, + indicates mean +/- one standard deviation.

Vestibular transfer functions for the G-seat on and off conditions were also compared. For this portion of the analysis, vestibular transfer functions were computed using the equations for the G-seat off condition. Vestibular transfer functions computed in this way were expected to indicate the sum of the true vestibular transfer function and the tactile transfer function, since sled acceleration was fed forward to the G-seat. This was expected to result in differences between the vestibular transfer functions for the G-seat on and G-seat off conditions.

For individual subjects' data, significant differences between vestibular transfer functions for the G-seat on and off conditions were found in only 7 of the 72 comparisons. Significant differences were found, however, in the mean vestibular transfer functions. Figure 6.7 shows the mean plus and minus one standard deviation for all subjects of the vestibular transfer functions for the G-seat on and G-seat off conditions. Ten of the twelve magnitude differences were significant, with the G-seat on vestibular transfer function magnitude significantly higher at 8 frequencies and significantly lower at 2 frequencies.

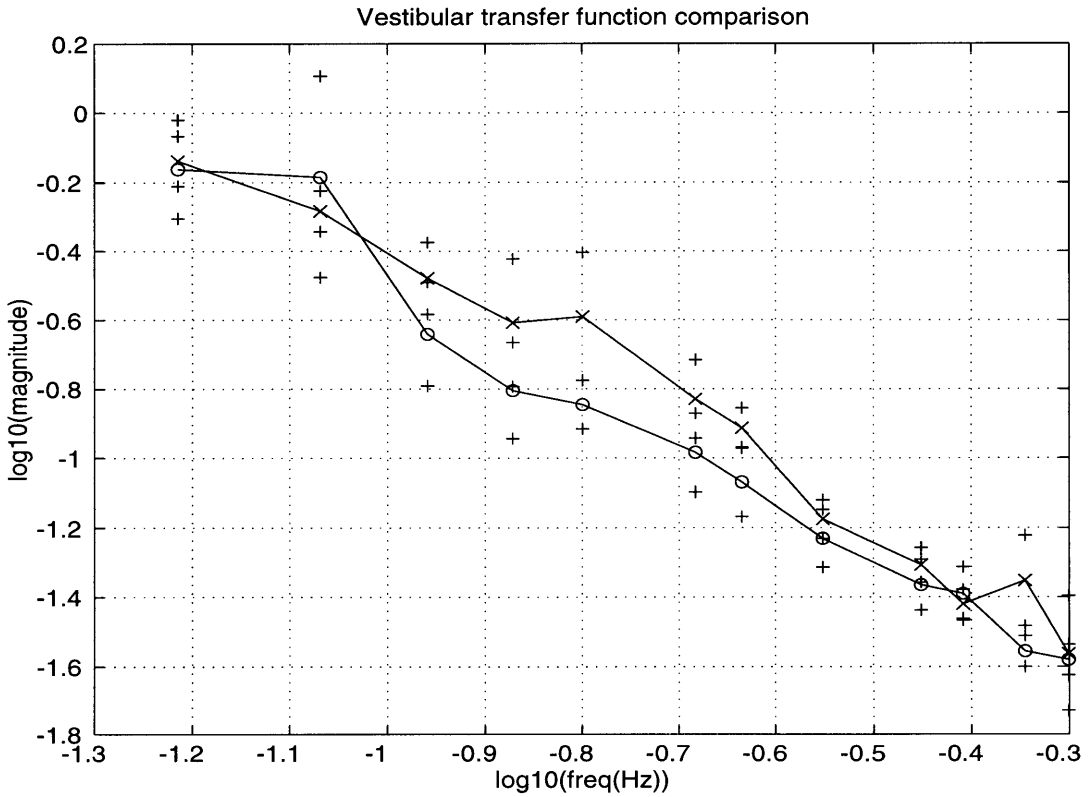

Figure 6.7: Mean over all subjects, vestibular transfer function comparison. x indicates G-seat on, o indicates G-seat off, + indicates +/- one standard deviation.

6.3 Fitted transfer functions

Transfer functions were fitted to the vestibular and tactile frequency responses. Since the phase data were considered unreliable, only magnitude data were used to compute the fitted transfer functions. The transfer function fitting method and goodness-of fit measures

are described in Sections 5.5 and 5.6.

Transfer functions were fitted to the tactile magnitudes for the G-seat on condition only. Four of the eight subjects' tactile magnitudes were significantly fit by a transfer function which had one zero and no poles in the frequency range of the disturbances used in the experiment. The other four subjects' tactile responses showed higher magnitudes at higher frequencies, but a transfer function that significantly fit this data could not be found. The mean of tactile magnitudes over all subjects was significantly fit by a one zero, no poles transfer function. Bode plots of the fitted transfer functions are shown in Figure 6.8 for the mean of the four subjects with lead transfer functions. Figure 6.9 shows the mean tactile transfer function for the other four subjects, and Figure 6.10 shows the data and fitted transfer function for the mean over all subjects.

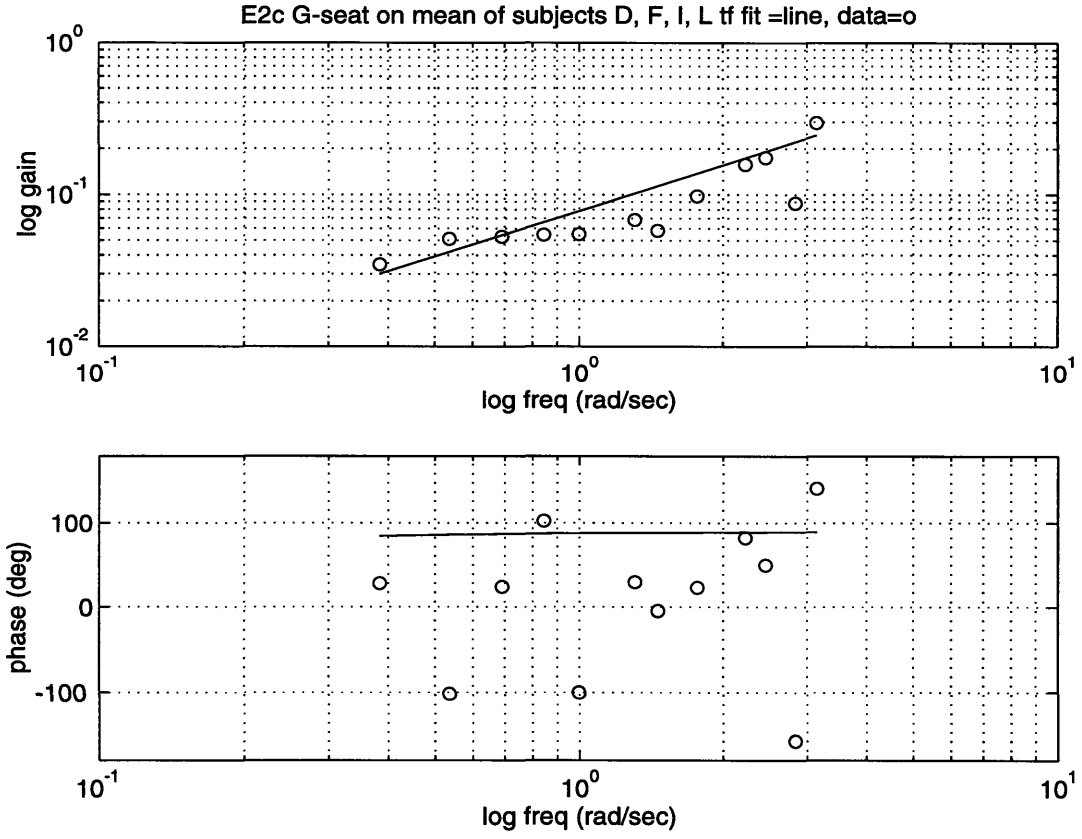

Figure 6.8: Tactile transfer function mean for subjects D, F, I, and L

$$E_2C(s) = 0.0782(s + 0.0375)$$

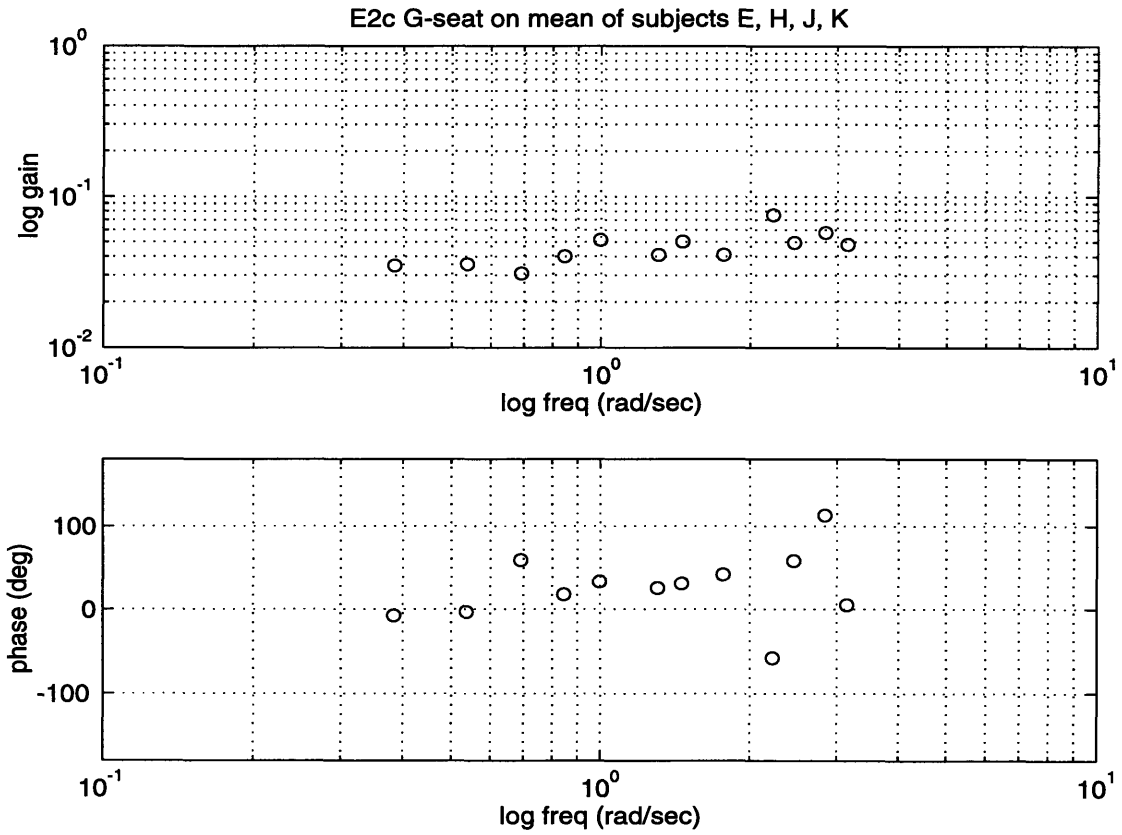

Figure 6.9: Tactile transfer function mean for subjects E, H, J, and K

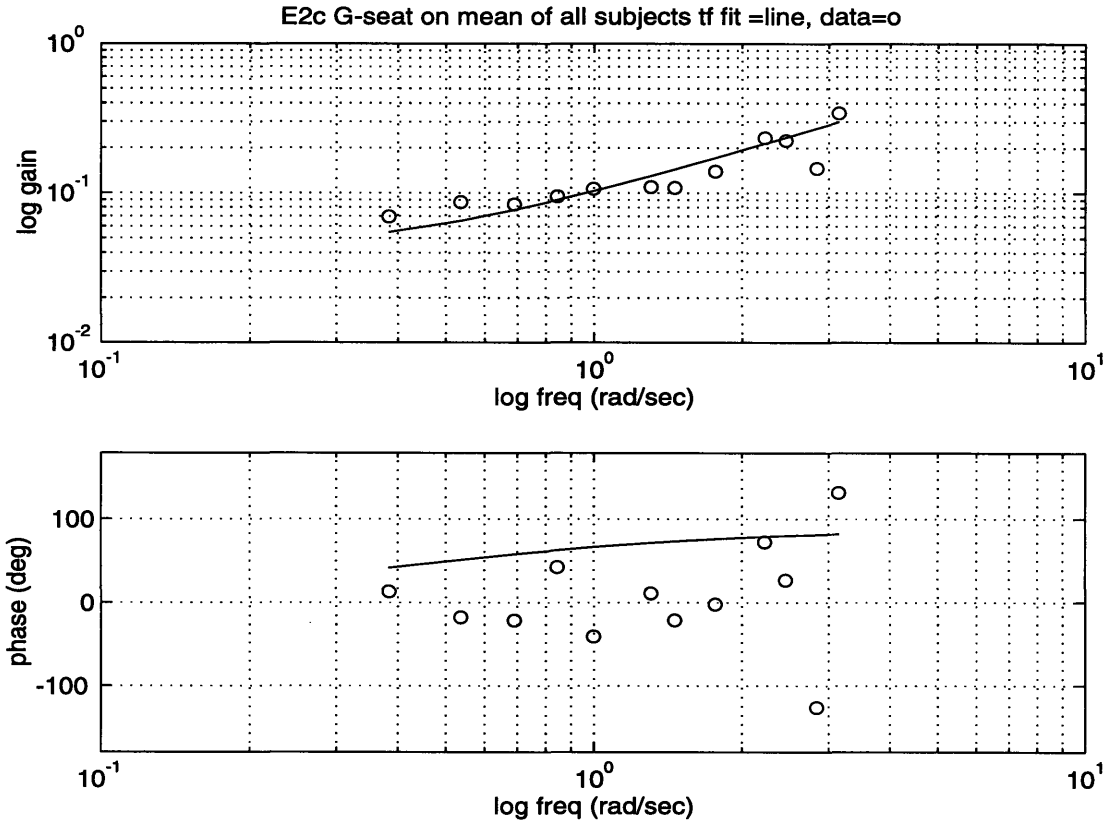

Figure 6.10: Tactile transfer function mean over all subjects

$$E_2C(s) = 0.0945(s + 0.435)$$

The fitted transfer functions for subjects D, F, I, and L have one zero which is either at or below the lowest frequency data point. Since the break frequency for the zero is not within the frequency range of the data, the fitted transfer function should be considered to be a differentiator over the frequency range of interest. It also should be noted that the zero frequency and the gain are not independent; for a selected gain, there is one zero frequency which will result in a transfer function that fits the magnitude data.

Transfer functions were fitted to the computed vestibular transfer function for both the G-seat on and G-seat off conditions. Only magnitude data was used for transfer function fitting. Figure 6.10 shows the fitted vestibular transfer function for the G-seat on condition, and Figure 6.11 shows the fitted vestibular transfer function for the G-seat off condi-

tion. Both transfer functions have two poles which are near or below the lowest disturbance frequency, so they should be regarded as double integrators over the frequency range of the experiment. As with the fitted tactile transfer functions, the gains of the fitted vestibular transfer functions are not independent of the pole frequencies.

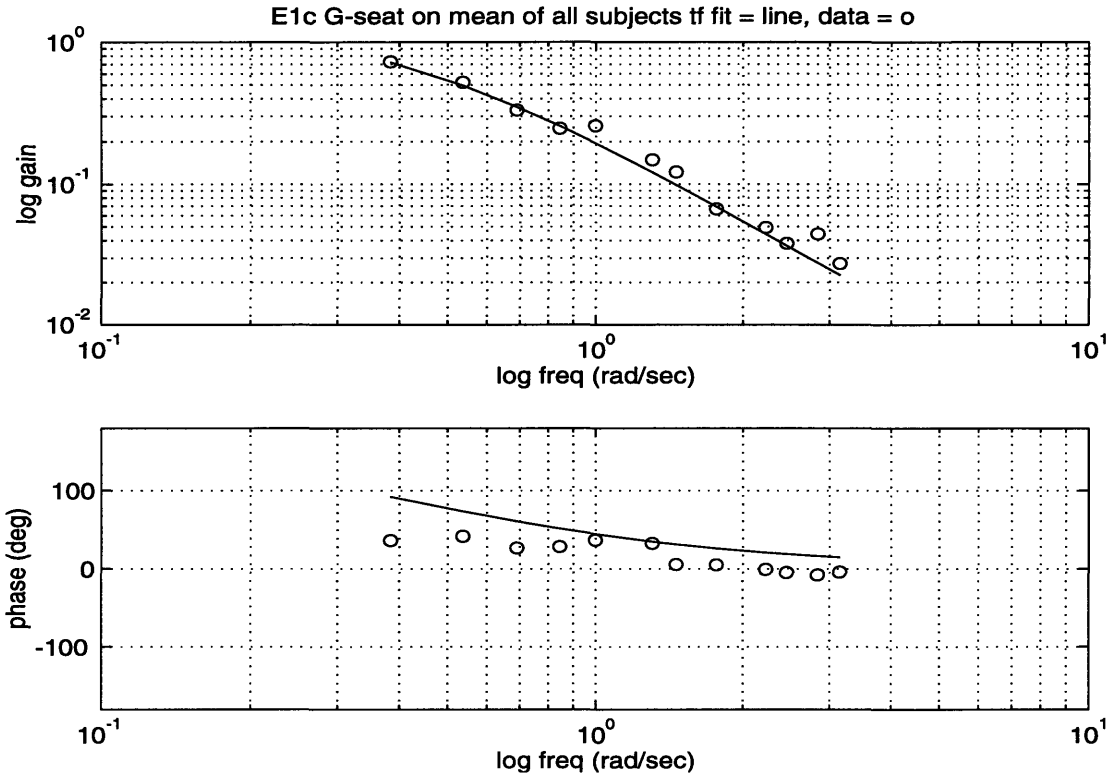

Figure 6.11: Fitted vestibular transfer function, G-seat on

$$E_1C = \frac{-0.2272}{(s+0.56)(s+0.21)}$$

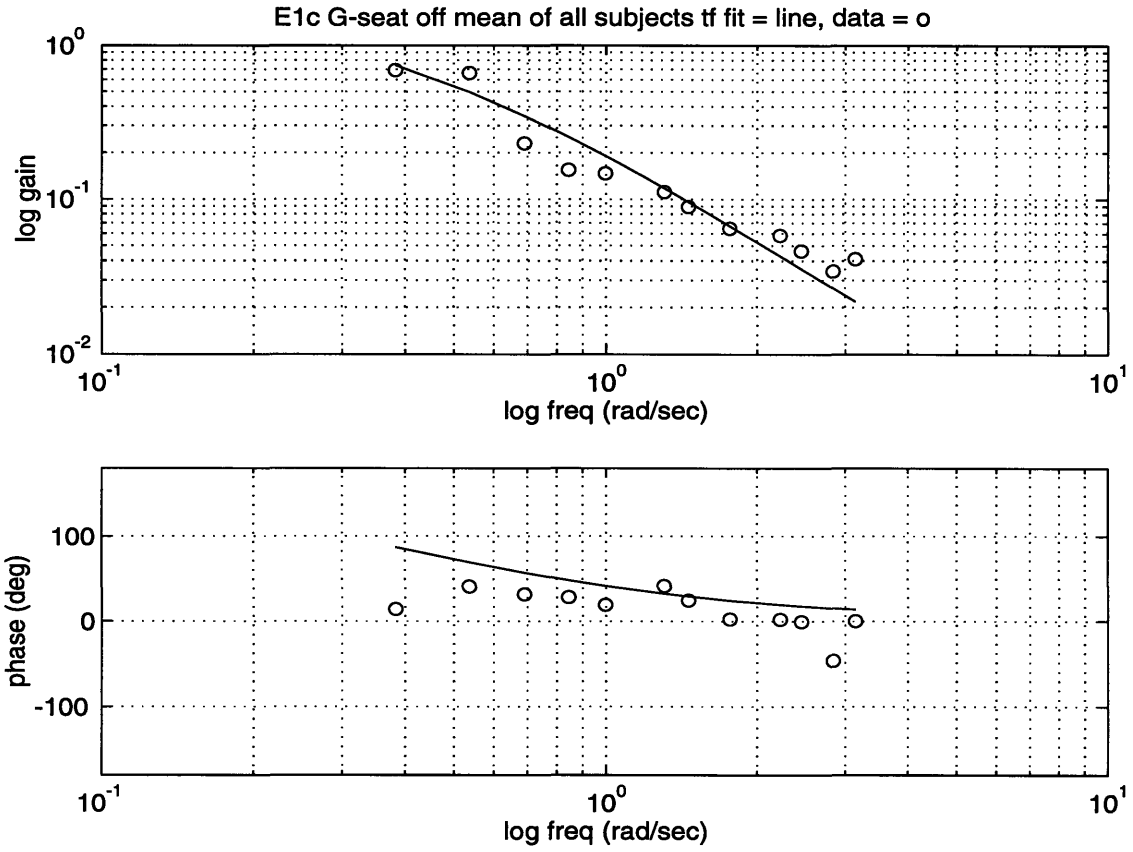

Figure 6.12: Fitted vestibular transfer function, G-seat off

$$E_1C = \frac{-0.2272}{(s+0.46)(s+0.31)}$$

Chapter 7

Discussion

7.1 Influence of G-seat on motion perception

The comparison between the tactile channel transfer function for the G-seat on condition and the computed tactile transfer function for the G-seat off condition clearly shows a subject command response to G-seat pressure. Determining whether the G-seat had a significant effect on motion perception was necessary because there was no assurance based on previous experimental work that subjects would have a measurable response to the G-seat in its present configuration on the MIT sled.

Although the ALCOGS G-seat has been shown to produce illusory tilt (Snell, Flach, McMillan 1985), and the pneumatic G-seat has been demonstrated to improve pilot performance in simulation tasks, (Ashworth, McKissick, Parrish 1984), the effect of the pneumatic seat on motion perception has not previously been demonstrated outside of a flight simulation environment. In addition, the G-seat was used in a horizontal, rather than its usual vertical, configuration, which changes the dynamics of the body-seat interaction. The subject's body position in the sled chair and other tactile cues due to the harness, headrest and footrest are also different from those found in a flight simulator. Furthermore, it was not known whether the data acquisition and analysis methods would be able to distinguish responses to the G-seat from manual control remnant and measurement noise.

Significant differences between the tactile channel transfer functions for the G-seat on and off conditions indicate that there was, in fact, a measurable subject command response to G-seat pressure.

7.2 Tactile transfer function

The computed tactile transfer functions had zeros near or below the lowest disturbance

frequency. For the frequency region tested, the mean tactile transfer function, which was calculated from pressure input to commanded velocity output, was

$$E_2C(s) = \frac{Velocity\left(\frac{m}{s}\right)}{Pressure(psi)} = 0.10s.$$

The above transfer function from pressure to velocity command includes sensor dynamics, the estimator, and the subject's control strategy. The units of velocity are meters per second (m/s) and the units of pressure are pounds per square inch (psi).

The differentiator in the tactile transfer function indicates that subjects react to the time rate of change of G-seat pressure, rather than the static pressure value. This finding supports the role of G-seat tactile cueing in indicating onset of acceleration. Neglecting the elastic behavior of the seat, the G-seat pressure is equal to the force exerted by the subject's body on the seat divided by the area of contact between the subject and the seat. The inertial force exerted by the subject's body on the seat is the product of the subject's mass and the sled acceleration. Therefore, seat pressure would be correctly interpreted as being proportional to sled acceleration. However, the computed tactile transfer functions indicate that subjects respond to pressure rate, which is proportional to the rate of change of acceleration.

Based on the results of previous research on tactile receptors, the kinematics of velocity estimation from acceleration measurements, and characteristics of the data collected in this experiment, several estimation and control schemes could account for these results. (Relevant previous research on tactile receptors is presented in Chapter 2.)

Research on tactile receptors indicates that the adequate stimulus for cutaneous tactile receptors is the sum of skin displacement and skin displacement rate, rather than static displacement. (Burgess and Perl 1973) Because of this property of tactile receptors, it is likely that important tactile sensor dynamics are included in the computed transfer func-

tion from pressure to command output. Kinematics also indicates that since tactile stimulation caused by motion must be a function of acceleration, there should be one integrator in the estimator if velocity is the estimated quantity. However, because of the limited frequency range of this experiment and the lack of phase data, it is possible that poles and zeros of the estimator and control strategy transfer functions can cancel each other and thus be unobservable from the recorded data.

The following three control and estimation schemes could account for the observed results.

1. The dominant receptor dynamics are a low frequency zero, which appears as a differentiator in the frequency range studied, while the estimator and control strategy have no observable poles or zeros within this frequency range. Figure 7.1 shows the block diagram for this scheme. The sensor dynamics in scheme 1 agree best with previous research, while the limited frequency range of the experiment allows estimator and control strategy dynamics to be unobservable.

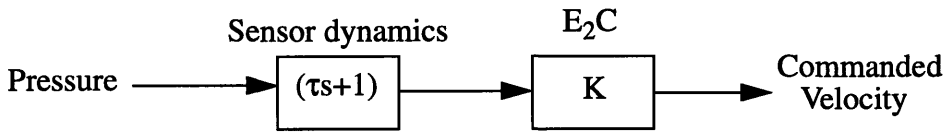

Figure 7.1: Block diagram for scheme 1.

2. The receptor dynamics include two differentiators, and the control strategy contains an integrator to convert acceleration to estimated velocity. Figure 7.2 shows the block diagram for scheme 2. The integration in E_2C agrees with the kinematics of velocity estimation from acceleration measurements, but the double differentiator in the sensor dynamics does not correspond with models of tactile receptors.

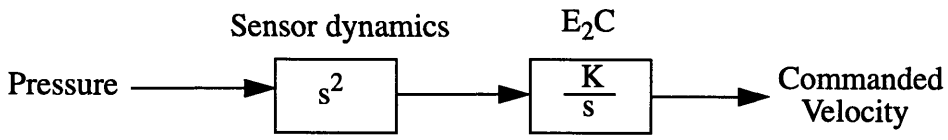

Figure 7.2: Block diagram for scheme 2.

3. There are no poles or zeros of the tactile receptors in the frequency region studied. Pressure is detected by the receptors and the differentiator is included in the estimator or control strategy. Figure 7.3 shows the block diagram for scheme 3. Since cutaneous receptors do not sense pure position, this scheme is unlikely.(Burgess and Perl, 1973)

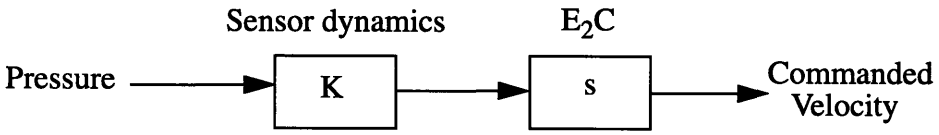

Figure 7.3: Block diagram for scheme 3.

All three of these schemes are equivalent from an input-output point of view and cannot be distinguished without further experiments to both find the subject's control strategy transfer function and a lumped-parameter model of the relationship between G-seat pressure and tactile sensation. However, the sensor dynamics of scheme 1 seem to be the most consistent with research on tactile receptors, while the limited frequency range of study could explain the lack of other observed estimator and control strategy poles or zeros.

Although the mean over all subjects of the tactile transfer function indicated magnitudes characteristic of a differentiator, differences between individual subjects' tactile transfer functions were seen. Four of the subjects (D, F, I, and L) had tactile transfer functions that were well fit by a differentiator, while the remaining four had tactile transfer functions that were not well fit by a differentiator. Figure 6.9 shows the mean tactile trans-

fer function for subjects E, H, J, and K. It should be noted that high frequency magnitudes for subjects E, H, J, and K were higher than low frequency magnitudes, although the large scatter in the data points prevents a significant transfer function fit.

No correlation between the two subject groups and values of root mean square sled velocity or root mean square control signal was seen. Subjects E, H, J, and K did have more frequencies at which tactile magnitudes were not significant. This comparison was somewhat obscured, however, by the loss of some data for subject K, which resulted in many more non-significant tactile magnitudes for subject K than for any other subject.

7.3 Vestibular transfer function

Another interesting result was that vestibular transfer functions changed only slightly when G-seat cueing was present at the sled stimulus frequencies. The fact that there were increases in the vestibular transfer function magnitudes, particularly at the higher frequencies, when the G-seat was on, supports the conclusion that the G-seat did affect motion perception. However, the increase in magnitude was not as large as that which would be predicted by a linear, time-invariant estimation process. The implication is that, while the linear estimator model is a useful tool in understanding the motion estimation process for a specified set of conditions, the real estimation process is more complex, with important contributions due to nonlinear elements such as the acceleration detection threshold and time varying processes, such as changes in control strategy due to learning.

7.4 G-seat drive algorithm

The observed effect of G-seat cuing on motion perception supports the use of the G-seat to provide linear motion cues in flight simulation, while the computed tactile transfer functions provide a basis for G-seat drive algorithms.

The computed tactile transfer functions lead to the following drive algorithm, where P is the G-seat pressure, a is the acceleration of the simulated aircraft, positive upwards (towards the head), and K is a constant.

$$P = P_{bias} + Ka$$

The bias pressure, P_{bias}, must be set so that the pilot does not come into contact with the hard seat base, in order for the pressure-firmness relationship to remain valid. The differentiation in the tactile transfer function indicates that subjects only respond to changes in the G-seat pressure, not its static bias value.

The polarity of the pressure-acceleration relation is based on the computed tactile transfer function phases. The mean tactile transfer function phases are scattered over an interval of -100 degrees to +100 degrees, indicating that the control response is roughly in phase with G-seat pressure. Together with the sign conventions of the pressure and subject command signals, the phase of the tactile transfer functions indicate that an increase in G-seat pressure corresponds to illusory headward motion.

The pressure-acceleration relation given above results in seat firmness characteristics that correspond with realistic body-seat dynamics, while changes in the G-seat height with acceleration are in the opposite direction of real seat displacement under acceleration. Since the subjects in this experiment were blindfolded and not able to see changes in the seat height, this apparent conflict did not play a role in subjects' responses. The seat height-firmness conflict would seriously diminish the effectiveness of the G-seat when subjects can observe changes in seat height by detecting shifts in eyepoint position with respect to the interior of the simulator cockpit.

7.5 Pneumatic G-seat in flight simulation

One possible application of a pneumatic G-seat in flight simulation could provide z-axis acceleration cues while avoiding a major weakness of the pneumatic G-seat.

An important shortcoming of pneumatic G-seats such as the Langley G-seat used in this experiment is that seat firmness and seat height cannot be independently controlled. This can cause inconsistencies between seat firmness cues and position cues, such as eye-point position relative to the cockpit instruments. For example, upward acceleration of the simulated aircraft should result in lowering of the eye position and an increase in firmness of the seat, while downward acceleration should result in raising of the eye position and a decrease in firmness of the seat. However, a pneumatic seat cushion is very firm at minimum height, when the pressure is very low and the pilot's weight is supported by the rigid seat base, it decreases in firmness as the pressure and height increase and the cushion begins to bear weight, and firmness increases again as the cushion reaches maximum pressure and height. The non-monotonic relationship between firmness and height can lead to inconsistencies in motion cues when the subject is able to detect both changes in seat height and seat firmness. The ALCOGS G-seat design addressed this problem by using hydraulic actuators to raise and lower sections of the seat pan and pneumatic bladders to control seat firmness. (Krohn and Kleinwaks, 1978)

An interesting possible application of the Langley G-seat in flight simulation is in a fixed-base flight simulation in which the visual scene, including both the out-the-window view and the cockpit instruments, is provided in a helmet-mounted display. Linear z-axis acceleration cues can be generated using both the helmet-mounted display and the G-seat. Shifts in eyepoint position can be provided in the visual display, while the associated changes in seat firmness can be provided with the G-seat. This configuration avoids the seat height-firmness conflict which is associated with pneumatic G-seats and could pro-

vide a significant increase in the realism of fixed-base simulation using a relatively simple, low cost mechanical system.

Chapter 8

Conclusions and Recommendations for Future Work

8.1 Conclusions

A great deal of research has been conducted to quantify the contributions of the visual and vestibular systems to motion perception. Tactile cueing also plays a significant role in motion perception, as shown by the successful use of G-seats for tactile stimulation in flight simulation.(Snell, Flach, and McMillan, 1985) However, tactile cueing of motion has been mentioned in only one of the current overall models of spatial orientation.(Borah, Young and Curry, 1978) This study was intended to assess the contribution of tactile stimulation to motion perception under experimental conditions and to quantify its contribution in the frequency domain, so that tactile cueing may be incorporated into an overall model of human spatial orientation.

This study came to the following conclusions.

1. With the G-seat in a horizontal orientation on the sled, G-seat cues did have an effect on motion perception.

2. The transfer function from G-seat pressure disturbance to the subject's commanded velocity has characteristics of a differentiator for the frequency range tested (.05 Hz-.5 Hz). This transfer function includes sensor dynamics, the estimator transfer function, and the subject's control strategy transfer function.

3. Smaller than expected increases in the magnitude of the transfer function from sled acceleration to the subject's commanded velocity, when the G-seat was on, indicated that the velocity estimation process is not simply a sum of contributions from linear, time invariant tactile and vestibular estimators. Rather, the estimation process has important

contributions from non-linear and time-varying elements, such as the acceleration detection threshold and changes in the subject's control strategy due to learning.

8.2 Recommendations for Future Work

Future experimental work can provide information that will allow components of the tactile transfer function to be separated. One possible area of investigation is to do an experiment similar to this work, using a larger frequency range. A wider range of disturbance frequencies may reveal interesting features of the estimation and control transfer functions.

Another area of possible work is the development of a large-scale model of cutaneous tactile receptors. The majority of existing experimental data on tactile receptors deals with recording from single units. A large-scale model of tactile sensation would be useful in the development of improved methods of tactile cueing of motion, and could uncover interesting spatial properties of tactile sensation, like those found in other receptors, such as retinal photoreceptors.

The data obtained in this work could be used to develop and validate a model of the tactile and vestibular estimation process at near-threshold acceleration levels, which may be relevant to pilots' awareness of aircraft altitude changes. One possible model is based on signal detection theory, and the observation that subjects in this experiment tended to make discrete control responses. In this probabilistic estimation and control model, discrete control responses would be generated with a probability of occurrence that is a function of acceleration and the rate of change of G-seat pressure. If validated, the model could be used to make predictions about pilots' responses to near-threshold accelerations.

Chapter 9

References

Ashworth, B. "A Seat Cushion to Provide Realistic Acceleration Cues for Aircraft Simulators," NASA TM X-73954, 1976

Ashworth, B., McKissick, B., Parrish, R., "Effects of Motion Base and g-Seat Cueing on Simulator Pilot Performance," NASA TP2247. March 1984.

Borah, J., Young, L.R., and Curry, R.E. "Sensory Mechanism Modeling", AFHRL-TR-78-83, Wright-Patterson AFB, Ohio: Advanced Systems Division, Air Force Human Resources Laboratory, 1978.

Burgess, P. R. and Perl, E. R. "Cutaneous Mechanoreceptors and Nociceptors" in *Handbook of Sensory Physiology Vol. II: Somatosensory System.* edited by A. Iggo, Springer-Verlag, Berlin, 1973.

Chapanis, A., *Research Techniques in Human Engineering.* Johns Hopkins Press, Baltimore, 1965,

Fernandez, C., and Goldberg, J., "Physiology of Peripheral Neurons Innervating Otolith Organs of the Squirrel Monkey. I. Response to Static Tilts and to Long-Duration Centrifugal Acceleration," Journal of Neurophysiology, 39:970-1008, 1976.

Flach, J., Riccio, G., McMillan, G., Warren, R. "Psychophysical Methods for Equating Performance Between Alternative Motion Simulators," *Ergonomics* Vol. 29, no 11, pp. 1423-1438, 1986.

Hiltner, D. *A Closed-Loop Otolith Assessment Procedure.* S.M. Thesis, Massachusetts Institute of Technology, 1983.

Kron, G.J., "G seat, G suit and Shaker Simulation." Flight Simulation Short Course, University of Dayton, March 11-14, 1980.

Kron, G.J. and Kleinwaks, J. M. "Development of the Advanced G Cuing System." AIAA 78-1572., 1978.

Levison, W., McMillan, G., Martin, E. "Models for the Effects of G-Seat Cuing on Roll-Axis Tracking Performance." *Proceedings of the 20th Annual Conference on Manual Control.* June, 1984

Loewenstein, W. R., "Mechano-electric Transduction in the Pacinian Corpuscle, Initiation of Sensory Impulses in Mechanoreceptors," *Handbook of Sensory Physiology, Vol. 1: Principles of Receptor Physiology*, edited by W.R. Loewenstein, Springer-Verlag, Berlin, 1971.

Looft, F. J. and Baltensperger, C.M. "Linear Systems Analysis of Cutaneous Type I Mechanoreceptors. *IEEE Transactions on Biomedical Engineering.* Vol. 37, No. 6, June, 1990.

Markmiller, M. *Sensory Interaction in Human Perception of Motion.* S.M. Thesis,

Massachusetts Institute of Technology, 1996

Martin, E., Osgood, R., McMillan, G. "The Dynamic Seat as an Onset Cuing Device," AIAA 87-2438-CP. *AIAA Flight Simulation Technologies Conference*, Monterrey, CA, August, 1987.

Merfeld, D.M. *Spatial Orientation in the Squirrel Monkey: An Experimental and Theoretical Investigation.* Ph.D. Thesis, Massachusetts Institute of Technology, 1990.

Oman, C, "A Heuristic Mathematical Model for the Dynamics of Sensory Conflict and Motion Sickness", *Acta Otolaryngologica* Supplement 392, 1982.

Pommelet, P. *Suboptimal Estimator for the Spatial Orientation of a Pilot.* S.M. Thesis, Massachusetts Institute of Technology, 1990.

Rolfe, J. M. and Staples, K. J., *Flight Simulation.* Cambridge University Press, Cambridge, 1986.

Rosner, B. *Fundamentals of Biostatistics,* 2nd Edition. PWS Publications, Boston, 1986.

Snell, M., Flach, J., McMillan, G,. Warren, R. "Tactual Cuing Can Produce Better Performance than Visual Cuing," *Proceedings of the Third Symposium on Aviation Psychology*, Columbus, OH, Ohio State University 1985.

Zacharias, G. *Motion Sensation Dependence on Visual and Vestibular Cues*, Ph.D. Thesis, MIT, 1977

Appendix A

Consent Form and Subject Instructions

Informed Consent Statement

Participation in this experiment is voluntary and you are free to withdraw your consent and to discontinue participation at any time without prejudice.

You have been asked to participate in an experiment aimed at better understanding the way in which people perceive motion. The investigation focuses on the interaction between visual, vestibular (inner ear), and tactile senses. During the experiment, you will be using the following three pieces of equipment, either alone or in conjunction: the MIT Sled, G-seat, and a visual display. The experimenter will brief you on the use of these devices, and will answer any questions you may have regarding them. Throughout, you will be seated in either a supine or upright position, wearing an aircraft-style safety harness. You will also be given a hand-held controller that you will use to indicate or control your motion--the experimenter will instruct you on its function beforehand. You comfort and safety are of utmost importance, and at no point will you be asked to do anything discomforting or dangerous. As with any motion simulation, there is a small risk that you may experience symptoms of motion sickness. If you experience discomfort at any time, or have any misgivings about continuing, tell us and we will stop the experiment.

Please feel free to ask any questions you care to about the experiment.

In the unlikely event of physical injury resulting from participation in this research, I understand that medical treatment will be available from the MIT Medical Department, including first aid emergency treatment and follow-up care as needed, and that my insurance carrier may be billed for the cost of such treatment. However, no compensation can be provided for medical care beyond the foregoing. I further understand that making such medical treatment available, or providing it, does not imply that such injury is the investigator's fault. I also understand that by my participation in this study, I am not waiving any of my legal rights. (For more information, call the Institute's Insurance and Legal Affairs Office at 253-2822.) I understand that I may also contact the Chairman of the Committee on the Use of Humans as Experimental Subjects, MIT 253-6787, if I feel I have been treated unfairly as a subject.

I have been informed as to the procedures and purpose of this experiment and agree to participate.

Signed:_____

Witness:_____

Date:_____

Subject Instructions

The goal of this experiment is to measure how the sense of touch contributes to the perception of motion. We are using a G-seat, which is a seat with inflatable cushions, to provide tactile stimulation.

During the experiment, you will be seated on the sled, wearing a blindfold. The sled will be moved in a seemingly random way, while the G-seat is inflated and deflated. The sliding controller allows you to control the velocity of the sled. We would like you to judge as best you can how you are moving and move the controller to counteract the sled's motion, in order to keep the sled still. Position on the track is not important; we would like you to attempt to make the sled's velocity zero.

We will do 4 practice trials, 16 data trials with the blindfold, and 4 data trials without the blindfold.

If the sled reaches the end of the track, a brake will engage and stop the sled's motion. You also have an emergency stop button which will engage the brake and immediately stop the sled. If you would like to stop the experiment at any time, tell the operator and she can bring the sled to a more gradual stop.

Appendix B

Practice Disturbance Profiles

Frequency (Hz)	**Profile 1** sled velocity (m/s)	G-seat command (volts)	**Profile 2** sled velocity (m/s)	G-seat command (volts)
.0610	.13			3.0
.0854		3.0	.13	
.110	.12			2.8
.134		2.6	.11	
.159	.12			2.8
.208		2.6	.11	
.232	.10			2.3
.281		2.6	.11	
.354	.09			2.1
.391		1.6	.07	
452	.07			1.6
.500		1.4	.06	

Phase offset = 103 degrees.

Appendix C

Sled Checklist

Sled General Checklist
Revised February, 1997

Pre-Experiment

1. Power on

1.1 CART: Make sure that everything on the sled is secured.

1.2 CART: Make sure that the umbilical area behind the sled is clear and that cables are intact and free to move. Nothing other than the umbilical should be behind the sled.

1.3 SLED ELECTRONICS CABINET: Sled disabled (toggle switch down)

1.4 240 VOLT MAIN POWER BOX: Main power on.

1.5 Turn on power strip on desk by door and Northgate 386 computer.

1.6 CART: Remove covers from rails

2. Mechanical Safety Checks

2.1 Cart: Verify all components are securely fastened, including harness and all cables.

2.2 SLED CONTROL PANEL: Press SLED ENABLE.

2.3 CART: Verify that subject's emergency stop button works.

2.4 CART: Verify limit switch operation.

Press SLED ENABLE. Manually slide sled over left limit switch

Press SLED ENABLE: Slide sled over right limit switch.

Press SLED ENABLE: Move sled off limit switch; press HARD ABORT.

2.5 Calibrate position potentiometer (2 volts/meter).

2.6 Log procedures in sled log book.

3. Sled computer

3.1 At sled prompt, type 'sled'

3.2 Enter user id and password, then press return again.

4. Sled preparation

4.1 Make sure all personnel and equipment are clear of the sled (behind the yellow and black line)

4.2 Post sign on sled room door: "Experiment in Progress"

4.3 SLED CONTROL PANEL: Press HARD ABORT

4.4 SLED ELECTRONICS CABINET: Enable sled (toggle switch up)

4.5 SLED CONROL PANEL: Enable sled (toggle switch up)

4.6 SLED CONTROL PANEL: Press SLED ENABLE
4.7 SLED CONTROL PANEL: Run through profiles with sled empty
4.8 SLED CONTROL PANEL: Press HARD ABORT

5. Subject Preparation
5.1 Log experiment in sled log book
5.2 Explain experiment to subject.
5.3 Have subject sign consent form
5.4 Have subject complete pre-experiment questionnaire
5.5 Post sign on sled room door: "Experiment in Progress"
5.6 SLED ELECTRONICS CABINET: sled disabled (toggle switch down)
5.7 SLED CONTROL PANEL: sled disabled (toggle switch down)
Press HARD ABORT
5.8 Have subject enter sled, making sure that he/she doesn't step on rails or cloth part of the cart base.
5.9 Fasten head and foot restraints and shoulder harness
5.10 Ask if subject is comfortable.

Post-Experiment
6. Subject Egress
6.1 SLED CONTROL PANEL: Press HARD ABORT
6.2 SLED CONTROL PANEL: Disable sled (toggle switch down)
6.3 SLED CONTROL PANEL: Disable sled (toggle switch down)
6.4 CART: Verify that brake is on.
6.5 Remove subject restraints
6.6 Have subject exit sled, without stepping on rails or cloth

Shut-down
8.1 CART: Secure all items on cart
8.2 SLED ELECTRONICS CABINET: Disable sled (toggle switch down)
8.3 SLED CONTROL PANEL: Disable sled (toggle switch down)
Press SLED ENABLE
8.4 CART: Move sled manually to center position.
8.5 SLED CONTROL PANEL: Press HARD ABORT
8.6 240 VOLT MAIN POWER BOX: Main power off.
8.7 Replace rail covers
8.8 Remove sign from door
8.9 Exit sled program and shut off computer and power strip.

Appendix D

G-seat checklist

First time power-up

1. Remove 8 servo amp cards from servo amp chassis.
2. Turn on power supplies, 28 volt last.
3. Turn on +10 volt, +-15 volt, -15 volt power switches on servo amp chassis.
4. Verify that voltage corresponds to label at each fuse, including +28 volt.
5. Turn all power switches off

Every time servo amp chassis powered up

1. Turn 3 power switches on, clockwise from lower left. Leave +28v power off.
2. Wait 20-30 minutes for cards to warm up.
3. Check voltage at TP2, and adjust to 0 volts, using POT1. Repeat for all cards.
4. Check drive signal at TP5. Adjust drive signal bias using POT4 to get desired G-seat bias inflation level. Repeat for all cards.

Operation

1. Open nitrogen tank valve.
2. Turn on power amp fan.
3. Turn on +28v power switch.
4. Verify that knob on bias controller is set to min and turn on bias controller power switch
5. Press on each seat cushion and check that cushion deflates and re-inflates when released.

Shutdown

1. Turn off bias controller power switch and 28v power switch on servo amp chassis.
2. Close nitrogen tank valve.
3. Turn off power amp fans.
4. Do not turn off +10 v, +-15 v, -15 v power switches.

Test points and potentiometers are listed in Table D.1. Note that POT2 is glued in place. No adjustments to POT2 or POT3 are necessary.

Number	Test Point (TP)	Potentiometer (POT)
1	not connected	pressure offset
2	pressure	pressure filter (glued)
3	filtered pressrue	pressure gain
4	inverted drive	drive offset
5	drive	external command gain

Table D.1: G-seat servo amp card test points and pots

Appendix E

Matlab Scripts

cutleadtail.m

```
function [trimmed,istart,iend] = CutLeadTail(untrimmed)
% Trims data leader and tail from original data. For GSeat
experiment
% Uses section of leader on velocity data. Michael Mark-
miller 8/96
% modified for new gseat experiment Patricia Schmidt 5/97

SAMPRATE = 50;                    % Data sampling rate
TRIALLEN = 81.92;                 % Trial length in sec
VELOFFSET = -0.0126;% Mean noise value (if not zero mean)
SLOFFSET=mean(untrimmed(1:50,5));
SLSTD    = 0.007;                 % Std. Dev of noise
MINLEADER=200;
MAXLEADER = 3000;                      %    maximum    leader
before data
MAXTRAILER= 2000;

% find start. This looks for the first index outside the
noise that is
% followed by at least 2 of 3 points outside noise on same
side of noise band

abovenoise  =  find(untrimmed(1:MAXLEADER,5)  >  (SLOFFSET  +
3*SLSTD));
for loop = 1:length(abovenoise)
                  flag = 0;
                  for innerloop = 1:3
                       if  (abovenoise(loop  +  innerloop)  ==
abovenoise(loop) + innerloop);
                            flag = flag +1;
                       end
                  end
if (flag >=2)
                  abovestart = abovenoise(loop);
                  break;
```

```
end
end

belownoise = find(untrimmed(1:MAXLEADER,5) < (SLOFFSET -
3*SLSTD));
for loop = 1:length(belownoise)
                flag = 0;
                for innerloop = 1:3
                     if (belownoise(loop + innerloop) ==
belownoise(loop) + innerloop);
                          flag = flag +1;
                     end
                end
if (flag >=2)
                belowstart = belownoise(loop);
                break;
end
end

if (abovestart < belowstart)% Pick the earlier good signal
                istart = abovestart - 1;
else
                istart = belowstart - 1;
end

if (istart==0)
                istart=1;
end %if istart

% find signal end. This will be checked against expected sig-
nal end
% discrepancies should be reported

abovenoise      =       find(untrimmed(length(untrimmed):-
1:(length(untrimmed)   -   MAXTRAILER),5)   >   (SLOFFSET   +
3*SLSTD));


for loop = 1:length(abovenoise)
                flag = 0;
                for innerloop = 1:3
```

```
                    if (abovenoise(loop + innerloop) ==
abovenoise(loop) + innerloop);
                         flag = flag +1;
                    end
               end
if (flag >=2)
               aboveend = abovenoise(loop);
               break;
end
end

belownoise     =     find(untrimmed(length(untrimmed):-
1:(length(untrimmed)  -  MAXTRAILER),5)  <  (SLOFFSET  -
3*SLSTD));

for loop = 1:length(belownoise)
               flag = 0;
               for innerloop = 1:3
                    if (belownoise(loop + innerloop) ==
belownoise(loop) + innerloop);
                         flag = flag +1;
                    end
               end
if (flag >=2)
               belowend = belownoise(loop);
               break;
end
end

if (aboveend < belowend)% Pick the later good signal. Notice
these indices count up from end of untrimmed
               iend = length(untrimmed) - (aboveend - 1) +
1;
else
               iend = length(untrimmed) - (belowend - 1) +
1;

end


% for short data files when sled reached end of track 7/31/97
```

```
if (istart-iend) < 3000
                  iend=istart+4097;
                  if iend>length(untrimmed)
                       iend=length(untrimmed);
                  end %if iend
end % if (istart...

% now cut ends off datafile. Don't forget to adjust time
trace!

totaltime = (iend-istart + 1)/SAMPRATE;
%disp(['Total time : ',num2str(totaltime)]);
if ((iend - istart)  > TRIALLEN*SAMPRATE)
                  iend = istart + TRIALLEN*SAMPRATE;
                  disp('Over expected length. Extra points
truncated.');
end
trimmed = zeros(TRIALLEN*SAMPRATE + 1,5);
trimmed(1:((iend-istart)+1),1:5)                              =
untrimmed(istart:iend,1:5);

% subtract starting time from time vector--preserves sample
times
trimmed(:,1)=trimmed(:,1)-
trimmed(1,1)*ones(size(trimmed(:,1)));

end
```

press.m

```
% press.m
% Created by Patricia Schmidt for gseat-sled data analysis
% Adds pressure trace to no-gseat data files for one sub-
ject's data.

trial=[3 4 5 6 9 10 15 16]; % numbers of no-gseat trials
% set subject designator
fname='ll';
eval('load MacintoshHD:users:Patricia:data:podd')
eval('load MacintoshHD:users:Patricia:data:peven')
```

```
for i=1:8
                  i
                  eval([`load       MacintoshHD:users:Patri-
cia:data:',name,':',fname,num2str(trial(i))]);
                  eval([`[blah,istart,iend]=CutLead-
Tail(`,fname,num2str(trial(i)),');']);

                  clear blah

                  if trial(i)/2==floor(trial(i)/2)

eval([fname,num2str(trial(i)),'(`,num2str(istart),':',num2st
r(iend),',2)=peven(1:iend-istart+1);']);
                  else

eval([fname,num2str(trial(i)),'(`,num2str(istart),':',num2st
r(iend),',2)=podd(1:iend-istart+1);']);
                  end %if

                  eval([`save       MacintoshHD:users:Patri-
cia:data:',name,':',fname,              num2str(trial(i)),'
`,fname,num2str(trial(i))]);
                  eval([`clear `,fname, num2str(trial(i))]);
end %for
```

loadsubt.m

```
% LOADSUBT
%                          Created by Patricia Schmidt for
gseat-sled expt data analysis
%
%          Computes transfer function for each pair of con-
secutive trials.
%           Loads subject data file, files containing gseat
pressure
%          and sled velocity profiles. Then calls findtf2 to
get
%             csd ratios. Calls solvefortft to solve for 3
transfer
```

```
%           functions for gseat on trials, nofbktf for gseat
off trials
%           Saves file containing csd ratios, transfer func-
tions for each block
%          of two trials.

%              This script uses findtf2.m, csdtf.m, solve-
fortft.m, nofbktf.m,
%          makeplots.m, bplot.m

clear;

P=path;
path(P,'MacintoshHD:users:Patricia:new_scripts');

% set up array of strings indicating which trials use which
freqs

setfreq(1,:)=['sled=freql;gseat=freqh;'];
setfreq(2,:)=['sled=freqh;gseat=freql;'];
setfreq(3,:)=['sled=freql;gseat=freqh;'];
setfreq(4,:)=['sled=freqh;gseat=freql;'];
setfreq(5,:)=['sled=freql;gseat=freqh;'];
setfreq(6,:)=['sled=freqh;gseat=freql;'];
setfreq(7,:)=['sled=freql;gseat=freqh;'];
setfreq(8,:)=['sled=freqh;gseat=freql;'];
setfreq(9,:)=['sled=freql;gseat=freqh;'];
setfreq(10,:)=['sled=freqh;gseat=freql;'];
setfreq(11,:)=['sled=freql;gseat=freqh;'];
setfreq(12,:)=['sled=freqh;gseat=freql;'];
setfreq(13,:)=['sled=freql;gseat=freqh;'];
setfreq(14,:)=['sled=freqh;gseat=freql;'];
setfreq(15,:)=['sled=freql;gseat=freqh;'];
setfreq(16,:)=['sled=freqh;gseat=freql;'];
setfreq(17,:)=['sled=freql;gseat=freqh;'];
setfreq(18,:)=['sled=freqh;gseat=freql;'];
setfreq(19,:)=['sled=freql;gseat=freqh;'];
setfreq(20,:)=['sled=freqh;gseat=freql;'];


% array of load commands corresponding to different trials
```

```
ldistfreq(1,:)=['load sledl; load gseath'];
ldistfreq(2,:)=['load sledh; load gseatl'];
ldistfreq(3,:)=['load sledl; load gseath'];
ldistfreq(4,:)=['load sledh; load gseatl'];
ldistfreq(5,:)=['load sledl; load gseath'];
ldistfreq(6,:)=['load sledh; load gseatl'];
ldistfreq(7,:)=['load sledl; load gseath'];
ldistfreq(8,:)=['load sledh; load gseatl'];
ldistfreq(9,:)=['load sledl; load gseath'];
ldistfreq(10,:)=['load sledh; load gseatl'];
ldistfreq(11,:)=['load sledl; load gseath'];
ldistfreq(12,:)=['load sledh; load gseatl'];
ldistfreq(13,:)=['load sledl; load gseath'];
ldistfreq(14,:)=['load sledh; load gseatl'];
ldistfreq(15,:)=['load sledl; load gseath'];
ldistfreq(16,:)=['load sledh; load gseatl'];
ldistfreq(17,:)=['load sledl; load gseath'];
ldistfreq(18,:)=['load sledh; load gseatl'];
ldistfreq(19,:)=['load sledl; load gseath'];
ldistfreq(20,:)=['load sledh; load gseatl'];


% two frequency vectors
per=81.92;
freql=1/per*[5 9 13 19 29 37];
freqh=1/per*[7 11 17 23 32 41];


% set subject designator
name='e';

% i= trial numbers to analyze i=1:16 is eyes closed trials
% i=17:20 is eyes open trials

for i=17:20

% k11 and k12 are missing--uncomment if for subject k
                %if ~(i==11 | i==12)
          % trial numbers
```

```
                    i
                    clear sledl sledh p1 slider;
                    fname=[name,num2str(i)];
                    fname
                    eval(['load        MacintoshHD:users:Patri-
cia:data:',name,':',fname])
                    ['load             MacintoshHD:users:Patri-
cia:data:',name,':',fname]


eval([fname,'(:,4)=vfilt(',fname,'(:,4));'])
                    eval([fname,'=cutleadtail(',fname,');']);

                    disp('loaded data file')

                    cd MacintoshHD:users:Patricia:data;
                    eval(ldistfreq(i,:));
                    disp('loaded profile file')
                    eval(setfreq(i,:));
                    data=eval(fname);

                    % convert p1,v,slider to engineering units
                    % [p]=psi, [v]=m/s, slider=[m/s]

                    slider=.113*data(:,5);
                    p1=-2.0580*data(:,2);
                    vel=1.9*data(:,4);

                    eval(['clear ',fname,' data']);
                    disp(['cleared ',fname])

                    % call findtf2 to get csd ratios

[a1(i,:),a2(i,:)]=findtf2(slider,vel,p1,sled-
vel,p,sled,gseat);
% uncomment end for subject k
%end %if
end % for i
```

```
% assemble a's into matrices A1 and A2 (8x12) 1 row for each
block,
% 1 col for each freq

A1=zeros(8,12);
A2=A1;

% k=block number-- k=1:8 for eyes closed trials, k=9:10 for
eyes open trials

for k=9:10

% data files missing for subj k, uncomment if for subj k
%if k~=6

A1(k,:)=[a1(2*k-1,1),a1(2*k,1),a1(2*k-1,2),a1(2*k,2),a1(2*k-
1,3),a1(2*k,3),a1(2*k-1,4),a1(2*k,4),...
a1(2*k-1,5),a1(2*k,5),a1(2*k-1,6),a1(2*k,6)];

A2(k,:)=[a2(2*k-1,1),a2(2*k,1),a2(2*k-1,2),a2(2*k,2),a2(2*k-
1,3),a2(2*k,3),a2(2*k-1,4),a2(2*k,4),...
a2(2*k-1,5),a2(2*k,5),a2(2*k-1,6),a2(2*k,6)];

% call solvefortf to find tf's for gseat on trials
[E1c(k,:),E2c(k,:),E1cm(k,:),
E1cp(k,:),E2cm(k,:),E2cp(k,:)]=                    solve-
fortft(A1(k,:),A2(k,:),k);

% uncomment for subj k
%else
%                A1(6,:)=zeros(size(A1(5,:)));
%end % if k

end %for k


freq=1/per*[5 7 9 11 13 17 19 23 29 32 37 41];

% find tfs for no gseat
% nofbktf2 uses no feedback formulas for _all_ trials
nofbktf
```

```
% plot all tf's
makeplots


% save file containing a1a a2a (means of a's at each freq),
% E1cm E1cp E2cm E2cp
% a1 a2  (a's at each frequency)

% results file naming: <subject>r = eyes closed
%                      <subject>ro = eyes open
%                     <subject>rn = no feedback formulas for
all tf's

filenum = input(['Enter number/letter to add to filename : '
name,'ro'],'s');
%filenum = input(['Enter number/letter to add to filename :
' name,'rn'],'s');

eval(['save                          MacintoshHD:users:Patri-
cia:data:',fname(1:1),'ro',filenum,' A1 A2 E1c E2c E1cm E1cp
E2cm E2cp freq']);
%eval(['save                          MacintoshHD:users:Patri-
cia:data:',fname(1:1),'rn',filenum,' A1 A2 E1c E2c E1cm E1cp
E2cm E2cp freq']);

for clearloop =1:16
                eval(['clear    ',fname(1:1),num2str(clear-
loop)]);
end % for clearloop
```

findtf2.m

```
function [a1, a2]= findtf2(slider,vel,p1,d1,d2,sled,gseat)
%
%%% Created by Patricia Schmidt for gseat-sled expt data
analysis
%
%%% Finds cross spectral density ratios at disturbance freqs
%%% calls csdtf.m
```

```
% set tolerance for frequency and input frequencies
tol=.01;
per=81.92;
%freq=1/per*[5 7 9 11 13 17 19 23 29 32 37 41];
freq1=1/per*[5 9 13 19 29 37];
freq2=1/per*[7 11 17 23 32 41];

K=.113; % joystick gain

vel=vel';
hmdv=hmdv';

% pad with zeros to make data, profiles same length
if length(d1)<length(slider),
                  disp('adding zeros to d1')
                  d1=[d1;zeros(length(slider)-
length(d1),1)];
                  length(d1)
end % if length

if length(slider)<length(d1),
                  slider=[slider;zeros(length(d1)-
length(slider),1)];
                  disp('adding zeros to p1, slider')
                  p1=[p1;zeros(length(d1)-length(p1),1)];
                  vel=[vel;zeros(length(d1)-length(vel),1)];
end % if length

% find ratios of csd's
% lambda=slider
% d1=sled profile
% d2=gseat profile
% p1=gseat pressure

% call csdtf to compute csd ratios

[a1r,a1i,f1]=csdtf(vel,slider,d1,length(vel),50,[]);
[a2r,a2i,f2]=csdtf(p1,slider,d2,length(p1),50,[]);
disp('took csds')
```

```
% throw away csd data for freq>1 hz

a1r=a1r(1:find(f1>1));
a2r=a2r(1:find(f2>1));

a1i=a1i(1:find(f1>1));
a2i=a2i(1:find(f2>1));

f1=f1(1:find(f1>1));
f2=f2(1:find(f2>1));

% find mags and phases at input frequencies by averaging over
% frequencies within tolerance

a1a=zeros(1,8);
a2a=a1a;

% convert real and imag parts to a+bj form
a1a=a1r + j*a1i;
a2a=a2r + j*a2i;

for i=(1:6),

%  *** average  a+bj
                 a1(i)=max(a1a(find(abs(f1-sled(i))<tol)));
                 a2(i)=mean(a2a(find(abs(f2-
gseat(i))<tol)));

end % for i

 disp('after for loop in findtf2')
```

csdtf.m

```
function [ar, ai, freq]=csdtf(in,out,d,nfft,fs,window)\
%  Created by Patricia Schmidt for gseat-sled expt data anal-
ysis
%
%  Finds transfer function between x and y by cross-correla-
tion
```

```
%  Returns tf in real, imag form

[Pxd, Fxd]=csd(in,d,nfft,fs,window);
[Pyd,Fyd]=csd(out,d,nfft,fs,window);

a=Pyd./Pxd;
ar=real(a);
ai=imag(a);


freq=Fxd;
```

solvefortft.m

```
function                    [E1c,E2c,E1cm,E1cp,E2cm,E2cp]=solve-
fortft(a1a,a2a,index)

%% solvefortft.m
%%   Created by Patricia Schmidt for gseat-sled expt data
analysis
%%  Given csd ratios, uses block diagram eqns to solve for
tf's
%%  for trials with gseat on.  Returns two transfer functions
in both
%%  a+bj form and mag*exp(j*phase) form.

% disturbance frequencies
per=81.92;
freq=1/per*[5 7 9 11 13 17 19 23 29 32 37 41];

%%%%% solve for estimator tf's

% joystick gain and low-pass filter
K=.113./((j*freq*2*pi)+10);

% gseat transfer function: pressure(volts)/cmd(volts)
% first order tf from 85lb load pressure data

G=3.0./((j*freq*2*pi)+10.3);
```

```
% gain of accel fbk to gseat
Kfbk=15;

% sled dynamics are flat for this frequency range
P=1;


% eqns for 6/16/97 two-channel block diagram
E1c=a1a./(j*freq*(2*pi))-G.*Kfbk.*a2a;
E2c=a2a;


% convert to mag, phase  deal with wrap-arounds in phase
E1cm=abs(E1c);

E1cp=rem(phase(E1c)*180/pi,360);

if E1cp>0
                E1cp=E1cp-360;
end %if

if E1cp<-360
                E1cp=E1cp+360;
end % if

E2cm=abs(E2c);


E2cp=rem(phase(E2c)*180/pi,360);

if E2cp>0
                E2cp=E1cp-360;
end %if

if E2cp<-360
                E2cp=E1cp+360;
end % if
```

nofbktf.m

```
% nofbktf.m
% Created by Patricia Schmidt for gseat-sled expt data anal-
ysis
%
% Computes transfer functions from csd ratios for no gseat
trials
% no gseat trials are 2,3,5,8


% select trials to use

%trial=[2 3 5 8];  % gseat off
%trial=[1 4 6 7];  % gseat on
trial=[9 10];      % eyes open

% joystick transfer function
K=1./((j*freq*2*pi)+10);


% Compute tf's for selected trials, using no fbk formulas
% tf's given as a+j*b and mag,phase

for index=1:length(trial)
                  trialno=trial(index)
                  E1c(trialno,:)=A1(trialno,:)/j./freq/(2
*pi);
                  E2c(trialno,:)=A2(trialno,:)+A2(tri-
alno,:).*A1(trialno,:).*K;

                  E1cm(trialno,:)=abs(E1c(trialno,:));
                  E1cp(trialno,:)=rem(phase(E1c(tri-
alno,:))*180/pi,360);

                  E2cm(trialno,:)=abs(E2c(trialno,:));
                  E2cp(trialno,:)=rem(phase(E2c(tri-
alno,:))*180/pi,360);
end %for
```

bplot.m

```
function bplot(mag,phase,w,lc)

% BPLOT.m
% Created by Patricia Schmidt for gseat system id
% Makes bode plot from mag, phase(deg), freq(rad/sec) data.
% Axes can be set or automatic.

subplot(211)
%cla
loglog(w,mag,lc)
hold on
loglog(w,mag,lc)

grid on
ylabel('log gain')
xlabel('log freq (rad/sec)')

subplot(212)
%cla
semilogx(w,phase,lc)
hold on
axis([.1,10,-180,180])
grid on
semilogx(w,phase,lc)
ylabel('phase (deg)')
xlabel('log freq (rad/sec)')
```

makeplots.m

```
%makeplots.m
% Created by Patricia Schmidt for gseat-sled expt data anal-
ysis
% Makes bode plots of vestibular, tactile tf's computed in
loadsubt.m
% for loaded results file.
% Select pause or print for screen display or printing
```

```
% i = block number i=1:8 for eyes closed, i=9:10 for eyes
open
for i=9:10
clg
bplot(E1cm(i,:),E1cp(i,:),freq,'o')
bplot(E1cm(i,:),E1cp(i,:),freq,'-')
subplot(211)
title(['Subject ',name,' vestibular block ',num2str(i),'
nofbk'])
%print
pause;

clg
bplot(E2cm(i,:),E2cp(i,:),freq,'x')
bplot(E2cm(i,:),E2cp(i,:),freq,'-')
subplot(211)
title(['Subject ',name,' tactile block ',num2str(i),'
nofbk'])
pause;
%print
end %for
```

Appendix F

Data

The plots on the pages that follow are the mean tactile and vestibular transfer functions for each of the eight subjects, under each of two conditions, G-seat on and G-seat off. The plots are as follows.

1. Tactile transfer function, G-seat on.
2. Tactile transfer function, G-seat off. Note that this transfer function serves as an indication of manual control remnant and measurement noise and does not contain information about the tactile feedback path.
3. Vestibular transfer function, G-seat on.
4. Vestibular transfer function, G-seat off.

Sections 5.2 and 5.3 describe the computation of these transfer functions.

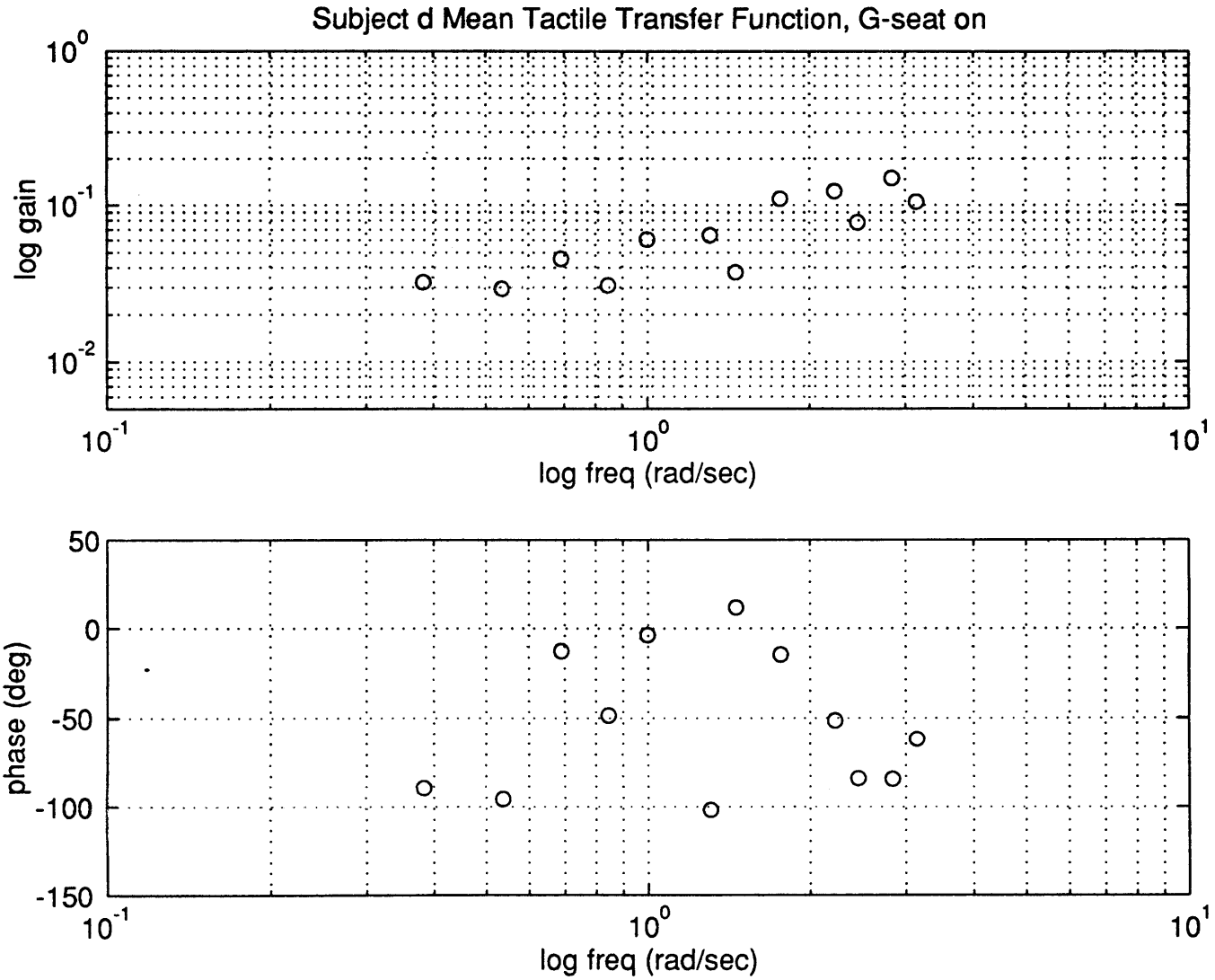
Subject d Mean Tactile Transfer Function, G-seat on
log gain
log freq (rad/sec)
phase (deg)
log freq (rad/sec)

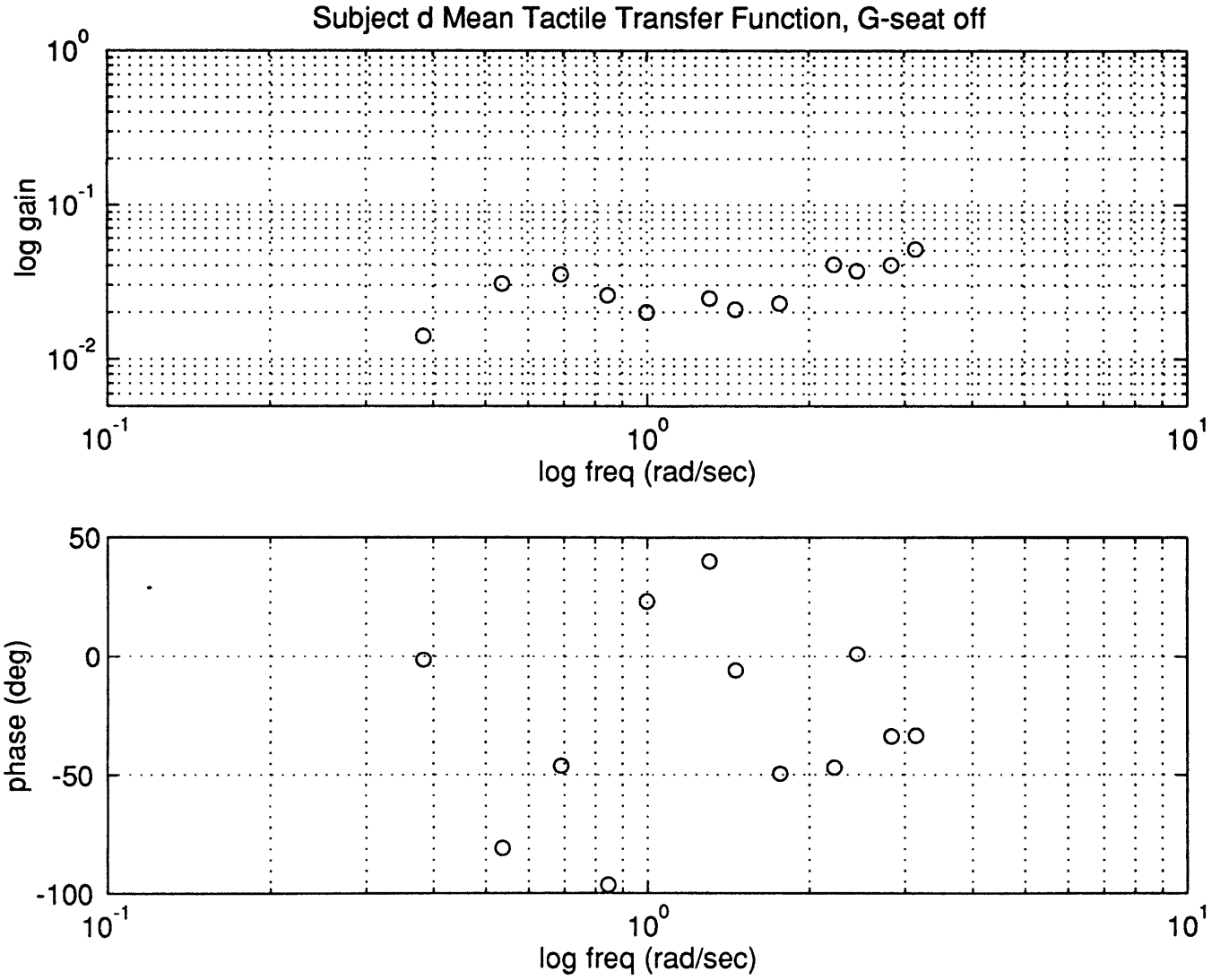
Subject d Mean Tactile Transfer Function, G-seat off
log gain
log freq (rad/sec)
phase (deg)
log freq (rad/sec)

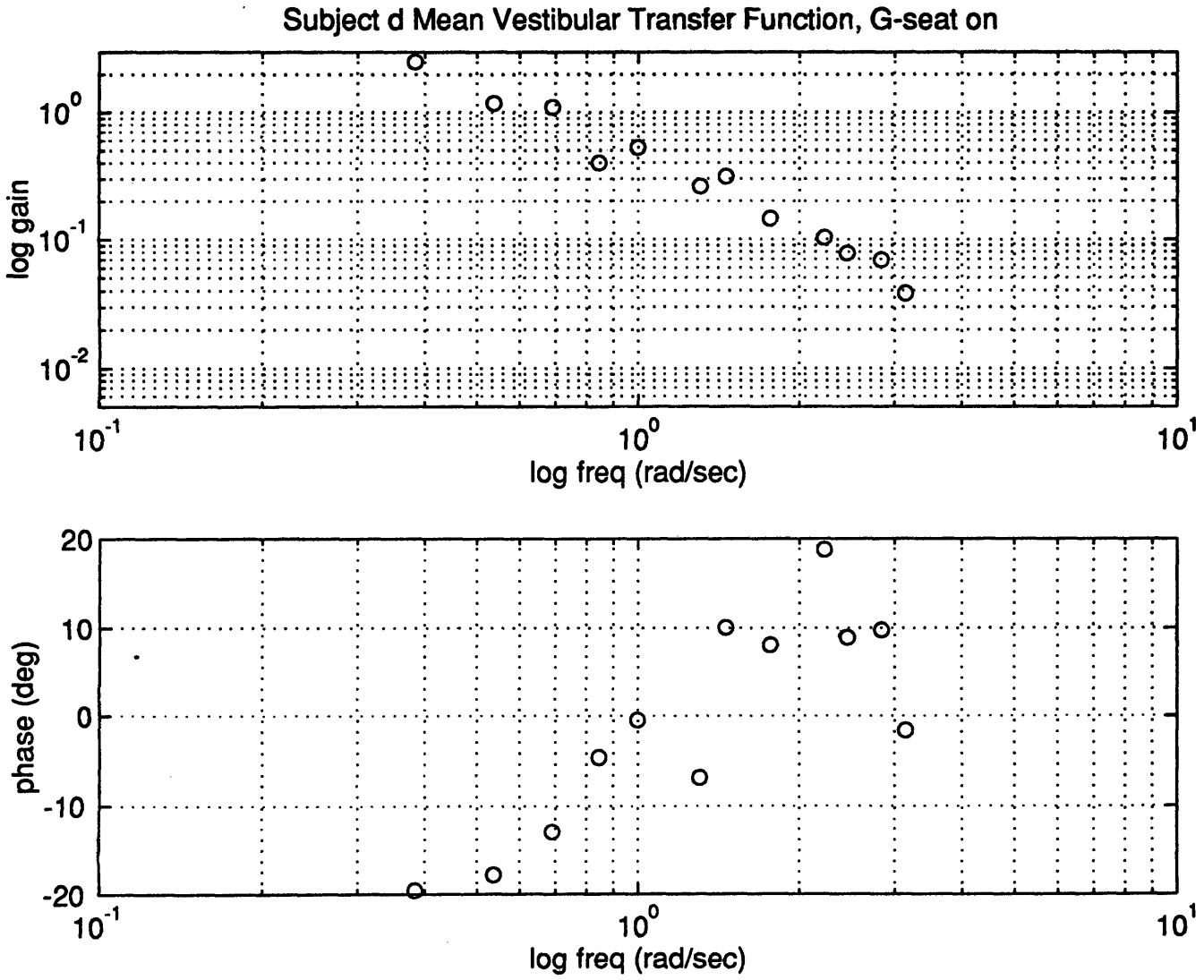
Subject d Mean Vestibular Transfer Function, G-seat on
log gain
10^{0}
10^{-1}
10^{-2}
10^{-1}
10^{0}
10^{1}
log freq (rad/sec)
phase (deg)
20
10
0
-10
-20
10^{-1}
10^{0}
10^{1}
log freq (rad/sec)

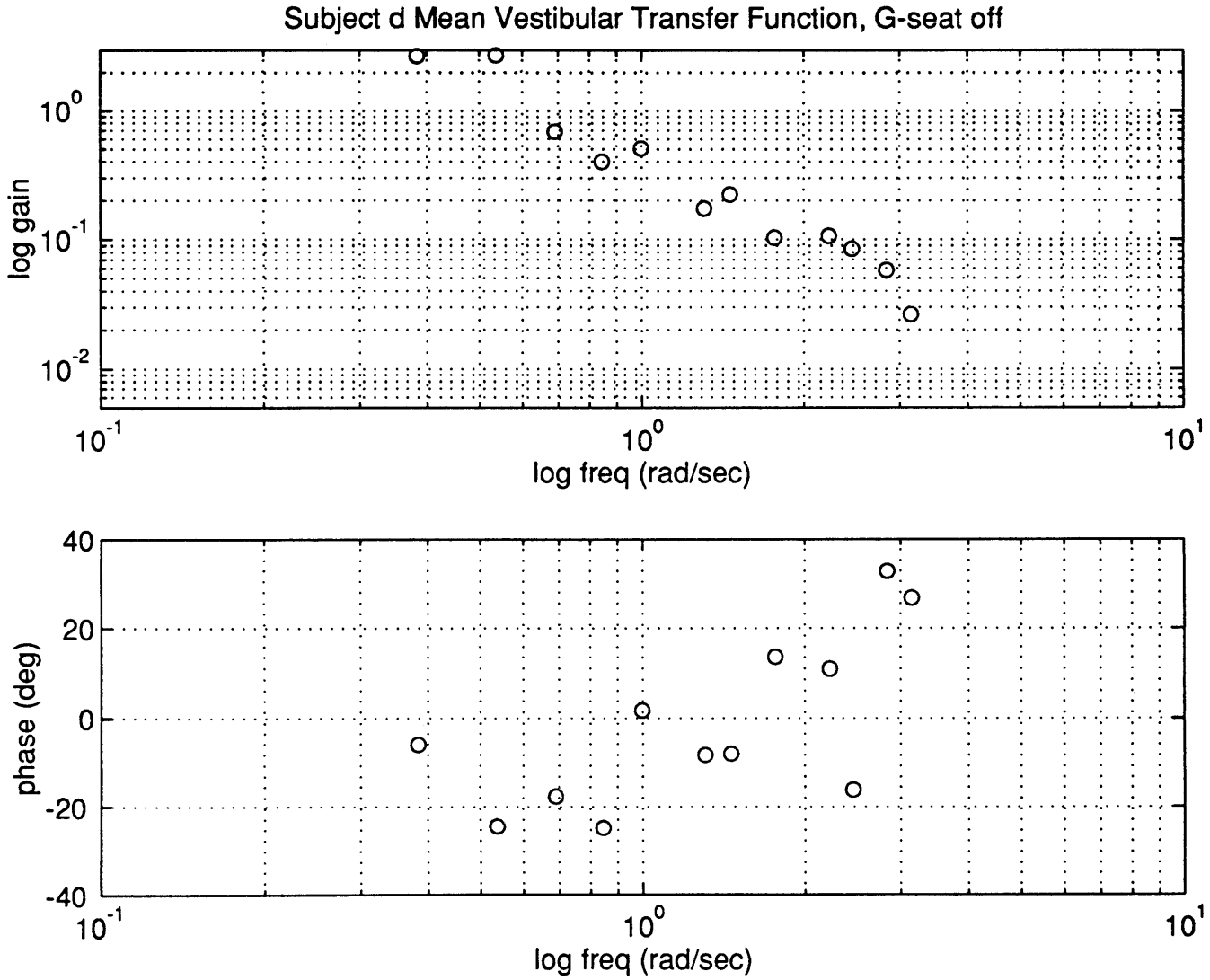
Subject d Mean Vestibular Transfer Function, G-seat off
log gain
10^{0}
10^{-1}
10^{-2}
10^{-1}
10^{0}
10^{1}
log freq (rad/sec)
phase (deg)
40
20
0
-20
-40
10^{-1}
10^{0}
10^{1}
log freq (rad/sec)

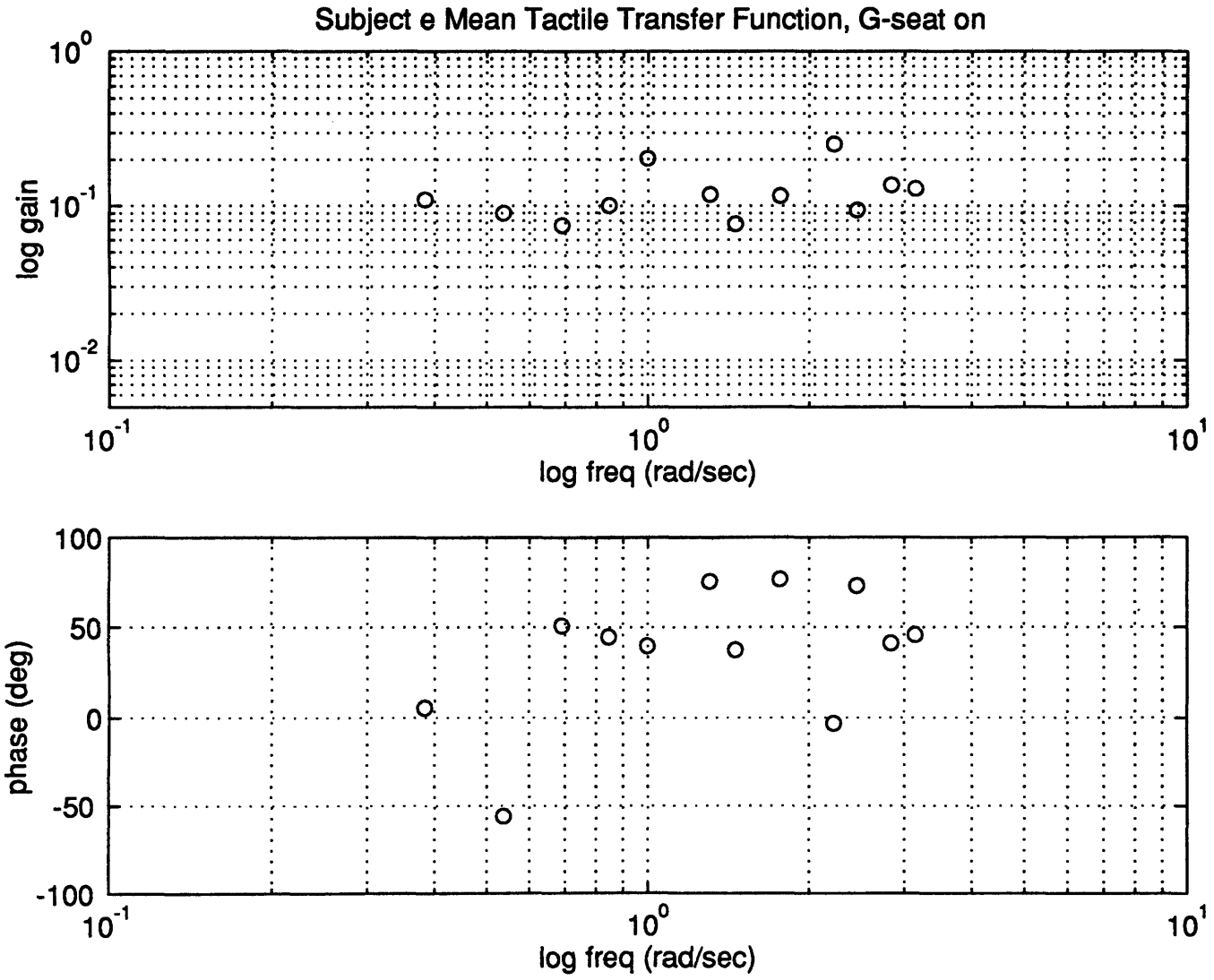
Subject e Mean Tactile Transfer Function, G-seat on
log gain
log freq (rad/sec)
phase (deg)
log freq (rad/sec)

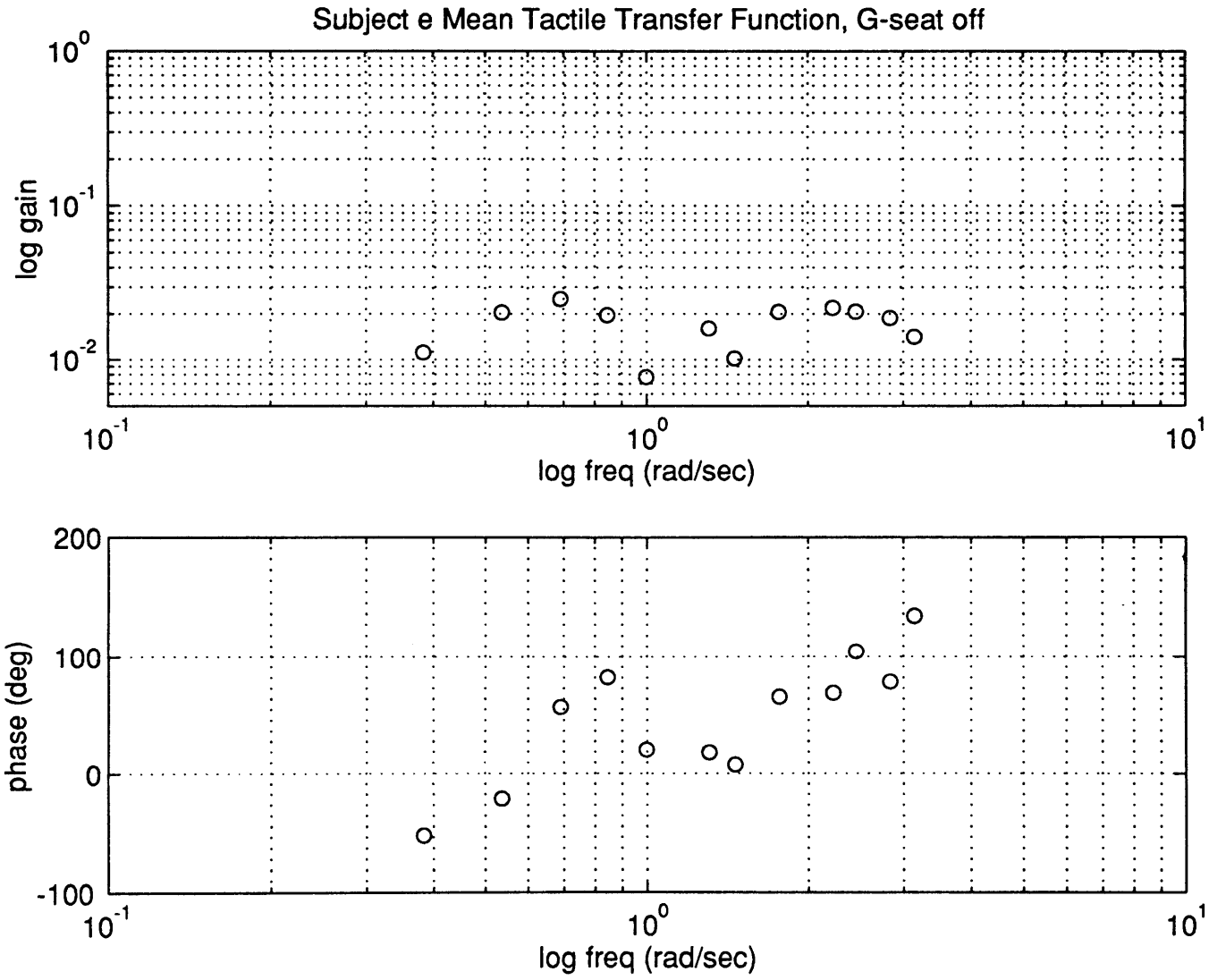
Subject e Mean Tactile Transfer Function, G-seat off
log gain
10^0
10^{-1}
10^{-2}
10^{-1}
10^0
10^1
log freq (rad/sec)
phase (deg)
200
100
0
-100
10^{-1}
10^0
10^1
log freq (rad/sec)

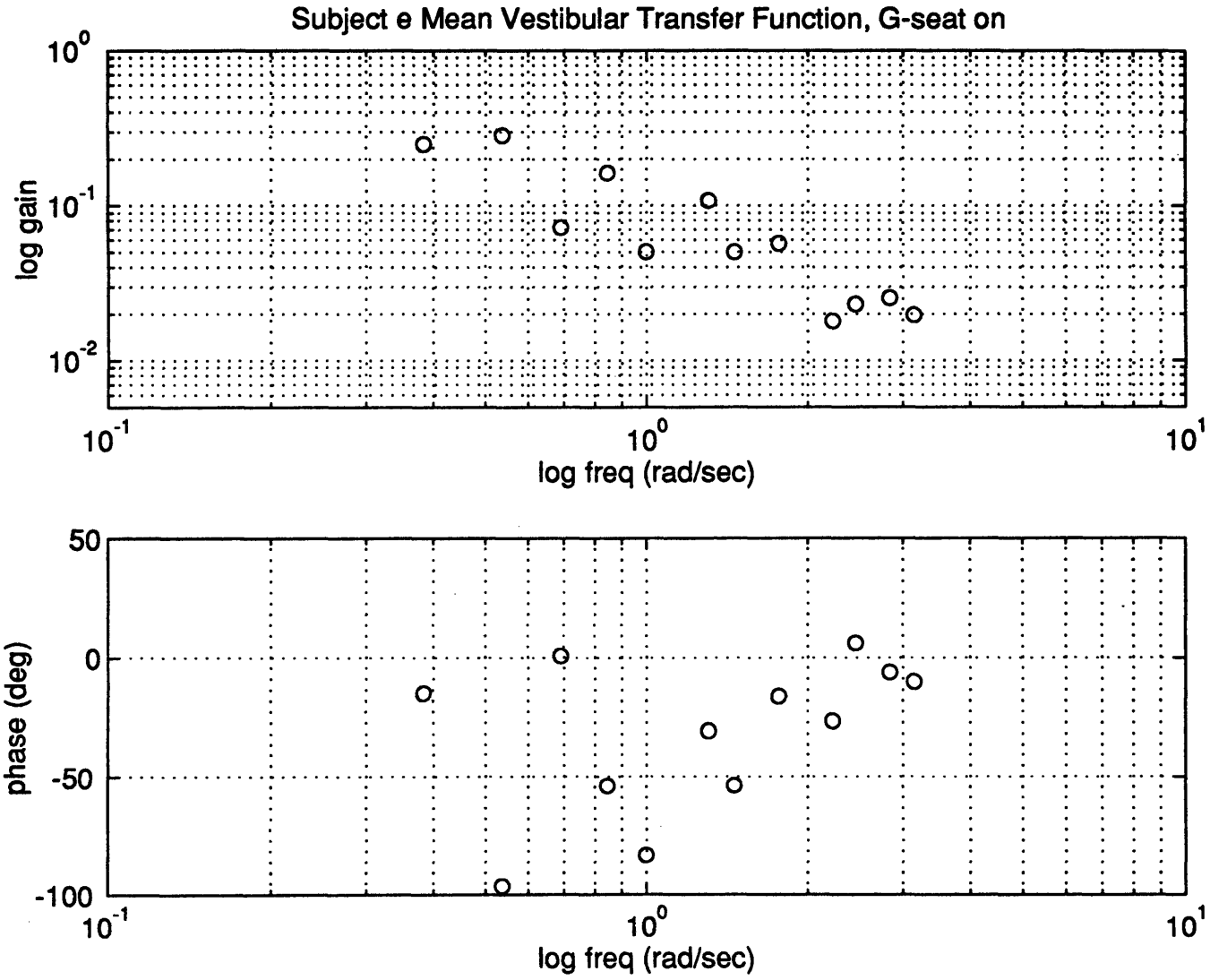
Subject e Mean Vestibular Transfer Function, G-seat on
log gain
log freq (rad/sec)
phase (deg)
log freq (rad/sec)

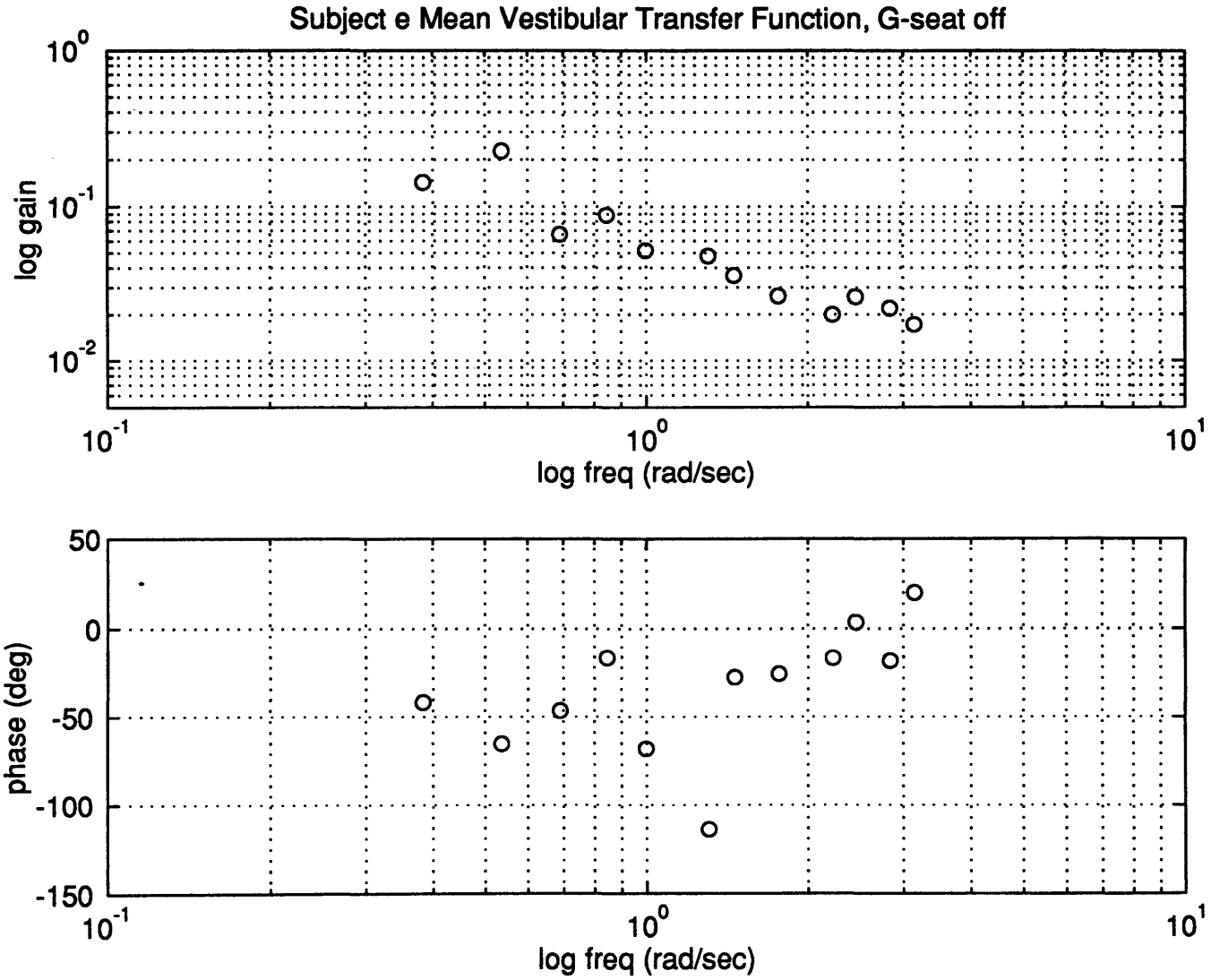
Subject e Mean Vestibular Transfer Function, G-seat off
log gain
10^0
10^{-1}
10^{-2}
10^{-1}
10^0
10^1
log freq (rad/sec)
phase (deg)
50
0
-50
-100
-150
10^{-1}
10^0
10^1
log freq (rad/sec)

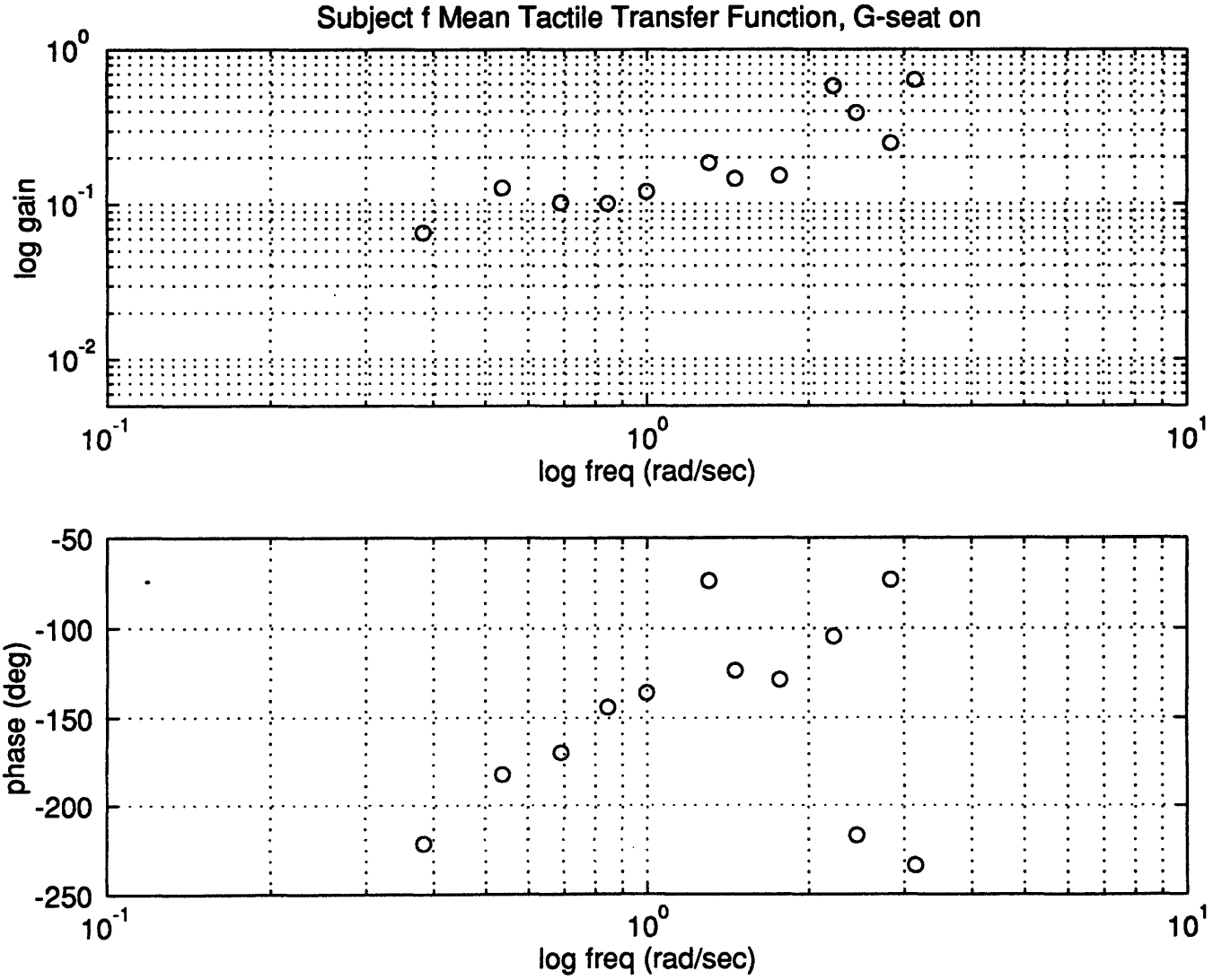
Subject f Mean Tactile Transfer Function, G-seat on
log gain
log freq (rad/sec)
phase (deg)
log freq (rad/sec)

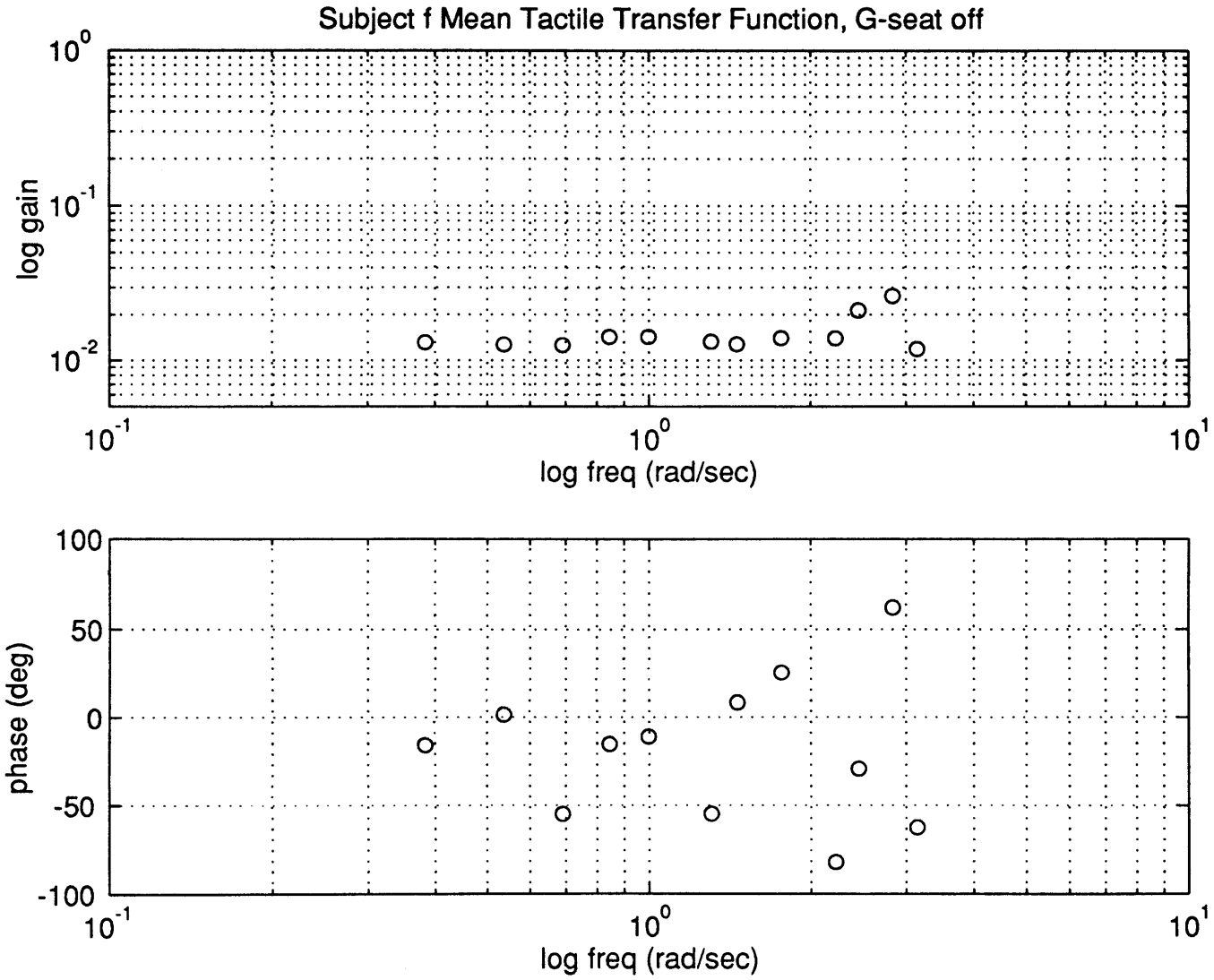
Subject f Mean Tactile Transfer Function, G-seat off
log gain
10^{0}
10^{-1}
10^{-2}
10^{-1}
10^{0}
10^{1}
log freq (rad/sec)
phase (deg)
100
50
0
-50
-100
10^{-1}
10^{0}
10^{1}
log freq (rad/sec)

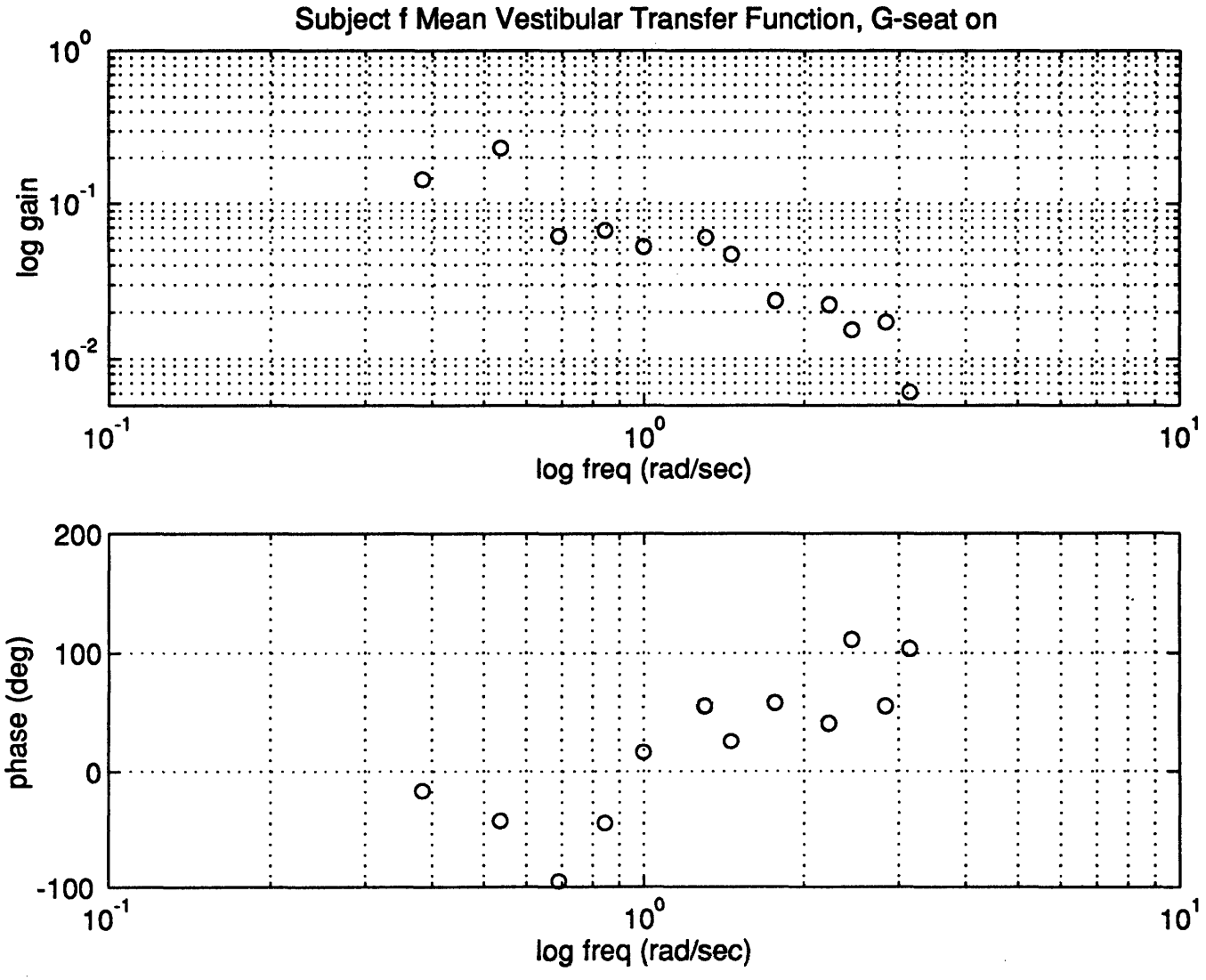
Subject f Mean Vestibular Transfer Function, G-seat on
log gain
log freq (rad/sec)
phase (deg)
log freq (rad/sec)

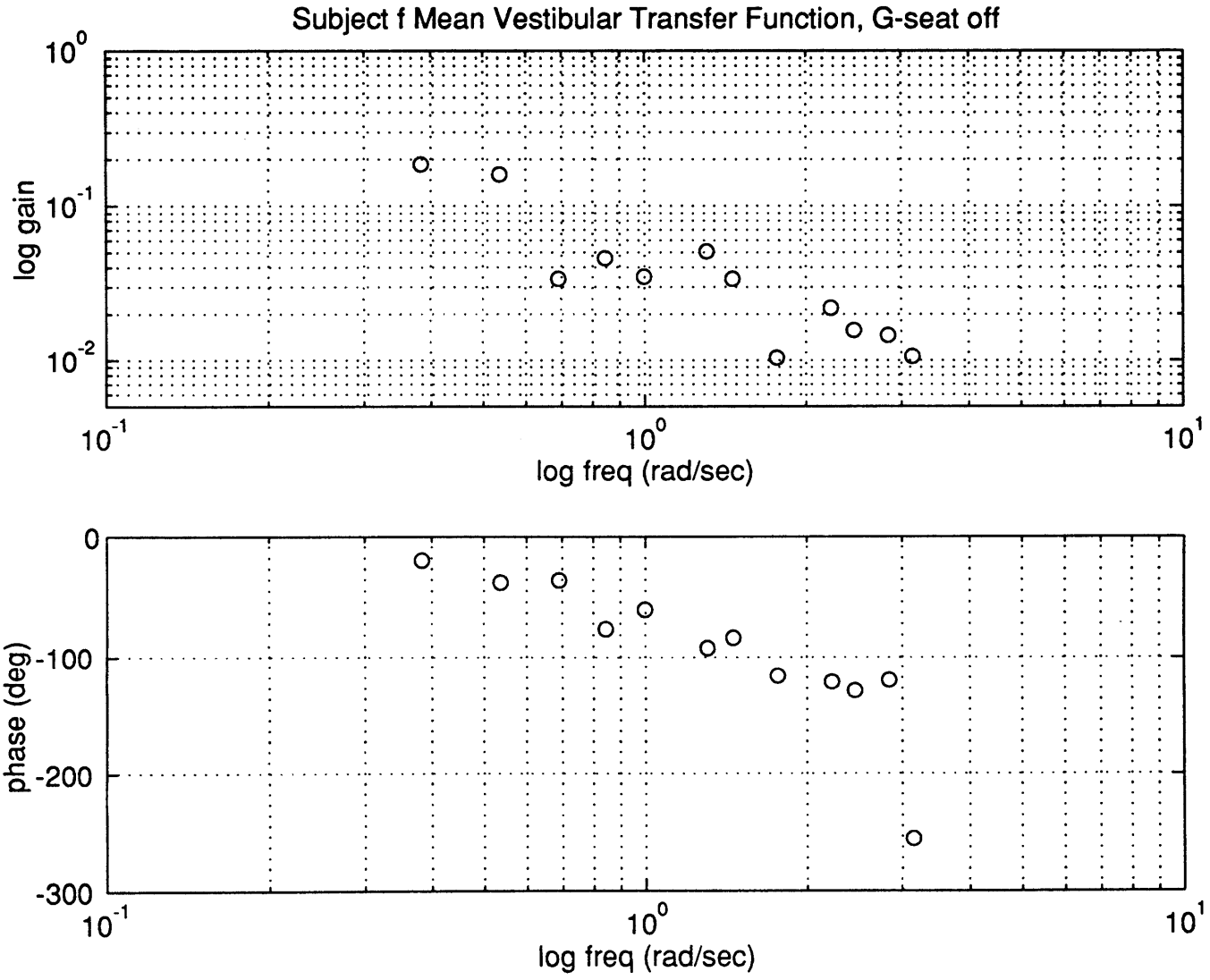
Subject f Mean Vestibular Transfer Function, G-seat off
log gain
log freq (rad/sec)
phase (deg)
log freq (rad/sec)

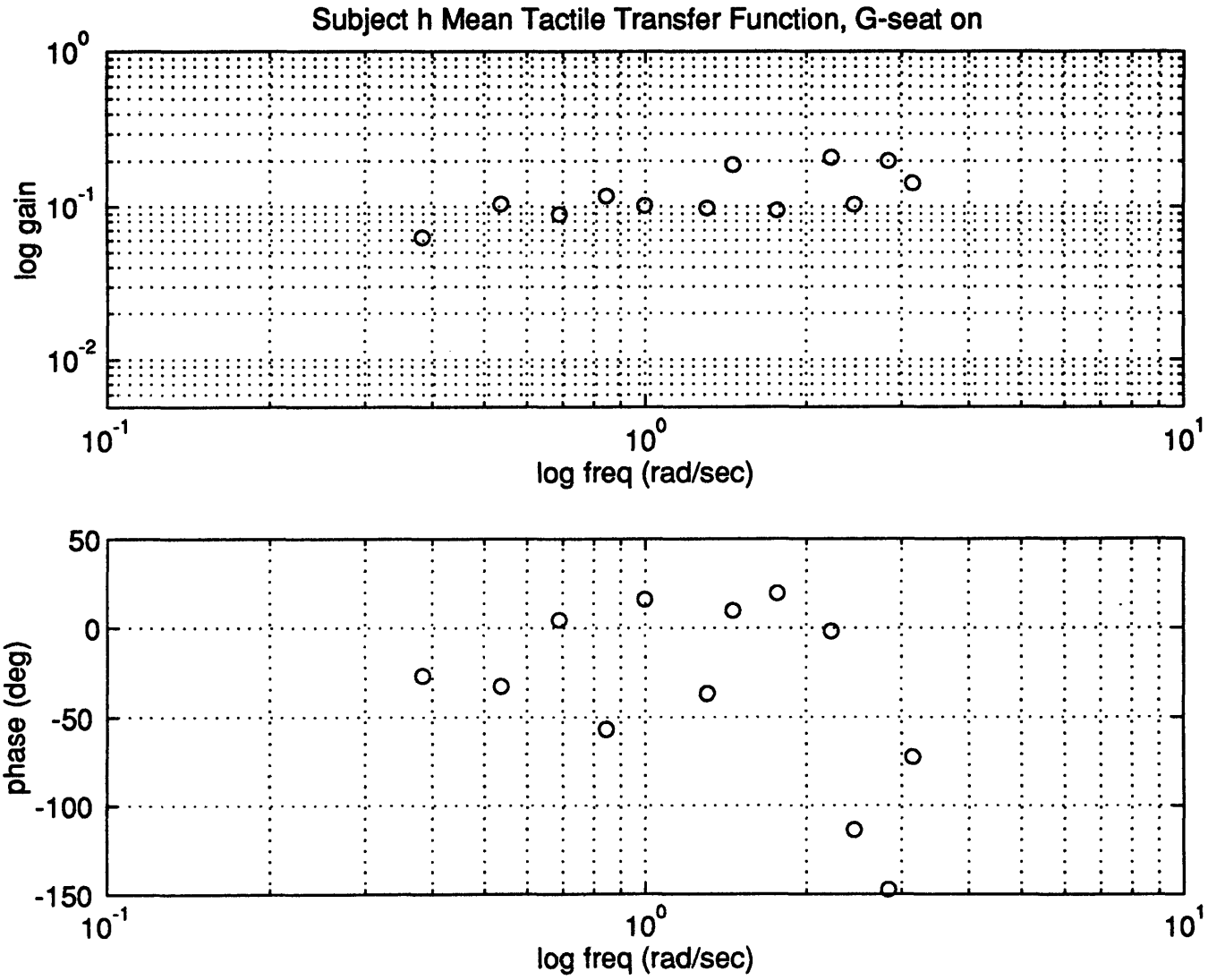
Subject h Mean Tactile Transfer Function, G-seat on
log gain
log freq (rad/sec)
phase (deg)
log freq (rad/sec)

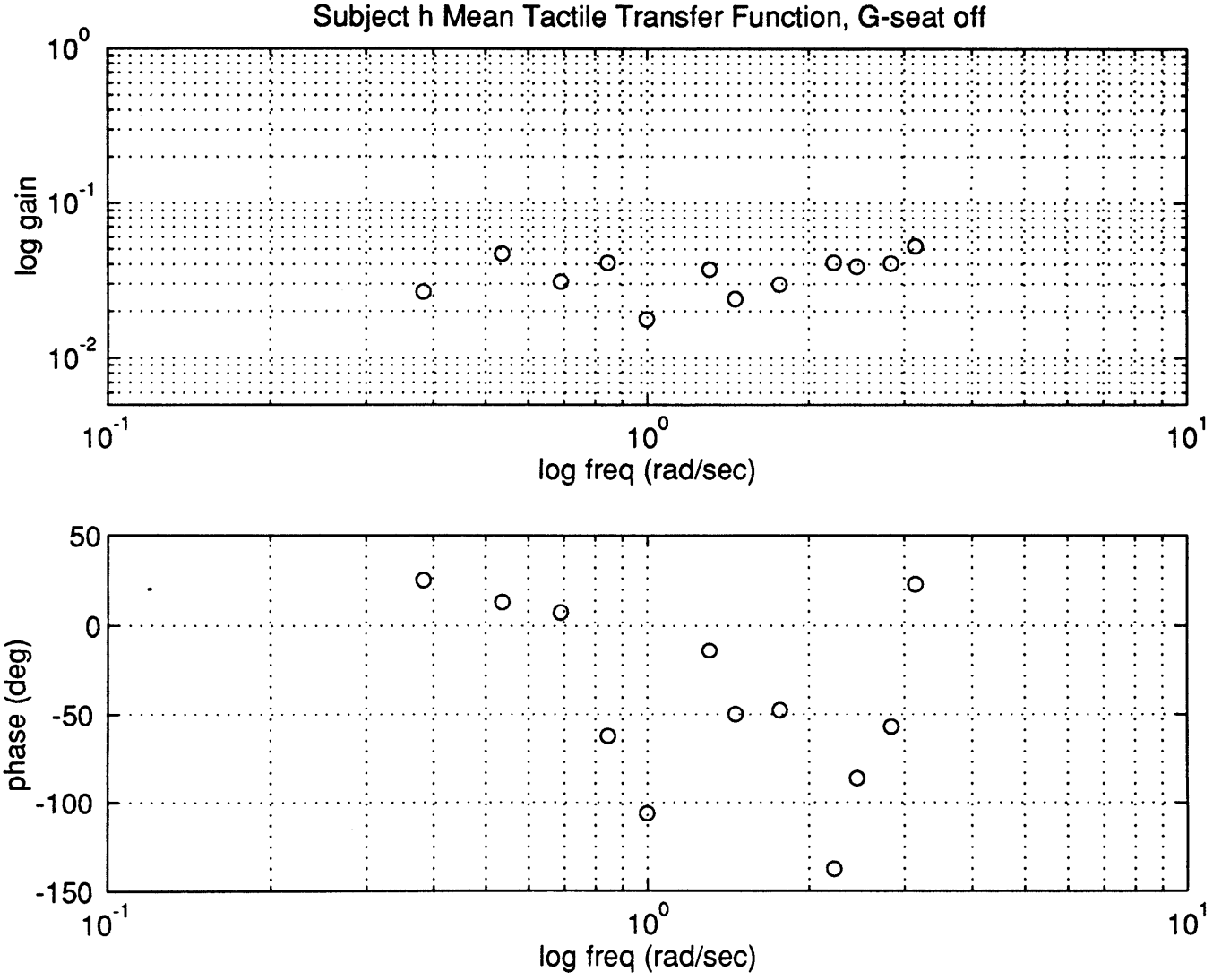
Subject h Mean Tactile Transfer Function, G-seat off
log gain
log freq (rad/sec)
phase (deg)
log freq (rad/sec)

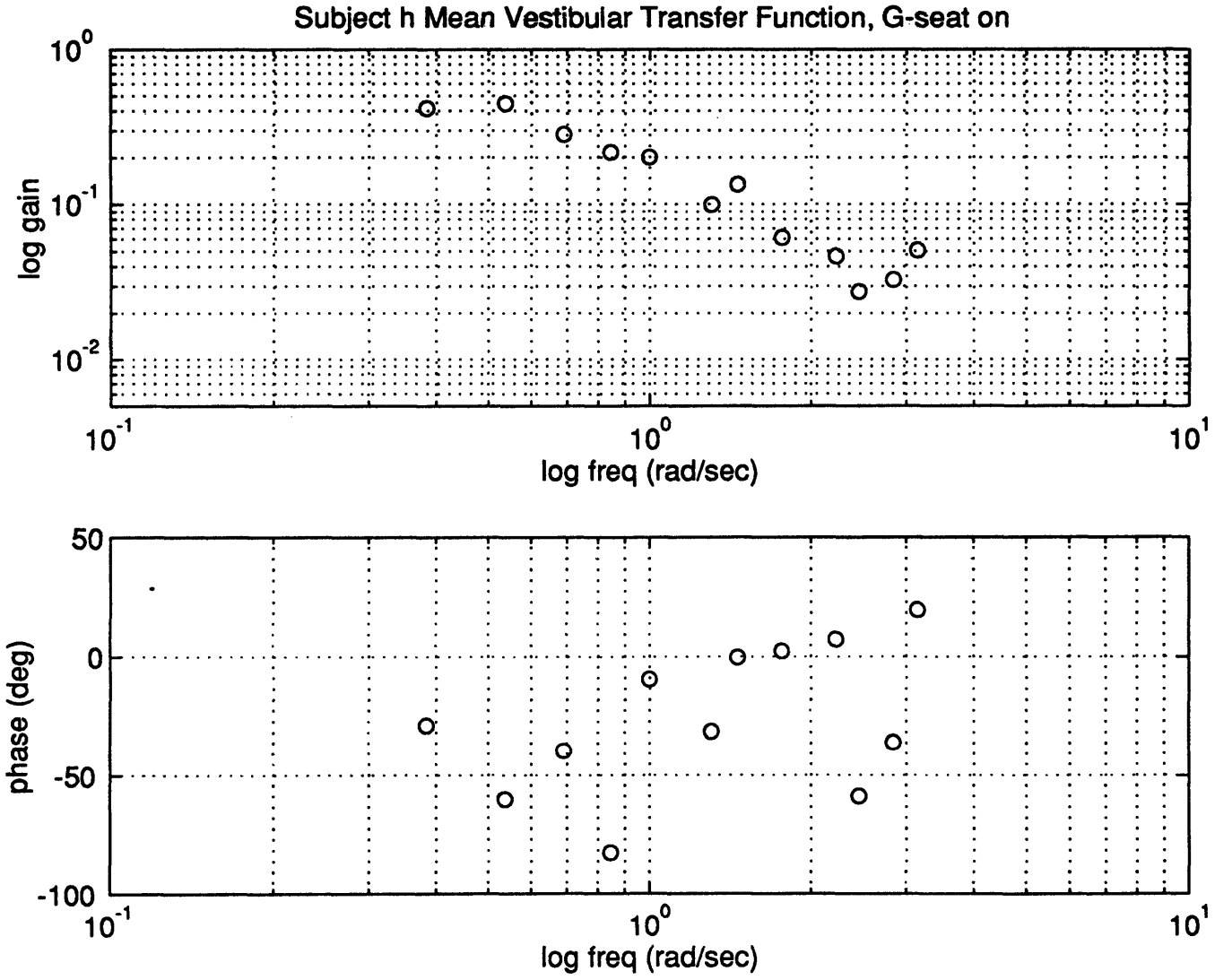
Subject h Mean Vestibular Transfer Function, G-seat on
log gain
log freq (rad/sec)
phase (deg)
log freq (rad/sec)

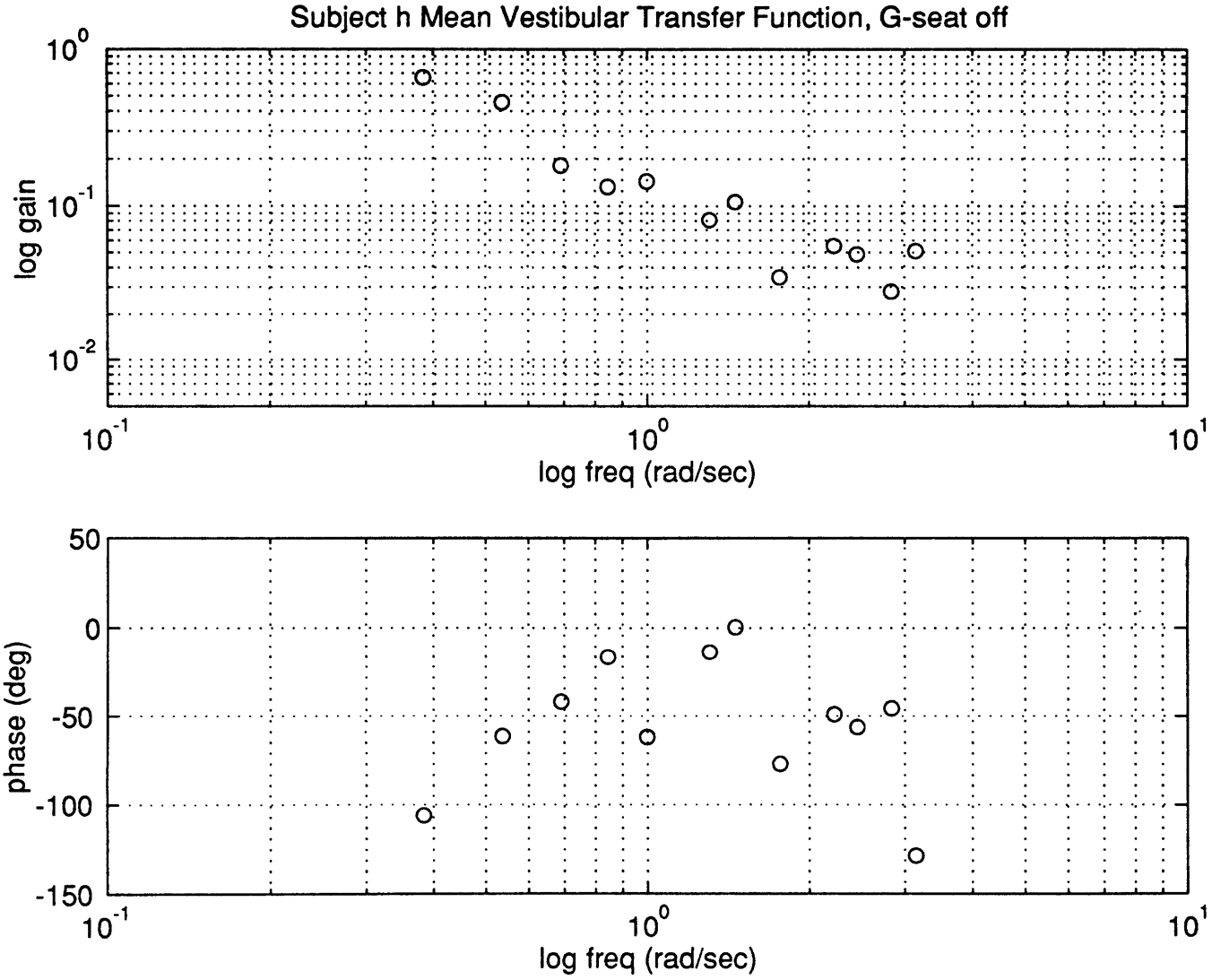
Subject h Mean Vestibular Transfer Function, G-seat off
log gain
log freq (rad/sec)
phase (deg)
log freq (rad/sec)

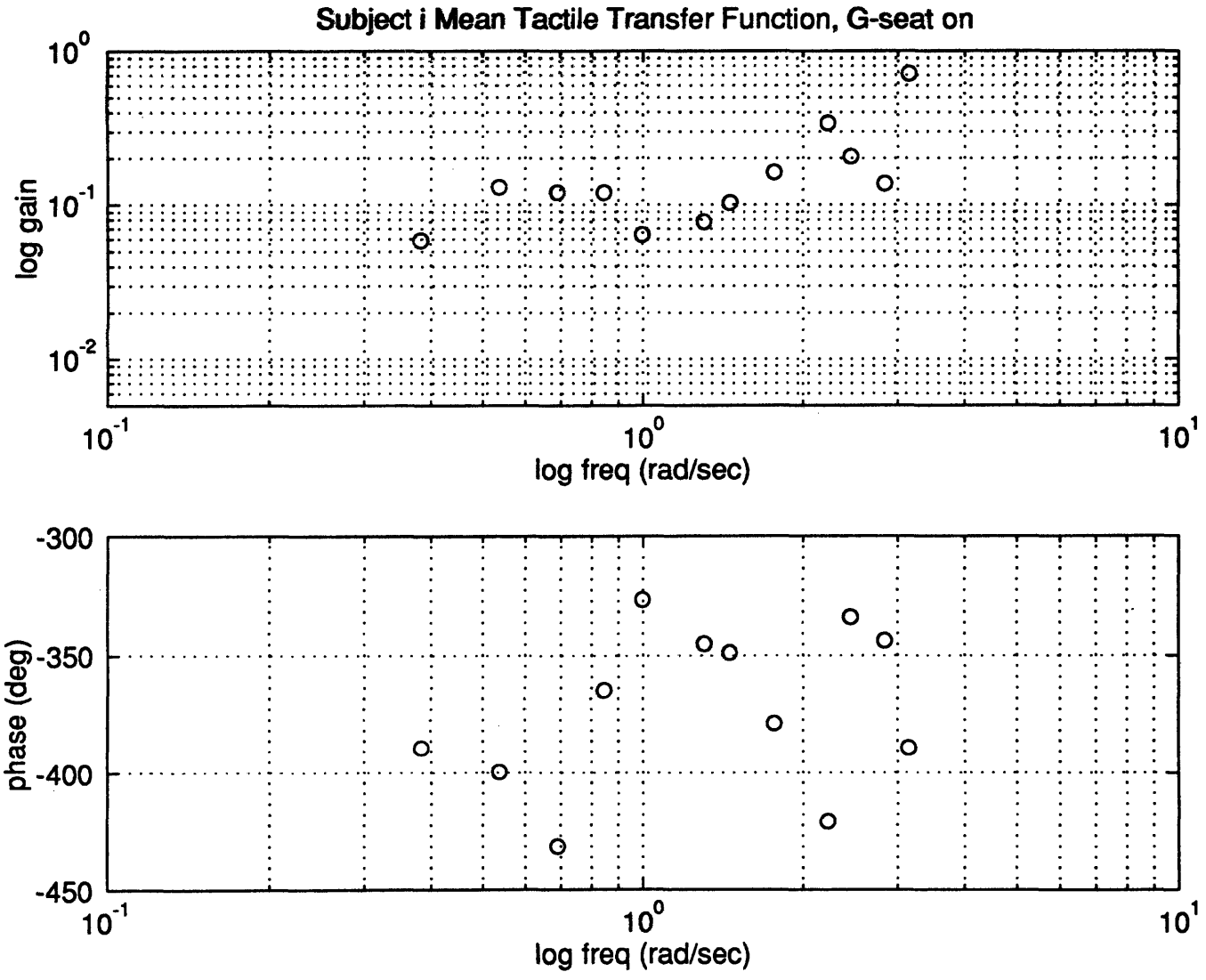
Subject i Mean Tactile Transfer Function, G-seat on
log gain
log freq (rad/sec)
phase (deg)
log freq (rad/sec)

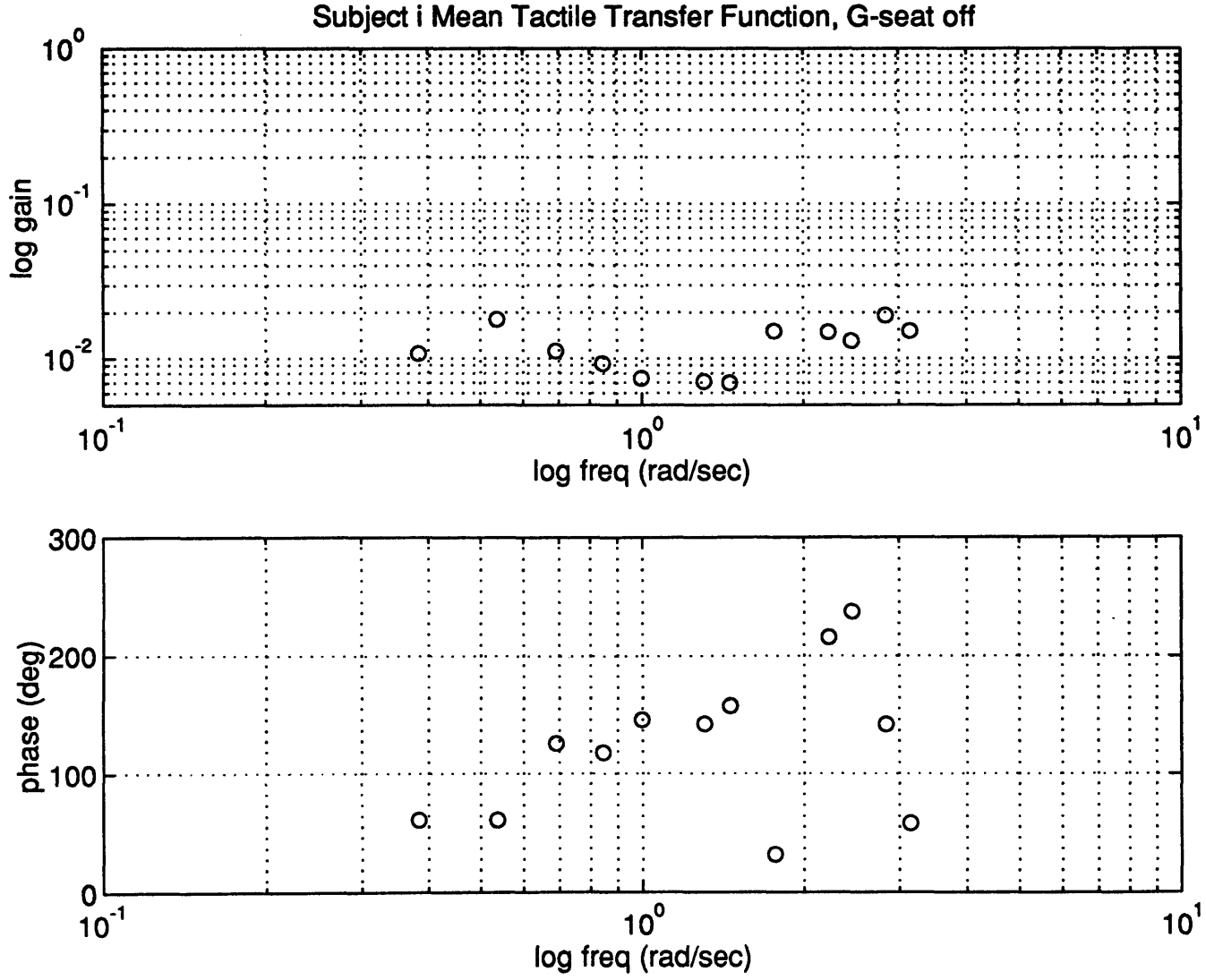
Subject i Mean Tactile Transfer Function, G-seat off
log gain
log freq (rad/sec)
phase (deg)
log freq (rad/sec)

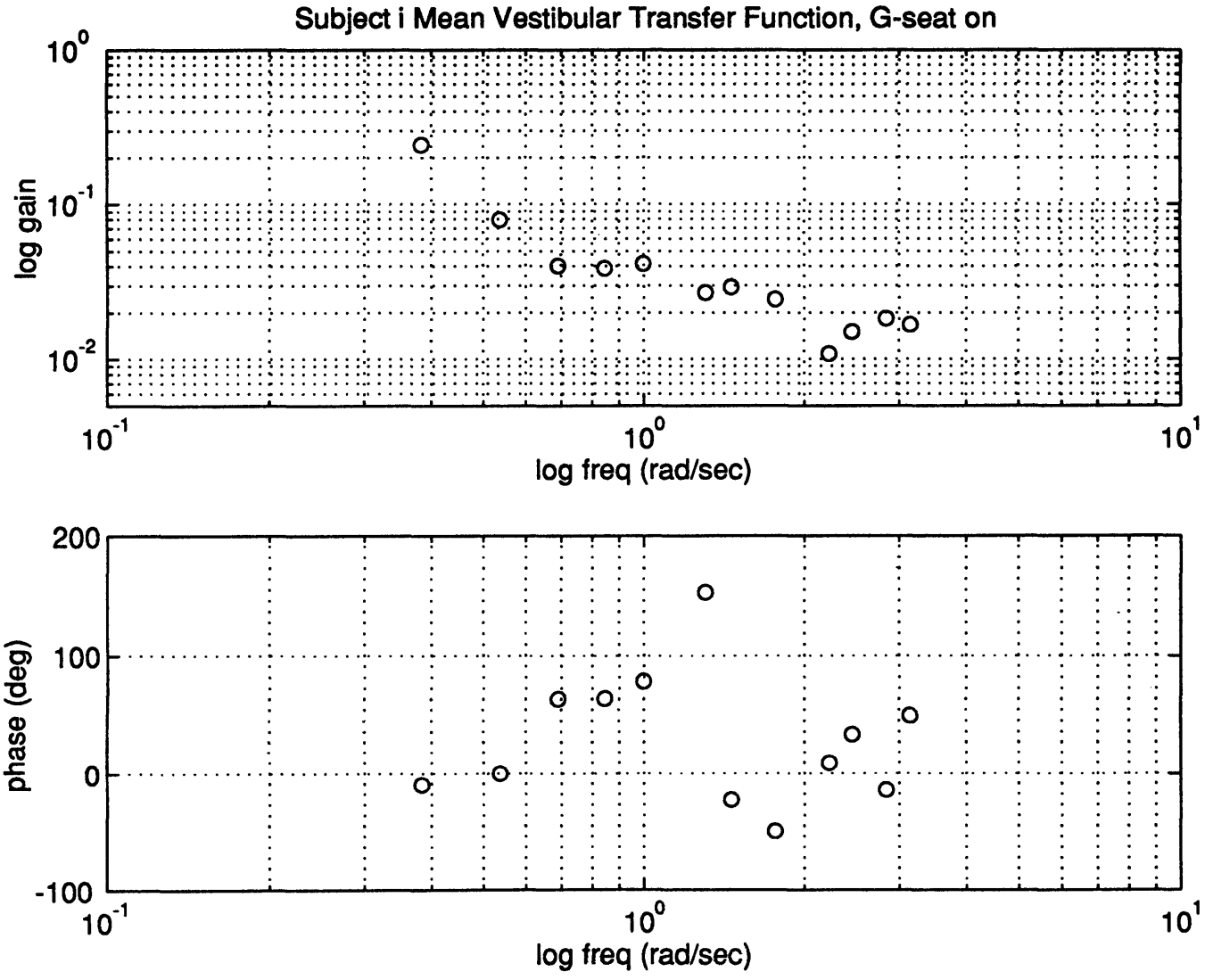
Subject i Mean Vestibular Transfer Function, G-seat on
log gain
log freq (rad/sec)
phase (deg)
log freq (rad/sec)

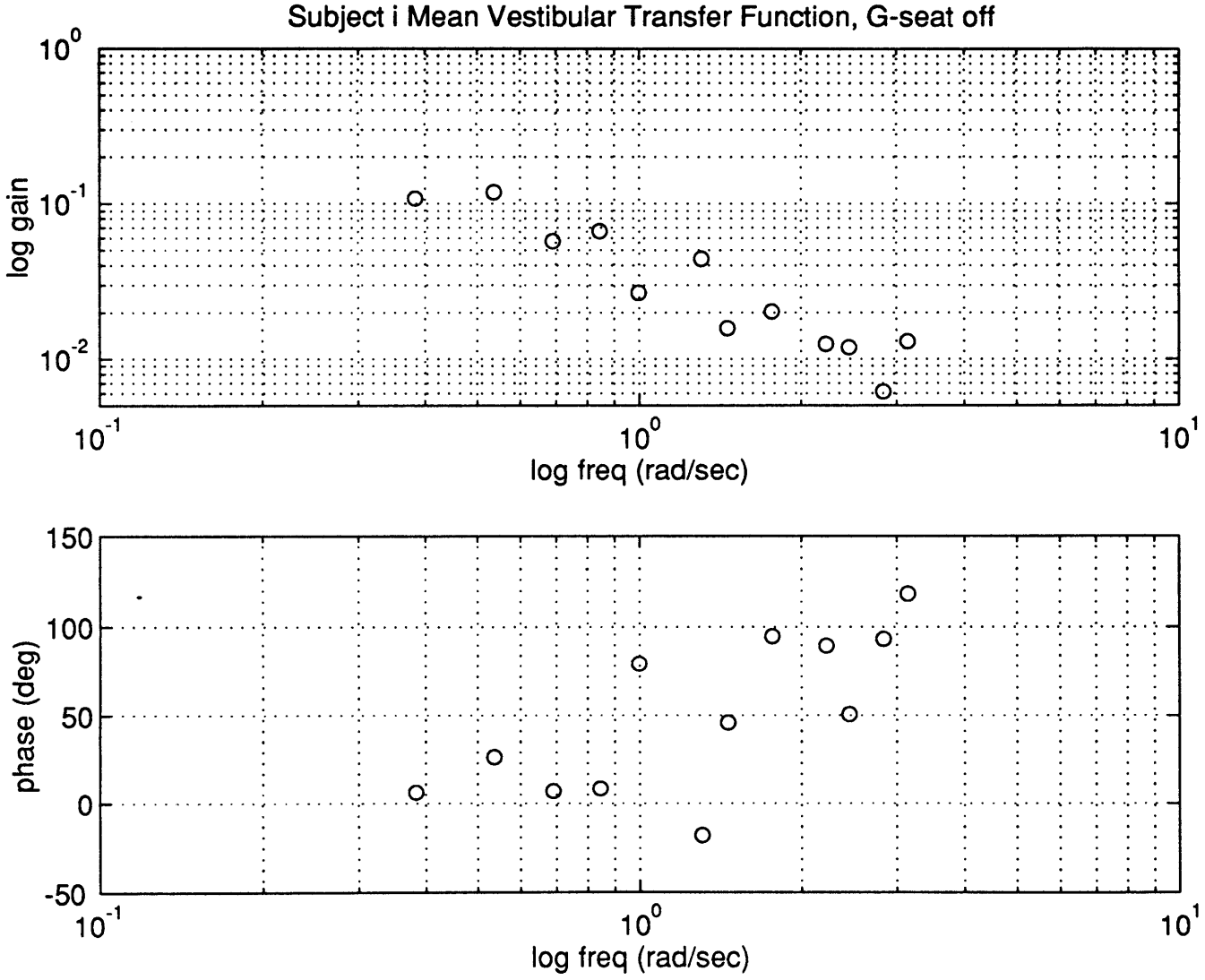
Subject i Mean Vestibular Transfer Function, G-seat off
log gain
10^{0}
10^{-1}
10^{-2}
10^{-1}
10^{0}
10^{1}
log freq (rad/sec)
phase (deg)
150
100
50
0
-50
10^{-1}
10^{0}
10^{1}
log freq (rad/sec)

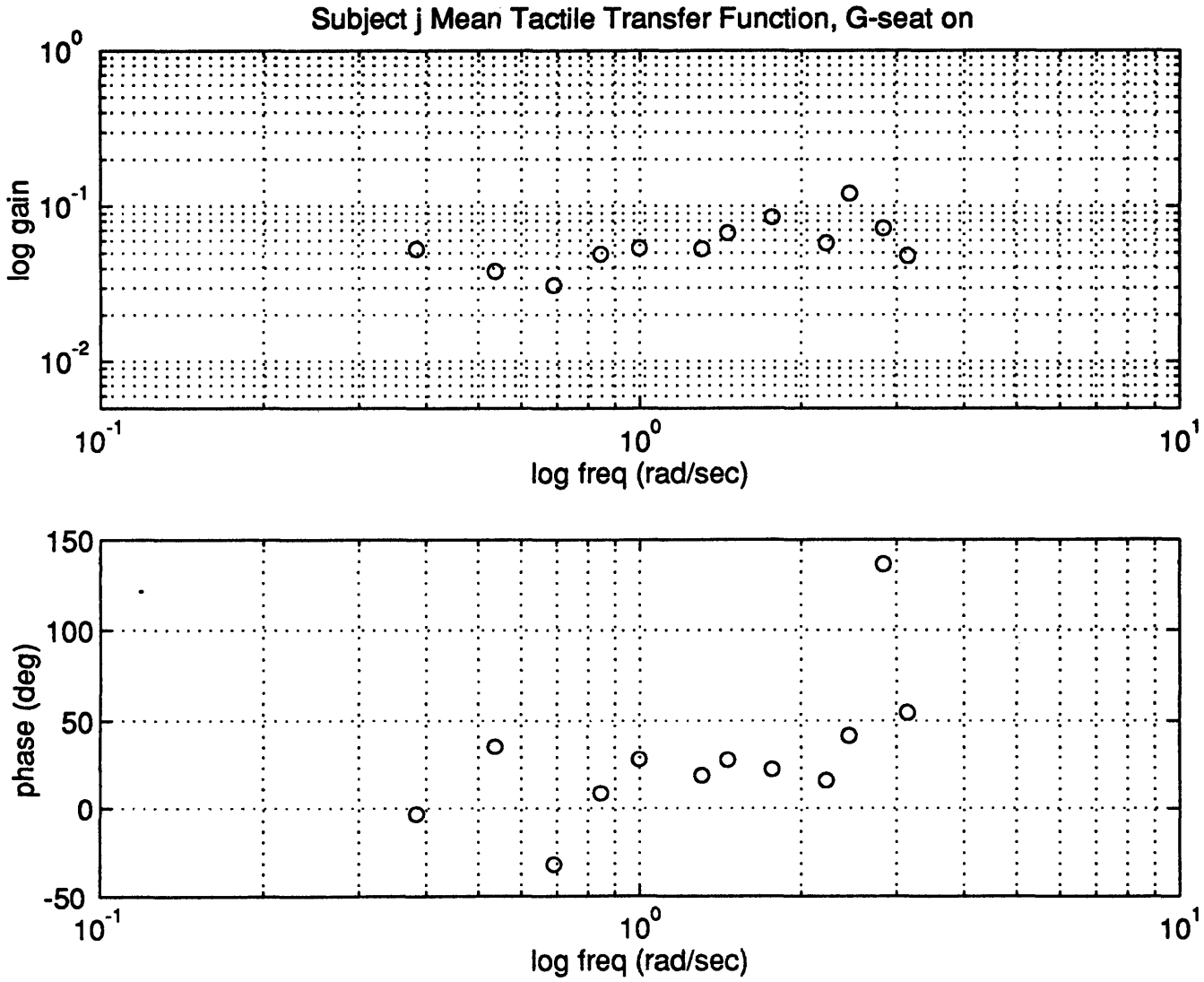
Subject j Mean Tactile Transfer Function, G-seat on
log gain
log freq (rad/sec)
phase (deg)
log freq (rad/sec)

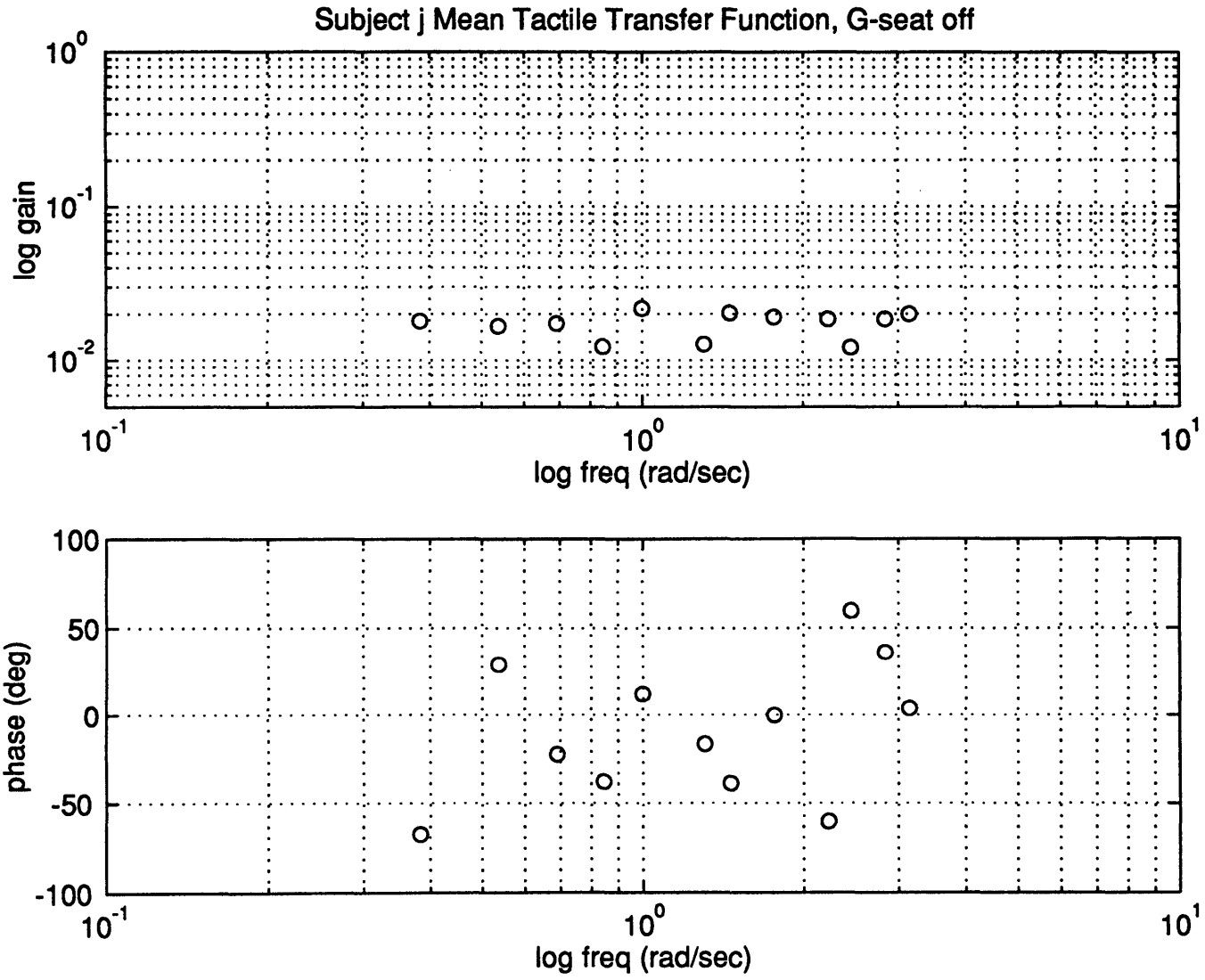
Subject j Mean Tactile Transfer Function, G-seat off
log gain
log freq (rad/sec)
phase (deg)
log freq (rad/sec)

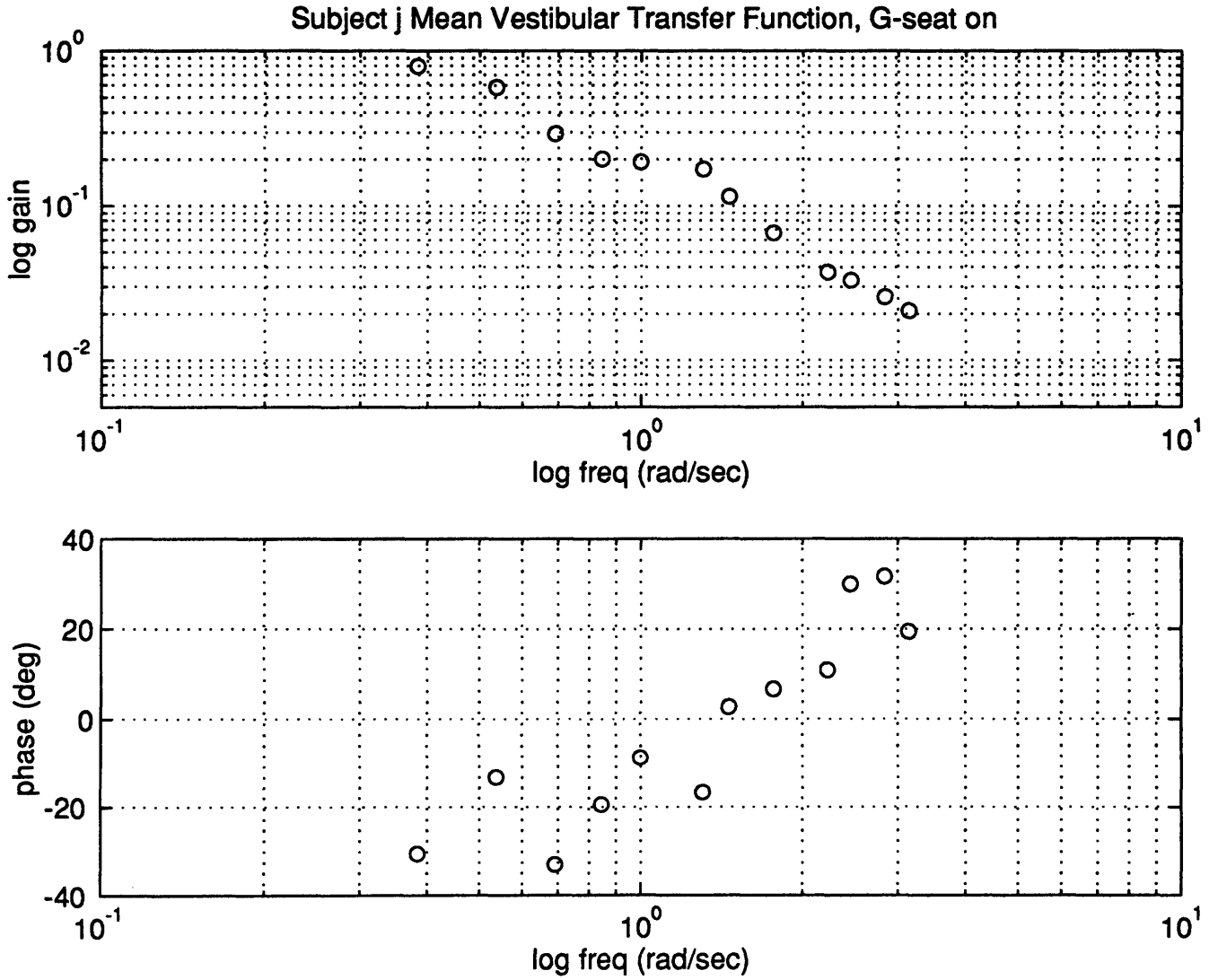
Subject j Mean Vestibular Transfer Function, G-seat on
log gain
log freq (rad/sec)
phase (deg)
log freq (rad/sec)

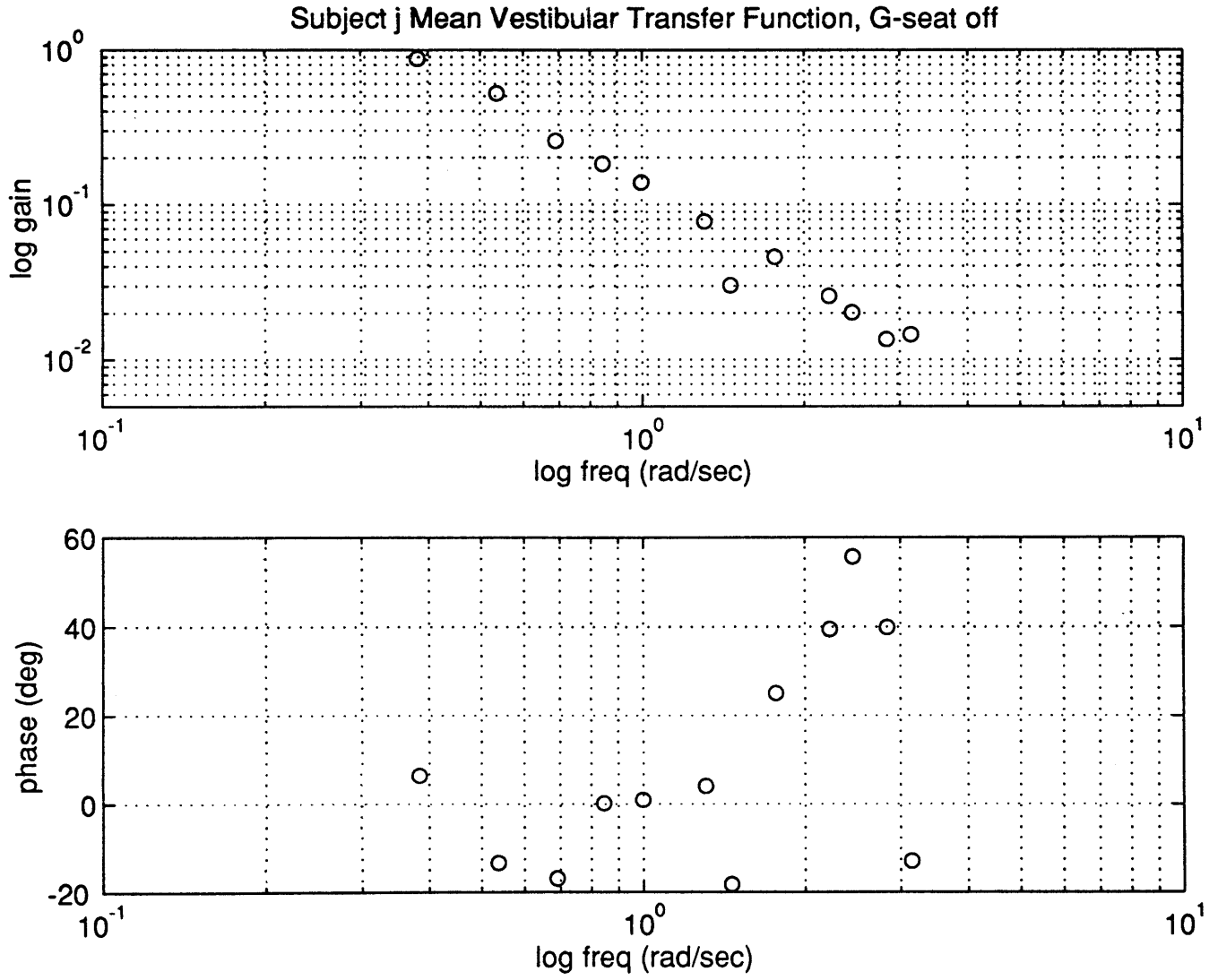
Subject j Mean Vestibular Transfer Function, G-seat off
log gain
log freq (rad/sec)
phase (deg)
log freq (rad/sec)

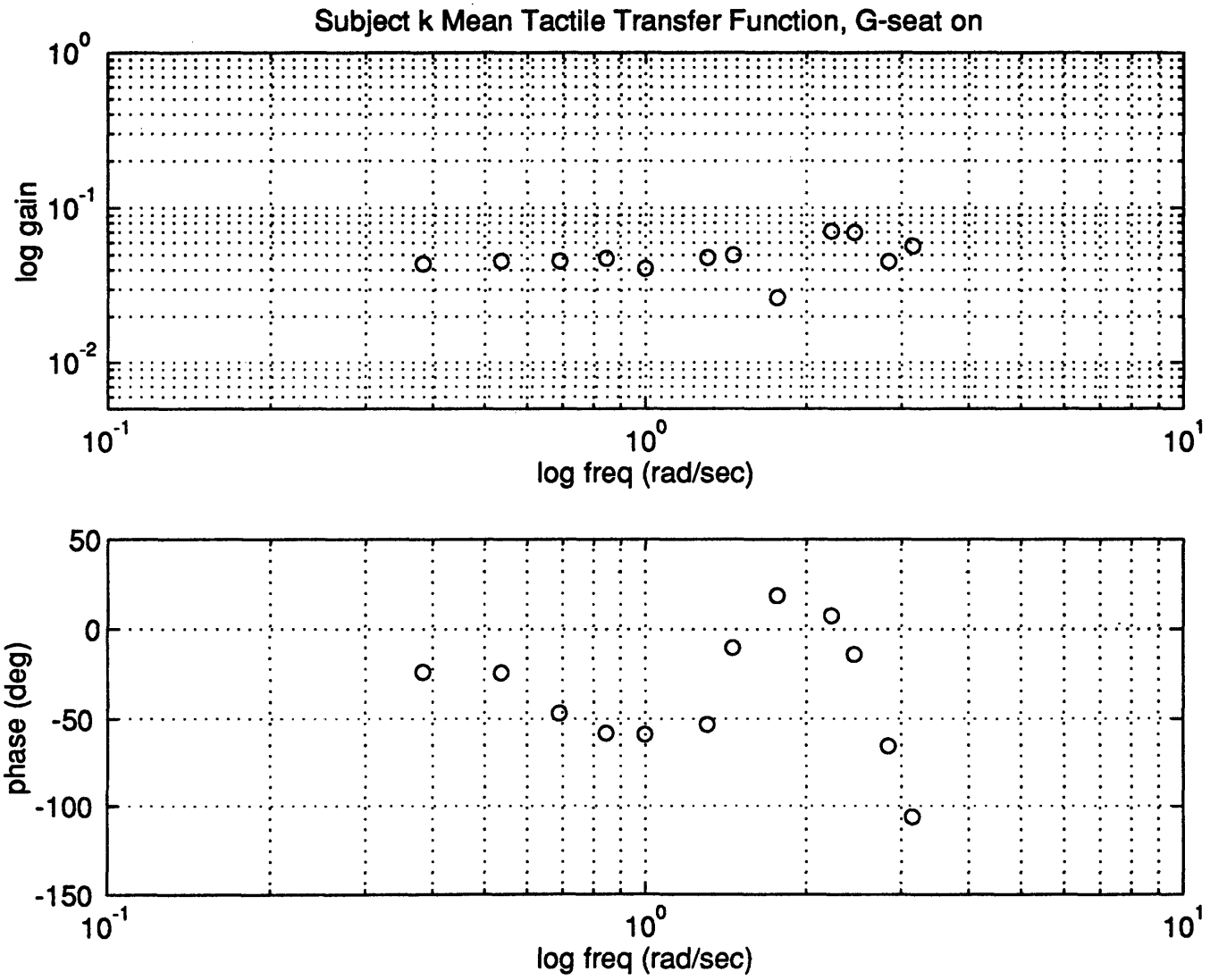
Subject k Mean Tactile Transfer Function, G-seat on
log gain
log freq (rad/sec)
phase (deg)
log freq (rad/sec)

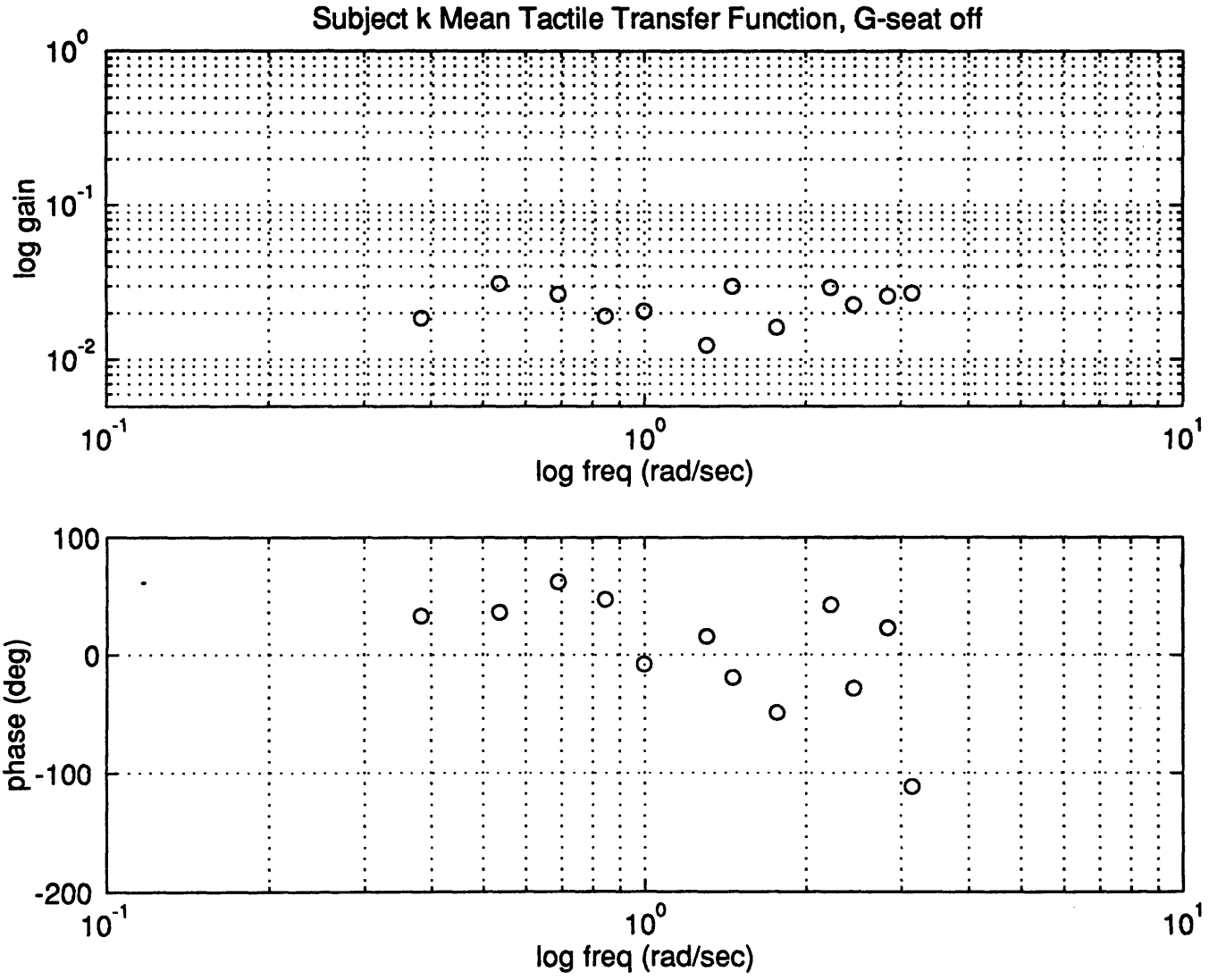
Subject k Mean Tactile Transfer Function, G-seat off
log gain
10^{0}
10^{-1}
10^{-2}
10^{-1}
10^{0}
10^{1}
log freq (rad/sec)
phase (deg)
100
0
-100
-200
10^{-1}
10^{0}
10^{1}
log freq (rad/sec)

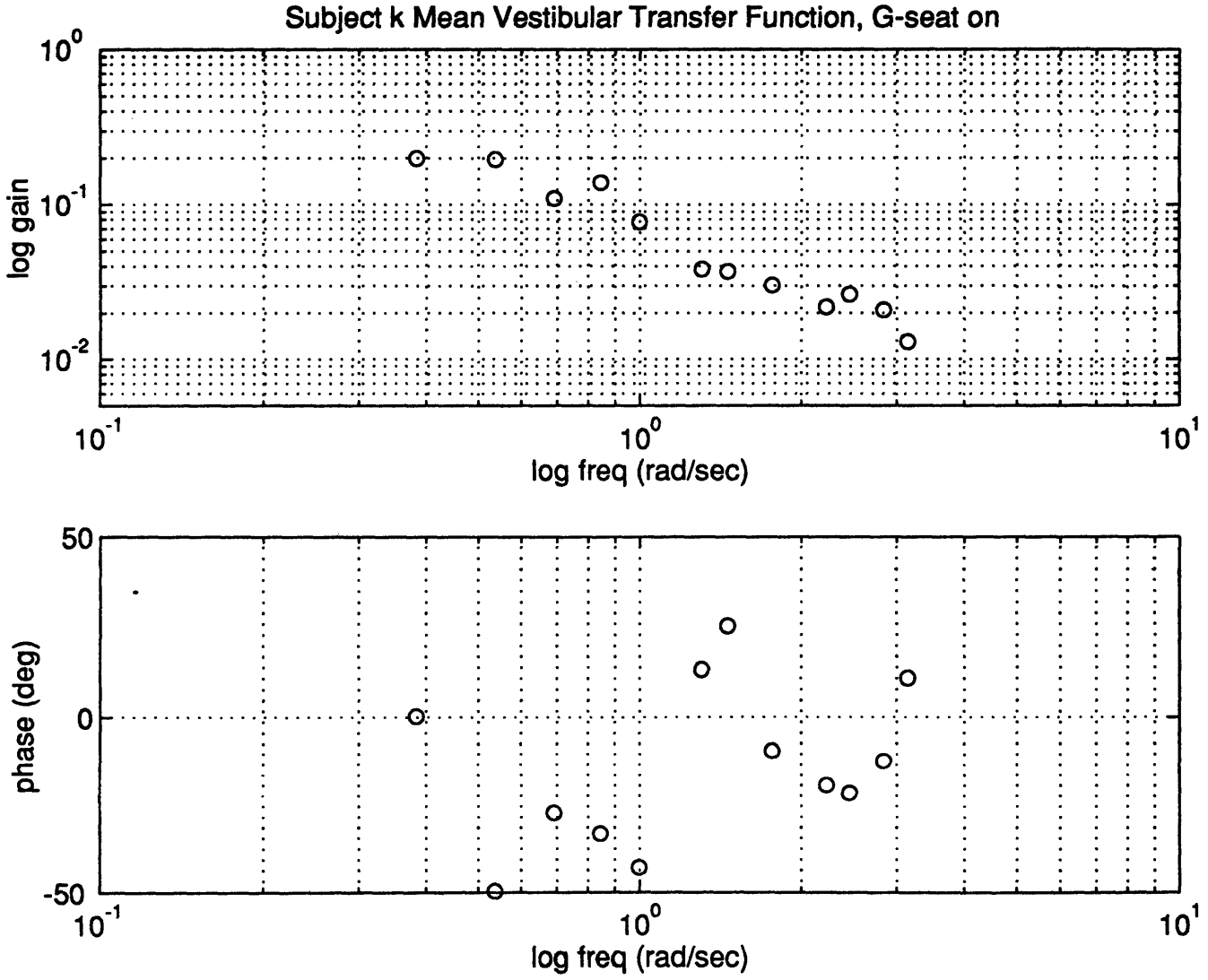
Subject k Mean Vestibular Transfer Function, G-seat on
log gain
10^0
10^{-1}
10^{-2}
10^{-1}
10^0
10^1
log freq (rad/sec)
phase (deg)
50
0
-50
10^{-1}
10^0
10^1
log freq (rad/sec)

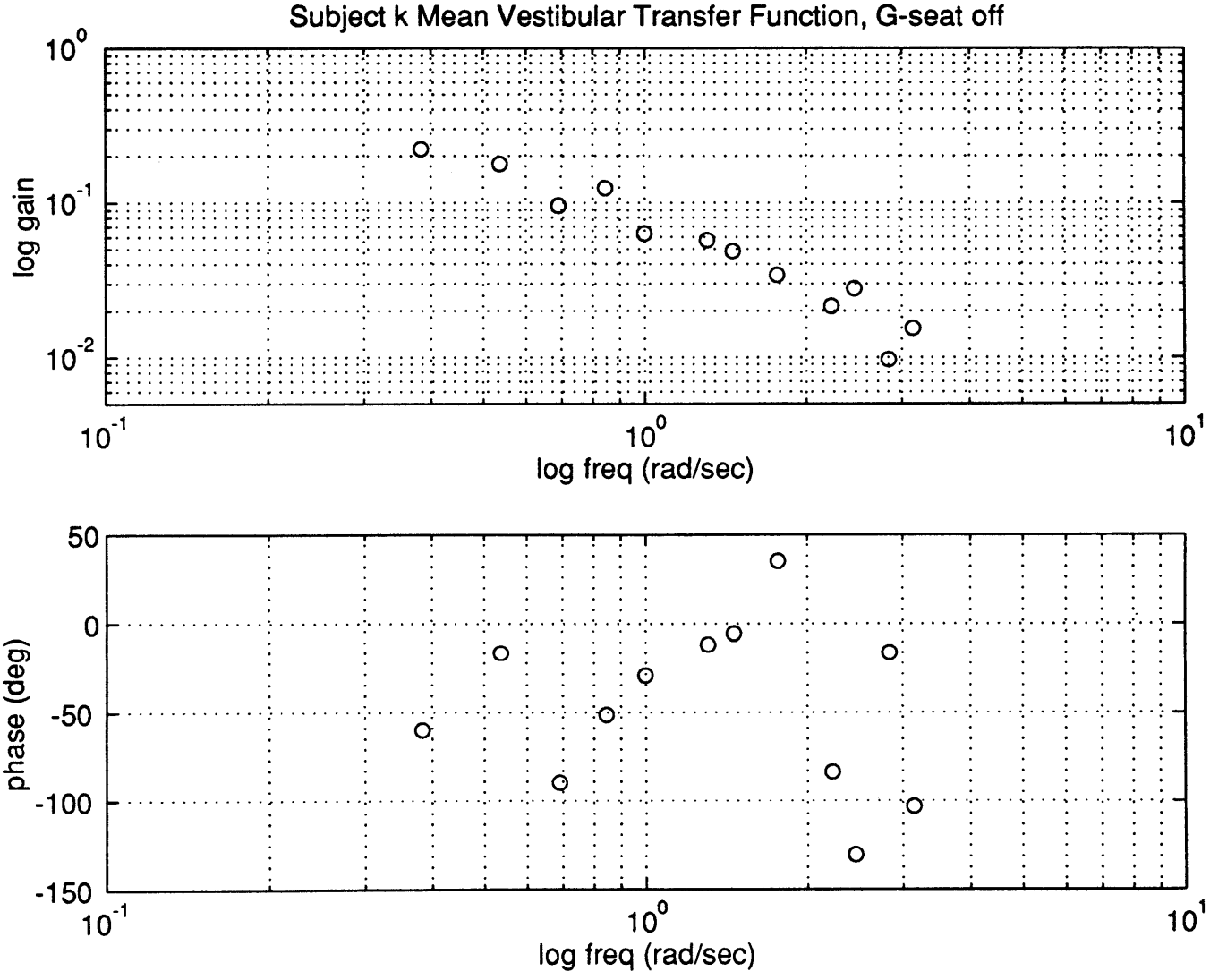
Subject k Mean Vestibular Transfer Function, G-seat off
log gain
10^{0}
10^{-1}
10^{-2}
10^{-1}
10^{0}
10^{1}
log freq (rad/sec)
phase (deg)
50
0
-50
-100
-150
10^{-1}
10^{0}
10^{1}
log freq (rad/sec)

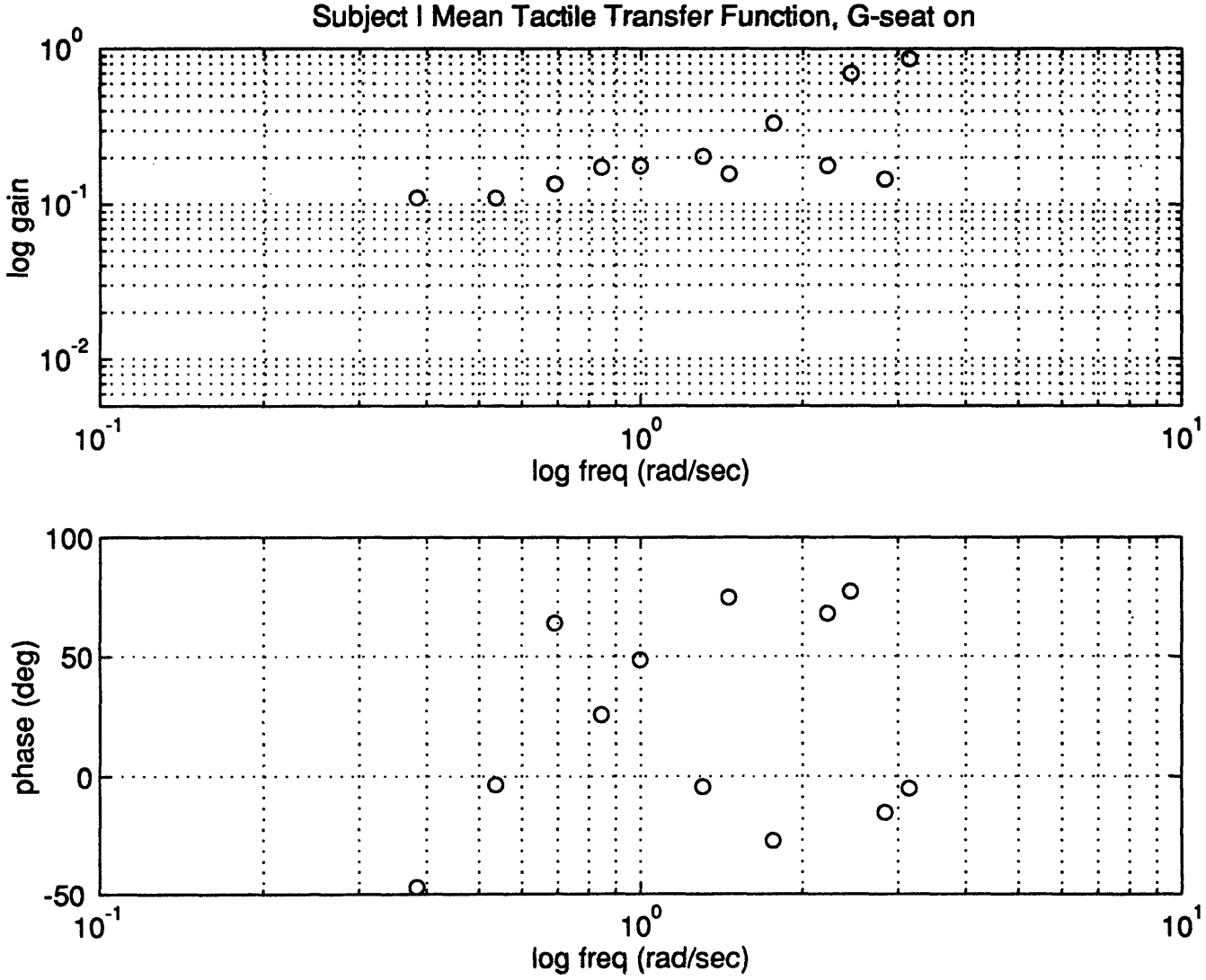
Subject I Mean Tactile Transfer Function, G-seat on
log gain
10^0
10^{-1}
10^{-2}
10^{-1}
10^0
10^1
log freq (rad/sec)
phase (deg)
100
50
0
-50
10^{-1}
10^0
10^1
log freq (rad/sec)

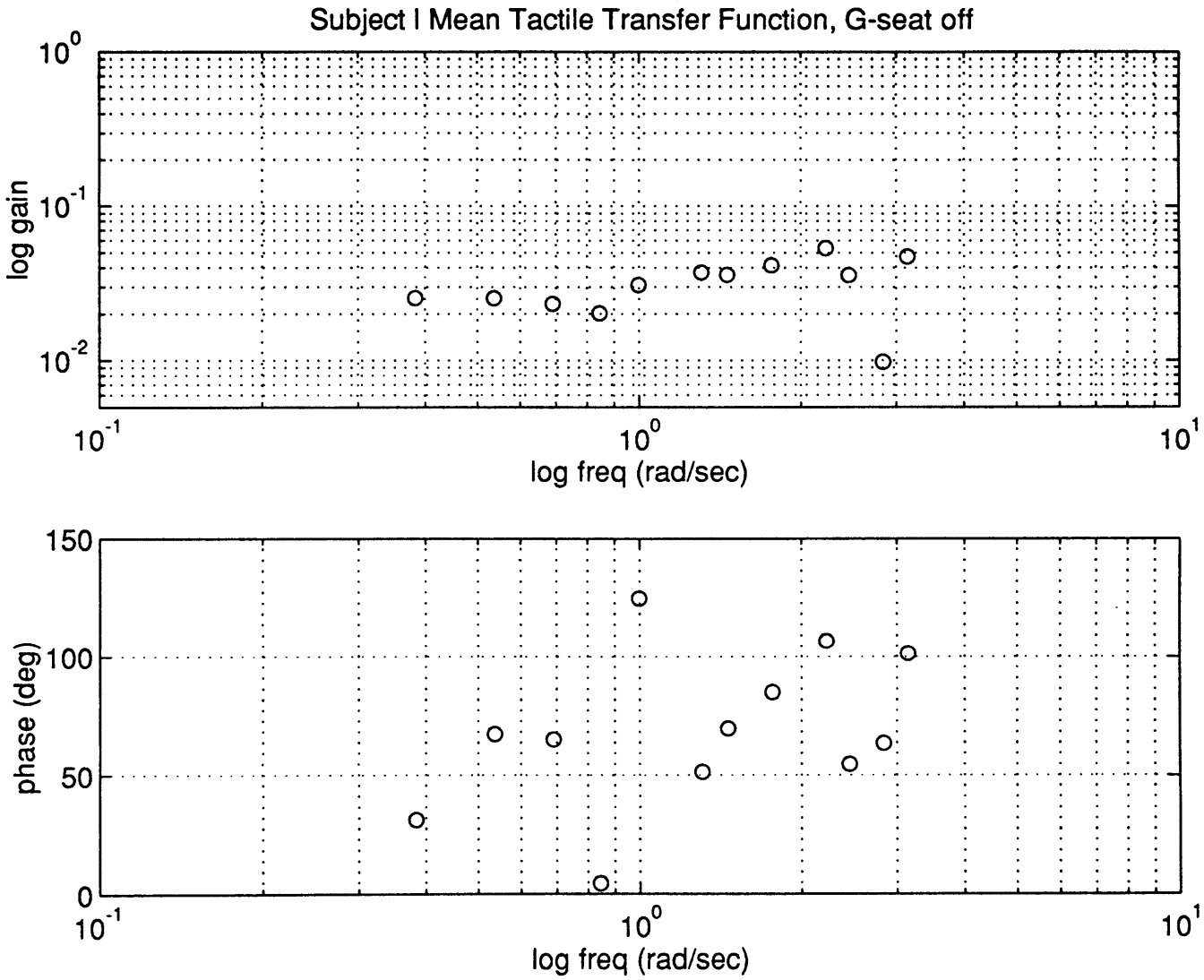
Subject I Mean Tactile Transfer Function, G-seat off
log gain
log freq (rad/sec)
phase (deg)
log freq (rad/sec)

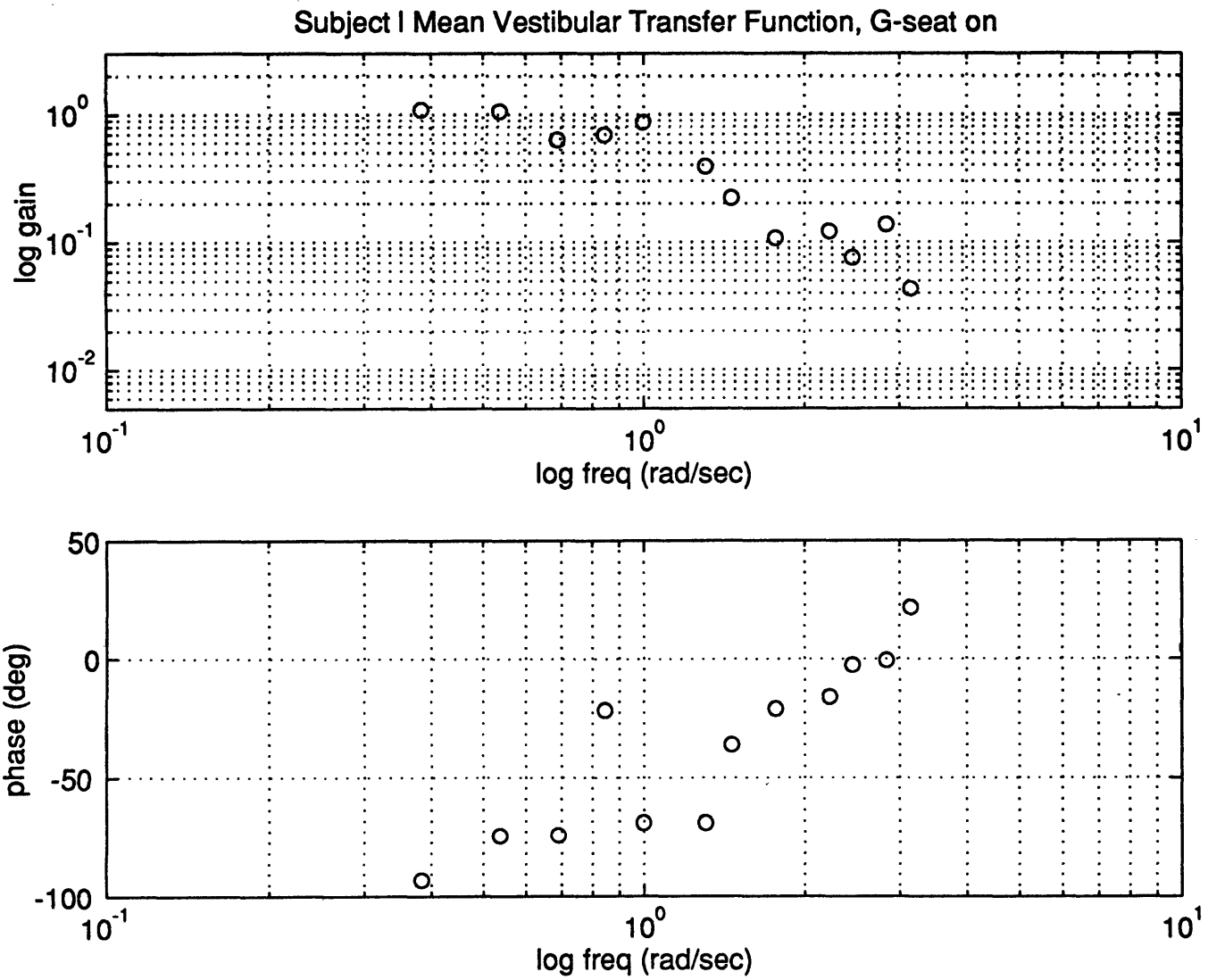
Subject I Mean Vestibular Transfer Function, G-seat on
log gain
10^{0}
10^{-1}
10^{-2}
10^{-1}
10^{0}
10^{1}
log freq (rad/sec)
phase (deg)
50
0
-50
-100
10^{-1}
10^{0}
10^{1}
log freq (rad/sec)

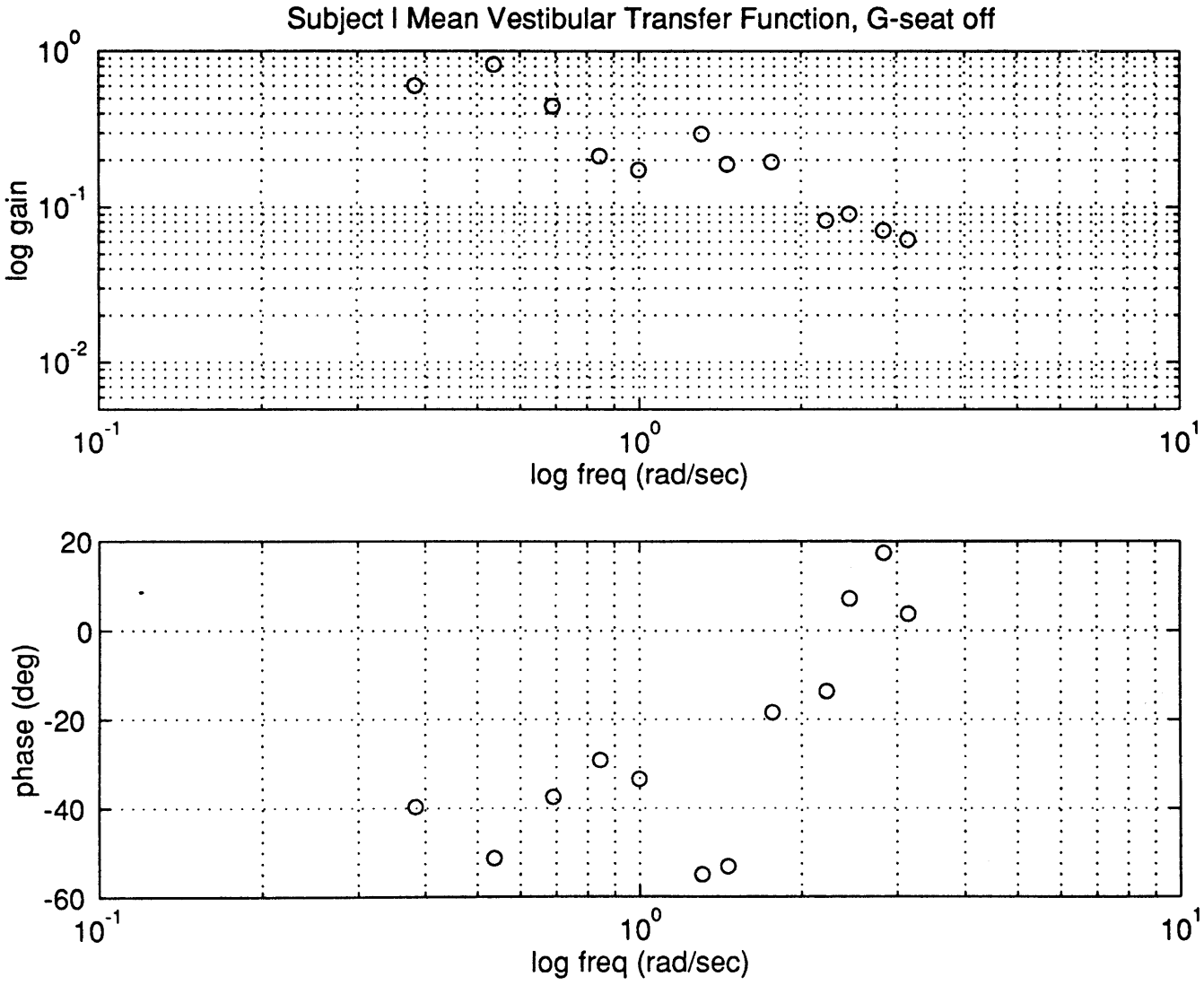
Subject I Mean Vestibular Transfer Function, G-seat off
log gain
10^0
10^{-1}
10^{-2}
10^{-1}
10^0
10^1
log freq (rad/sec)
phase (deg)
20
0
-20
-40
-60
10^{-1}
10^0
10^1
log freq (rad/sec)